Stony Brook University

Interferon-Gamma Fosters a Shift from Acute to Chronic Inflammation in Lyme Disease

A Dissertation Presented

by

Gregory John Sabino

to

The Graduate School

in Partial Fulfillment of the

Requirements

for the Degree of

Doctor of Philosophy

in

Molecular and Cellular Biology

(Immunology and Pathology)

Stony Brook University

December 2010

Stony Brook University

The Graduate School

Gregory John Sabino

We, the dissertation committee for the above candidate for the

Doctor of Philosophy degree,

hereby recommend acceptance of this dissertation.

Martha B. Furie, Ph.D., Dissertation Advisor
Professor, Department of Pathology

Richard R. Kew, Ph.D., Chairperson of Defense
Associate Professor, Department of Pathology

Jorge L. Benach, Ph.D.
Professor, Department of Molecular Genetics and Microbiology

Howard B. Fleit, Ph.D.
Associate Professor, Department of Pathology

Adrianus W. M. van der Velden, Ph.D.
Assistant Professor, Department of Molecular Genetics and Microbiology

This dissertation is accepted by the Graduate School.

Lawrence Martin
Dean of the Graduate School

Abstract of the Dissertation

Interferon-Gamma Fosters a Shift from Acute to Chronic Inflammation in Lyme Disease

by

Gregory John Sabino

Doctor of Philosophy

in

Molecular and Cellular Biology

(Immunology and Pathology)

Stony Brook University

2010

Borrelia burgdorferi is an extracellular bacterium that causes Lyme disease, an inflammatory, multi-systemic ailment. Interferon-γ (IFNγ) is present in lesions of human Lyme disease and positively correlates with severity of illness. Endothelial cells, which line the vasculature, mediate recruitment of immune cells to sites of infection and inflammation. To determine whether IFNγ contributes to development of Lyme disease through its actions on endothelium, cultured human umbilical vein endothelial cells (HUVEC) were exposed to *B. burgdorferi,* IFNγ, or the two stimuli together. Treatment of HUVEC with both stimuli enhanced the transendothelial migration of monocytes and diminished that of natural killer cells, compared to each stimulus alone. Adhesion molecules on endothelium are integral to guiding movement of leukocytes into infected tissues. Concurrent stimulation of HUVEC

with IFNγ and *B. burgdorferi* increased expression of two such adhesion molecules, compared to each stimulus singly, and caused a third to disperse from its usual junctional location. Macrophages secrete chemoattractant cytokines (chemokines) that recruit immune cells, which could contribute to accumulation of leukocytes in lesions of Lyme disease. In studies of cultured human and murine macrophages, IFNγ and *B. burgdorferi* synergistically induced several chemokines for T cells and monocytes, while synergistically downregulating others that attract neutrophils. To investigate the role of IFNγ in the development of Lyme carditis, wild-type and IFNγ-deficient mice were infected with *B. burgdorferi*. Histological analysis of infected mice revealed no difference in severity of carditis between wild-type and IFNγ-deficient mice at 14, 21, 25, and 28 days post-infection. However, a shift in the types of leukocytes within the hearts of IFNγ-deficient mice was observed at 25 days. In the absence of IFNγ, the number of neutrophils in the heart was increased, while T cells were decreased. Bacterial loads within these hearts were similar to those in wild-type mice. Thus, both in vitro and in vivo studies show that IFNγ and *B. burgdorferi* cooperate to enhance recruitment of monocytes and T cells, which typify chronic inflammation, and suppress that of neutrophils and natural killer cells, which accumulate during acute inflammation. These results support the hypothesis that IFNγ promotes a shift from acute to chronic inflammation in Lyme disease.

Table of Contents

List of Tables

List of Figures

Acknowledgments

I would like to thank John Schwedes of the Stony Brook University DNA Microarray Core Facility and Lance Palmer for performing and analyzing human and murine microarrays. I also thank Dr. Patricio Mena for his valuable work throughout the course of our *in vivo* studies, and Stephanie Burke of the Pathology Translational Research Laboratory at Stony Brook University Medical Center for her indispensable knowledge of histology techniques. Additionally, I thank Silvia Leonor of the Stony Brook University Hospital Non-Transplant Tissue Bank for the processing of sample blocks and slides. Lastly, I am grateful for the macrophages supplied by Galina Romanov, the excellent laboratory support provided by Indralatha Jayatilaka, and the contribution of Joseph Catanzaro, who repeated the experiments shown in Figure 8 as part of his rotation in the Furie laboratory.

Introduction

I. Overview

Borrelia burgdorferi is a Gram-negative, spirochetal bacterium that causes an inflammatory disorder known as Lyme disease. *B. burgdorferi* is transmitted to new hosts through the bite of an *Ixodes* tick. As the spirochetes enter the skin of a host, leukocytes migrate to the area in an effort to eliminate the bacteria. This local inflammatory response results in a rash known as an erythema migrans.[1,2] The infiltration of leukocytes into regions of infection is a hallmark of Lyme disease.[3,4]

If patients are left untreated, the bacteria can enter the bloodstream and disseminate to other areas of the body. As it progresses, Lyme disease can develop into a multisystemic disorder resulting in arthritis, myocarditis, and complications within the peripheral nervous system. In Lyme disease, the host inflammatory response is responsible for the severity of the illness. Over time, humans may develop a chronic phase of the disease, where there is a persistent infiltration of leukocytes into tissues and the destructive inflammation becomes self-sustaining.[5]

In an effort to protect itself from infection, trauma, or toxins, the body mounts an inflammatory response to prevent tissue damage, eliminate insults, and repair tissues.[6] During inflammation, a cascade of events results in the release of mediators that culminate in the recruitment of leukocytes to infected or injured areas.[7] There is an intricate interaction among leukocytes, adhesion molecules, endothelial cells, and chemical factors, which entails both synergy and redundancy.[8]

II. Inflammation

A. Acute and Chronic Stages

Inflammation is commonly categorized into two phases, acute and chronic, each with distinct properties.[9] Acute inflammation is the initial rapid response to an insult and consists of the influx of neutrophils and the secretion of pro-inflammatory cytokines and acute-phase proteins.[10] Typically, the acute stage of inflammation lasts only a few days if the resolution of inflammation proceeds normally.[11] If an insult is not cleared, the inflammatory response can develop into a chronic state. The leukocytic population in lesions of chronic inflammation is predominantly mononuclear cells, such as macrophages and T lymphocytes.[10] The neighboring vasculature proliferates to form new capillary-like vessels, and existing vessels can enlarge. Reactive oxygen species, used by leukocytes to eliminate microbes, can damage surrounding tissue due to their lack of specificity. During chronic inflammation, wound fibrosis and scarring occur to maintain structural integrity; however, these processes can impair the function of joints and organs.[11] Due to a consistent influx and activation of leukocytes in the region, chronic inflammation can be of long duration.[12]

B. Pro-Inflammatory Cytokines

Cytokines are small peptides that signal between cells to regulate a variety of downstream effects.[13] During acute inflammation, the pro-inflammatory cytokines interleukin (IL)-1 and tumor necrosis factor-α (TNFα) are promptly secreted from endothelium and immune cells.[6] Collectively, these cytokines foster proliferation of leukocytes, cytotoxicity, and the release of additional cytokines within the inflammatory lesion.[13] Moreover, they promote the secretion of certain chemoattractant cytokines

(chemokines) that promote infiltration of neutrophils.[6] One of three members in the IL-1 family, IL-1β, may be found in the circulation and is secreted primarily from monocyte/macrophages.[14,15] Human umbilical vein endothelial cells (HUVEC) also produce both IL-1α and IL-1β in response to lipopolysaccharide (LPS).[16] IL-1β is an integral factor in the progression of acute inflammation and is required for the manifestation of fever during inflammation and development of experimental arthritis.[17] Stimulation of endothelium with IL-1β also increases the expression of cell-surface adhesion molecules and binding of leukocytes.[18]

TNFα is secreted predominantly from macrophages as a response to infection or tissue damage. It can activate leukocytes to enhance their anti-microbial properties, such as natural killer (NK) cell cytolytic activity,[19] while also promoting secretion of mediators such as tissue factor from monocytes and endothelium. The secreted tissue factor in turn induces leukocytes to release additional TNFα.[10] TNFα increases the expression of cell-surface adhesion molecules on endothelium and promotes the adhesion of leukocytes.[19] TNFα plays an important role in the repair of damaged tissues. However, if resolution of inflammation is not complete, TNFα can participate in a destructive series of events, leading to chronic inflammation consisting of tissue and organ injury.[10]

C. Resolution of Inflammation

Elimination of the insult during the acute phase of inflammation will deter the further production of pro-inflammatory mediators and infiltration of leukocytes into tissue. The absence of a stimulus will initiate the clearance of leukocytes from the inflamed region,[6] while returning tissues to their previous structure and composition.[20] During clearance,

leukocytes are able to emigrate out of tissues and return to the circulating population.[21] As neutrophils migrate into lesions, they secrete a receptor for the cytokine IL-6. IL-6 and its receptor form a complex that shifts the expression of chemokines towards those that attract monocyte/macrophages involved in resolution.[6] In this instance, IL-6 directly opposes the pro-inflammatory activity of IL-1β and TNFα. In addition, leukocytes can undergo apoptosis locally and become phagocytosed by macrophages that are recruited to the region. While acting as an inducer of inflammation, IL-1β also can promote the release of lipoxins, which act as a chemoattractant for macrophages that are capable of accelerating the resolution of inflammation through phagocytosis of neutrophils.[22] These macrophages may also abandon the area via lymphatic drainage in a process controlled by the modulation of cell-surface adhesion molecules.[6,20]

During apoptosis of phagocytic cells, their membranes remain intact, which prevents release of cytotoxic granules. The apoptotic process causes cell-surface changes that allow macrophages to rapidly recognize and engulf the dying cells.[23] Ingestion of the apoptotic cells by macrophages can promote the secretion of anti-inflammatory cytokines such as IL-10 and transforming growth factor-β (TGFβ). These anti-inflammatory cytokines act as signals to other leukocytes in the locale to dampen the inflammatory response.[24] Macrophages can also release Fas ligand, which initiates apoptosis in neutrophils.[25] However, if their clearance is inhibited, these dying cells can become necrotic.[23] Necrosis leads to the loss of membrane integrity, enabling the release of intracellular components that will act as pro-inflammatory stimuli. Dysfunction in the clearance of inflammation leads to chronic inflammation.[23]

D. Chemokines

Chemokines are chemotactic cytokines that are primarily basic in electrostatic charge and range from 70 to 125 amino acids long. They play a role in the homeostatic trafficking of leukocytes and their response to inflammatory stimuli.[26] The chemokine super-family is subdivided into four smaller groups named C, CC, CXC, and CX3C.[27] This nomenclature is derived from the number of cysteine residues in the N-terminus of the protein and the number of amino acids between them.[28] As a whole, CC chemokines are attractants for mononuclear cells. However, the CXC family comprises chemokines that attract neutrophils or lymphocytes. An animo acid sequence of Glu-Leu-Arg before the first cysteine residue, known as the ELR motif, dictates on which cell type the chemokine acts. If a CXC chemokine possesses the ELR motif, it will attract neutrophils, while chemokines that lack the motif attract lymphocytes. XCL1 (lymphotactin) and XCL2 are the only members of the C family, and they act on T cells. The sole member of the CX3C family, fractalkine, is cell-surface bound and promotes the migration of T cells, monocytes, and NK cells.[29]

Chemokines that promote the infiltration of immune cells into areas of injury or infection are typically secreted by resident dendritic cells and macrophages.[30] Endothelial cells are also major sources of inflammatory chemokines.[31] These chemokines are the result of direct interactions of bacterial products, such as LPS, with cells or the effector function of pro-inflammatory cytokines present in the area.[32] Acting as mediators of inflammation, chemokines aid in the migration of leukocytes by altering leukocytic integrin expression, L-selectin shedding, and cytoskeletal organization.[27]

Chemokines signal though 7-transmembrane G protein-coupled receptors on target cells,[26,33] exhibit redundancy, and can often bind to more than one receptor.[26] Some specific

diseases are associated with the expression of certain chemokine receptors in patients.[34] In the case of rheumatoid arthritis, CXCR3 and CCR5 are upregulated on T cells found in synovial fluid.[35] Depending on their location, monocytes and macrophages differentially express chemokine receptors on their cell surface. If they are in the process of migrating out of the circulation into tissue, CCR1 and CCR2 are expressed. In the joint, CCR3 and CCR5 are prevalent and aid in retention of macrophages.[36]

Early forms of arthritis are typified by the infiltration of neutrophils into synovial tissue. In the context of rheumatoid arthritis, CXCL8, a major attractant of neutrophils, is highly secreted by synovial macrophages. It is observed in synovial fluid, synovial tissue, and sera of patients.[37,38] CXCL1 and CXCL5 also promote the migration of neutrophils and stimulate fibrosis in patients with rheumatoid arthritis.[37,39] As the disease develops further, CXCL9 and CXCL10 are released by synovial macrophages and fibroblasts and recruit lymphocytes and monocytes.[37] These chemokines are detected in sera of rheumatoid arthritis patients as well.[33]

E. Endothelium

Vascular endothelial cells form a physiological barrier between blood and tissue and play a vital role in promoting and resolving inflammation. Under homeostatic conditions, endothelial cells lining the blood vessels are anti-adhesive and anti-aggregatory.[40,41] Activated endothelial cells foster the migration of leukocytes into damaged tissue through adhesion molecules and the presentation of bound chemokines to leukocytes on the luminal surface.[40] Additionally, activation of endothelial cells enhances their production of cytokines and growth factors and increases vascular permeability.[41] Endothelial cells perpetuate the

inflammatory response through paracrine and autocrine stimulation by secreted chemokines.[42] The activation of endothelial cells promotes the surface presentation of chemokines to leukocytes through the expression of glycosaminoglycans (GAGs), which are negatively charged polysaccharides that form electrostatic bonds with chemokines.[43] In the absence of functional GAGs, the transmigration of leukocytes is nearly abolished.[44] Endothelial cells also produce large amounts of chemokines, which form a concentration gradient that guides migration of leukocytes out of the vasculature.[43]

The endothelium aids the resolution of inflammation in a variety of ways. While bound GAGs can direct migration, soluble GAGs can bind free chemokines and prevent their binding to immune cells, which can limit downstream migratory events.[43] The D6 chemokine receptor on endothelium can bind secreted chemokines, leading to their internalization and breakdown.[40] Superoxide dismutase (SOD) expressed by endothelial cells can also limit inflammatory responses by reducing the oxidative stresses that are the result of free radicals generated by nicotinamide adenine dinucleotide phosphate H (NADPH) oxidase.[40] As described previously, endothelial cells and leukocytes produce lipoxins during acute inflammation. These can also act as anti-inflammatory mediators by limiting vascular permeability.[40]

F. Recruitment of Leukocytes by Endothelium

At inflammatory lesions, the vascular endothelium and leukocytes engage in a cascade of events that enables leukocytes to enter the surrounding tissues through a process known as diapedesis.[45,46] In general, pro-inflammatory mediators stimulate endothelial cells to express chemokines, selectins, and immunoglobulin super-family members on their

surface.[47] Leukocytes undergo a loose tethering to endothelium, which is followed by tight adhesion, and lastly, transendothelial migration. Throughout this process, chemokines play an integral role.[46]

Leukocytes are initially recruited to the surface of endothelium by low-affinity interactions between selectins that are expressed on both activated endothelium and the leukocytes. Without selectins, leukocytes are unable to roll along the endothelium.[48,49] There are three types of structurally similar selectins involved in the early stages of transmigration named P-, E-, and L-selectin. They are transmembrane glycoproteins that bind to surface receptors that contain sialylated carbohydrates. P-selectin is constitutively produced by endothelial cells but expressed on the surface only upon activation. P-selectin binds to P-selectin glycoprotein ligand (PSGL)-1 on leukocytes, forming one of the earliest interactions between the vascular endothelium and immune cells. Expression of E-selectin by endothelial cells is induced by TNFα, IL-1β, and LPS and peaks about 4 hours into the inflammatory response.[50] On the surface of leukocytes, L-selectin forms loose tethering through a number of receptors on endothelial cells, such as glycosylation-dependent cell adhesion molecule-1, CD34, podocalyxin, and Sgp2000.[51] The binding of L-selectin is important for rolling of neutrophils.[52] The binding of selectins to their receptors can upregulate the surface expression of integrins and initiate internal Ca^{2+} signaling.[53,54]

The rolling of leukocytes positions them to detect chemokines that are presented on the surface of activated endothelial cells.[46] The recognition of these ligands by the chemokine receptors on leukocytes triggers a series of events within the cells. Conformational changes in the β1 integrin very late antigen (VLA)-4 and β2 integrins lymphocyte function-associated antigen (LFA)-1 (CD11a/CD18) and Mac-1 (CD11b/CD18) on leukocytes foster tight

adhesion to the vascular endothelium.[55] These integrins bind to specific immunoglobulin superfamily members, resulting in a high-affinity binding to the endothelial surface.[46,56] Vascular cell adhesion molecule (VCAM)-1 on endothelial cells interacts with VLA-4 expressed mostly on lymphocytes and monocytes.[46] LFA-1 and Mac-1 on leukocytes, such as neutrophils, bind to intercellular adhesion molecule (ICAM)-1 and ICAM-2 on the surface of endothelium.[57] Pro-inflammatory cytokines and bacterial agents can stimulate an increase in endothelial surface expression of ICAM-1, but not ICAM-2. The expression of ICAM-1 peaks around 8 hours after endothelial activation.[58] In addition to promoting the generation of chemokines,[59] binding of ICAM-1 can promote the remodeling of the cytoskeleton of endothelial cells.[56,60]

The process of migration across the vascular endothelium can occur in two ways. Transcellular migration is the process of a leukocyte passing through an individual endothelial cell.[47] This process is due to bound ICAM-1 translocating to actin- and caveolae-rich regions. There, lipid rafts containing ICAM-1 link together forming vesiculo-vacuolar organelles, which create an intracellular channel through which a leukocyte can migrate.[61] Paracellular transmigration occurs when a leukocyte passes through the junctions between endothelial cells.[47] This step in diapedisis is controlled by homophilic and heterophilic binding between various receptors on leukocytes and in endothelial junctions.[47]

At interjunctional spaces during paracellular migration, ring clustering of ICAM-1 and LFA-1 around migrating leukocytes inhibits the function of VE-cadherin, which contacts the actin skeleton,[45] resulting in an increase in the permeability of the endothelial monolayer.[46,47] Platelet endothelial cell adhesion molecule (PECAM) is a member of the

immunoglobulin superfamily and when ligated can induce increased binding of integrins to VCAM-1.[56] PECAM is continually recruited to endothelial cell junctions by constant recycling within the lateral border recycling compartment (LBRC).[62] At junctional borders, kinesin family molecular motors play a crucial role in the recycling of LBRCs, which surround migrating leukocytes and are required for diapedesis of these transmigrating cells.[62,63] Blocking the motor domain of kinesins results in the inhibition of transendothelial migration of neutrophils and monocytes.[62] Interjunctional adhesion molecule CD99 is a homophilic receptor located on leukocytes and the lateral borders of endothelial cells.[61] It is required for the migration of neutrophils,[64] monocytes,[65] and T cells[66] and acts on these leukocytes during paracellular migration downstream of PECAM.[61] Endothelial cell-selective adhesion molecule (ESAM) is also present at endothelial junctions and believed to mediate migration of neutrophils and maintain contacts between endothelial cells.[67]

G. Leukocytes of the Immune Response

1. T Lymphocytes

T lymphocytes are derived from lymphoid progenitor cells in the bone marrow and mature in the thymus.[68] Each cell develops a T cell receptor that is specific for a single antigen, which is acquired through gene rearrangement during development.[68] In humans, the population of naïve T cells (T cells that have never encountered antigen) can be as large as 100 million, each with unique antigen specificity.[69] T cells migrate to secondary lymphoid organs where they can encounter antigen being presented by dendritic cells on the major histocompatibility complex (MHC) for peptide antigens or CD1 for lipid antigens.[69] Recognition of antigen results in the clonal expansion of the antigen-specific T cell. This T

cell population differentiates and develops a range of effector functions such as cytotoxicity and cytokine secretion.[68] These cells then travel to sites of infection where they can influence the progression of the immune response.[69]

There are two types of T cells, which are defined by their co-receptor. These co-receptors restrict which type of MHC the T cell can recognize. $CD4^+$ T cells only interact with MHC class II molecules, while $CD8^+$ T cells only bind to MHC class I molecules.[68] $CD4^+$ T cells are integral components of the cellular and humoral immune response and can be further divided into two sets, T helper (Th) 1 and Th2, depending on their cytokine secretion profile.[68] Th1 cells are major producers of the pro-inflammatory cytokine interferon-γ (IFNγ) and induce an inflammatory response that is macrophage-mediated. Th2 cells, however, produce IL-4 and IL-5 and foster functionality of mast cells and eosinophils.[70] $CD8^+$ T cells are cytotoxic and are capable of killing cells infected with pathogens.[68]

When $CD4^+$ T lymphocytes are activated, cytokines and interactions between the T cell and antigen-presenting cell determine their developmental fate.[71] Differentiation of Th1 cells is influenced by IL-12 and the engagement of LFA-1 between antigen-presenting cells and T cells.[71,72] Newly activated dendritic cells stimulate the Th1 response.[71] Th1 cells secrete IL-2, IFNγ, and TNFβ and express on their surface CCR5 and CXCR3, which are receptors for inflammatory chemokines. In addition, Th1 cells upregulate ligands for P- and E-selectin on their surface.[69] Overall, Th1 cells mediate the activation of macrophages and $CD8^+$ cytotoxic T cells.[71] Development of Th2 cells is induced by IL-4 and IL-13 and signaling through the co-receptor CD28.[71,72] Exhausted dendritic cells, which are unresponsive to additional stimuli, typically induce the Th2 response.[71] Th2 cells promote the

humoral response by fostering the maturation of B cells and the degranulation of mast cells. The chemokine receptor CCR3 is present on Th2 lymphocytes, along with eosinophils, basophils, and mast cells.[69] Th2 cells also express CXCR5 and CCR4, which are receptors for chemokines that are produced in B cell follicles.[69]

Memory T cells develop as a sub-population of activated T cells that stop clonally expanding and return to a quiescent state.[68] Memory T cells are divided into two populations depending on expression or absence of CCR7. $CCR7^+$ T cells express L-selectin and migrate to lymph nodes and inflamed tissues. $CCR7^+$ T cells also differentiate into $CCR7^-$ memory T cells. $CCR7^-$ T cells do not express L-selectin and typically migrate to non-lymphoid tissues. Both types of T cells provide immunologic memory in their respective tissues.[69]

2. Neutrophils

Neutrophils are the most numerous leukocytes in humans and are the first to respond to an injury. They are categorized as a type of polymorphonuclear granulocyte, a designation that also includes eosinophils and basophils. Neutrophils migrate rapidly to an area of inflammation, where they phagocytose and degrade foreign molecules and bacteria.[73,74] The latter are killed through the production of reactive oxygen species and secretion of microbicidal agents.[75] Granulocyte colony-stimulating factor is responsible for granulopoiesis within the bone marrow, and, in response to inflammatory signals, neutrophils are released from the marrow and join the circulating population.[74] Chemokines such as CXCL1 and CXCL2 are able to mediate this process.[76]

Neutrophils have a variety of means to eliminate microorganisms. Activated neutrophils engulf bacteria, which triggers assembly of NADPH oxidase, a complex

membrane-bound enzyme that produces superoxide anions and hydrogen peroxide through the conversion of oxygen. In addition, the enzymes myeloperoxidase and nitric oxide synthase generate hypochlorous acid and nitric oxide, respectively.[77,78] Neutrophils also contain four types of granules, azurophilic, specific, gelatinase, and secretory, that contain a variety of cytotoxic molecules that can exocytose to eliminate an insult.[73] Inhibition of the apoptosis and clearance of neutrophils can result in the development of chronic inflammatory disorders. The agents produced by neutrophils are non-specific, and if not properly controlled, they can kill normal cells and destroy connective tissue at sites of inflammation.[79]

3. Natural Killer Cells

NK cells, like neutrophils, are recruited to tissues during early stages of infection.[80] They possess CX3CR1 and migrate towards CX3CL1 (fractalkine) and CXCL8.[81] NK cells are 5 to 15% of the total leukocyte population in the blood. NK cell precursors are located in the bone marrow and thymus. There, they mature before entering the periphery.[82] NK cell cytotoxicity and IFNγ production peaks within the first several hours to days of an infection. They are capable of discerning between virally infected cells and normal cells based on the interaction of MHC I on the target cells and inhibitory receptors on the NK cell.[80] Pathogens elicit production of IL-12 from phagocytic cells, which induces NK cells to synthesize IFNγ, IFNα, and IFNβ and activates their antiviral processes.[82,83]

During early stages of inflammation, NK cells react more swiftly than T cells, which supports the development of the Th1 immune response before Th1 cells arrive.[82] NK cells can modulate the inflammatory response by secreting IFNγ, TNFα, granulocyte/macrophage colony stimulating factor (GM-CSF), CXCL8, CCL3, CCL4, and CCL5.[81,83,84] NK cells can

also take on different effector roles through direct cell-cell interactions. The effector role is most evident in contacts with dendritic cells, where NK cells are induced to secrete IFNγ and enhance their cytotoxicity. In turn, NK cells can prime dendritic cells to foster $CD8^+$ T cell memory responses.[80]

In addition to cytokines and cell-cell interactions, engagement of receptors on the surface of NK cells can lead to activation. Toll-like receptors on NK cells induce cytotoxicity in response to various microbial or viral agents.[80] NK cell CD16 is a receptor for the Fc portion of IgG and can trigger antibody-dependent cellular cytotoxicity and the generation of IFNγ.[82,83] The binding of this receptor can initiate the lysis of infected cells in two ways. Perforin-mediated killing is due to pore formation in the membrane of the target cell, which disrupts osmotic pressure, leading to lysis. Additionally, Fc receptor-promoted Fas ligand expression induces apoptosis in the target cells.[81,85,86]

4. Monocytes

Monocytes are myeloid cells that originate from hematopoietic stem cells in the bone marrow.[87] They comprise 5 to 10% of the total population of peripheral blood leukocytes in humans.[88] They are a heterogeneous population that can vary in size, granularity, and nuclear morphology.[88] During homeostatic conditions, they circulate through the peripheral blood for several days before entering tissues and differentiating into tissue macrophages to maintain a steady population of the latter.[88,89] They, like macrophages, also help maintain equilibrium by eliminating apoptotic cells and scavenging for toxic compounds.[87]

During infection, monocytes can act as antigen-presenting cells, albeit not as efficiently as macrophages and dendritic cells.[90] Monocytes possess pattern recognition

receptors that are able to bind molecular determinants that are conserved among pathogens.[88] Depending on the activating agent, monocytes can act as effector cells by secreting prostaglandins, cytokines such as TNFα, IL-1β, IL-6, and IL-10, and chemokines such as CCL2 and CXCL8.[87] Monocytes act directly in host defense by generating reactive nitrogen and oxygen intermediates, while also lysing bacteria with phagolysosomal enzymes.[91]

In addition, monocytes provide a link between the innate and adaptive immune responses due to their ability to act as progenitor cells for other leukocytic sub-types.[87] The inflammatory response promotes their migration into tissues and differentiation into subsets of macrophages and dendritic cells based on the inflammatory mediators in the lesion.[89,90] During resolution of inflammation, monocytes aid macrophages in tissue repair and remodeling.[92]

Multiple species of monocytes exist in humans and mice. In humans, three sub-types of monocytes have been classified due to their expression of CD14 and CD16: $CD14^+$ $CD16^-$, $CD14^+$ $CD16^+$, and $CD14^{dim}CD16^+$.[87] The $CD14^+$ $CD16^-$ monocytes make up 80% to 90% of the monocytes found in the blood. On their surface, they express high levels of CCR2 and low levels of CX3CR1, and they often secrete IL-10 in response to LPS.[87] In contrast, the pro-inflammatory $CD14^+$ $CD16^+$ monocytes comprise only 10% of the monocytic population and are the major secretor of TNFα.[93] However, they are found in significant numbers in patients with inflammatory disease.[94] The function of $CD14^{dim}CD16^+$ monocytes is still being investigated.[87]

In mice, monocytes can be distinguished from other leukocytes by CD115. The majority of monocytes express the surface marker $Gr1^+$ and high levels of CCR2 and are relatively deficient in CX3CR1.[87] These monocytes are phenotypically similar to human

$CD14^+$ monocytes.[90] However, murine $Gr1^+$ $CCR2^{high}$ $CX3CR1^{low}$ monocytes are recruited to inflammatory lesions and produce high levels of TNFα and IL-1 during infection or tissue damage, such as early after myocardial infarct.[87,95] $Gr1^-$ $CCR2^{low}$ $CXCR1^{high}$ monocytes are smaller in size and play a role in monitoring for pathogens along the luminal side of the vascular endothelium.[87]

5. Macrophages

Tissue macrophages are derived from monocytes that leave the circulation. They then become resident phagocytes in lymphoid and nonlymphoid tissues. In addition to maintaining homeostasis, like monocytes, macrophages are major secretors of growth factors and cytokines when activated.[88] Macrophages are a heterogeneous population that exhibits a great deal of plasticity. They are able to specialize in function depending on the local signals that recruited them to the inflamed region and the subset of macrophage into which they have differentiated.[88,89]

In humans, macrophages are considered classically activated (M1) when stimulated by IFNγ or LPS and show high microbicidal activity by producing reactive oxygen species to eliminate pathogens and restricting iron and nutrients needed for bacterial replication.[88,96] On their surface, M1 macrophages present antigen to other leukocytes through their expression of MHC II. They are also responsible for secreting the pro-inflammatory cytokines TNFα, IL-1β, IL-12, and IL-18 and the chemokines CCL15, CCL20, CXCL8, CXCL9, CXCL10, CXCL11, and CXCL13. Alternatively activated (M2) macrophages are induced by IL-4, IL-10, and IL-13. These cytokines promote a phenotype that fosters tissue repair through the secretion of fibronectin, matrix metalloproteinases, and TGFβ.[88,96]

Myeloid-derived suppressor cells (MDSC) are an immature population of myeloid cells, typically found during infection and in tumors, that can suppress the immune response. In mice, they are characterized by their expression of Gr1 (Ly6C or Ly6G). They can be further divided into monocyte-like suppressor cells, which generate nitric oxide, and neutrophil-like suppressor cells, which produce reactive oxygen species. MDSC exhibit properties of both of M1 and M2 macrophages. Similar to alternatively activated macrophages, formation of MDSC is promoted by IL-4 and IL-13. However, IFNγ is required for their expression of nitric oxide and reactive oxygen species. If the host response to an infection develops towards adaptive immunity, a shift in the ratio of M1 macrophages, M2 macrophages, and MDSC is observed in lesions of inflammation. A macrophage is able to differentiate into the different subtypes based on the chemical mediators in the region.[96]

6. Dendritic Cells

Dendritic cells are short-lived cells that are major antigen-presenting cells and make up 1% of peripheral blood mononuclear cells in humans.[87] Specific subtypes of dendritic cells were once thought to develop from myeloid-restricted or lymphoid-restricted precursors, leading to heterogeneity within the dendritic cell population. However, each precursor is able to produce all of the mature splenic and thymic dendritic cell subtypes. In addition, the functionality of dendritic cell populations is not predetermined at this developmental stage.[70] Monocytes are also the progenitors of different subtypes of dendritic cells, such as Langerhans cells in the skin and dendritic cells found in gastrointestinal and respiratory tracts.[92] Dendritic cells phagocytose particles from the environment and process them for presentation on MHC complexes to T cells. Activated dendritic cells also secrete

cytokines that further regulate development of T cells.[90] During inflammation caused by infection, Ly6C^{high} monocytes that differentiate into monocyte-derived dendritic cells are essential for the initiation of the innate and adaptive immune responses.[92] They promote Th1 cell responses, prime antigen-specific CD8^{+} T cells, and add to the inflammatory environment by secreting TNFα and nitric oxide during viral, bacterial, and parasitic infections.[89,92] These dendritic cells are considered a subset different from those that monitor the environment at sites of antigen capture and in lymphoid organs during homeostatic conditions.[89]

H. IFNγ

IFNγ is a Type II interferon that forms homodimers with itself.[97] IFNγ forms a symmetrical complex with two of its receptor chains, IFNγR1 and IFNγR2. The binding of IFNγ in turn activates Jak1, Jak2, and Stat1, which induce the expression of genes containing the γ-activation sequence in the promoter. In addition, IFNγ can also initiate effector pathways involving phosphatidylinositol-30-OH kinase, serine/threonine kinase, and nuclear factor (NF)-κB.[97] Negative regulators, such as IL-4, IL-10, TGFβ, suppressors of cytokine signaling, and protein inhibitors of activated Stats down-regulate the signaling functions of IFNγ.[97,98] IFNγ plays a major role in immunity to bacteria, fungi, parasites, and some viruses.[99] IFNγ-deficiency disorders result in a predisposition to mycobacterial disease. [99]

IFNγ is a major cytokine secreted by Th1 cells. IFNγ influences the activation of many genes involved in the innate immune response by inducing genes of transcription factors.[98,99] This signaling can happen within 30 minutes of stimulation.[98] IFNγ promotes activation of macrophages,[100] effector functions of NK cells, and T cell activation and

cytotoxicity typical of the cellular immune response.[101] IFNγ is primarily secreted by NK cells, NK T cells, and T lymphocytes, but dendritic cells and macrophages can produce it under certain conditions.[99]

IFNγ fosters the generation of IL-12 by phagocytic cells and inhibits their production of IL-4. IL-12 secreted by macrophages in response to bacterial agents and IFNγ results in a positive feedback loop, which further increases the production of IL-12. This IL-12 can further enhance the secretion of IFNγ from other leukocytes, such as NK cells.[98] Macrophages stimulated by IFNγ increase their pinocytosis and phagocytosis. In addition, there is an increase in their ability to kill invading microorganisms through the NADPH oxidase system and production of nitric oxide.[98]

IFNγ is important in the activation and differentiation of T cells in the cellular immune response. IFNγ augments the efficiency of the MHC class II antigen-presenting pathway, which promotes the activation of $CD4^+$ T cells.[98] IFNγ also shifts differentiation of naïve $CD4^+$ T cells toward a Th1 phenotype. This shift towards the Th1 response influences the secretion of cytokines and chemokines in the area. IFNγ also promotes the migration of circulating leukocytes to sites of infection by up-regulating the expression of adhesion molecules and chemokines by both endothelium and leukocytes.[101]

IFNγ is an important mediator in host defense. However, IFNγ can contribute to the development of inflammatory diseases. The progression of pathology in systemic lupus erythematosus, multiple sclerosis, and insulin-dependent diabetes mellitus has been linked to production of IFNγ.[102] IFNγ can also promote tissue damage as observed in cardiovascular disease. Reactive oxygen species within the heart are chronically produced due to the high levels of IFNγ, which contributes to atherogenesis.[103]

III. Lyme Disease

A. *Borrelia burgdorferi*

Borrelia burgdorferi is a helical bacterium, which can range between 20 to 30 μm in length and 0.2 to 0.5 μm in width. Unlike that of most Gram-negative bacteria, the outer membrane of *B. burgdorferi* contains no LPS. Instead, it expresses on its surface an array of lipoproteins that aids the bacterium in various ways throughout the life cycle.[104] This motile bacterium also produces 7 to 11 flagella, which anchor in the cell membrane and protrude into the periplasm, propelling it to move in a corkscrew manner.[105] Genetically, *B. burgdorferi* contains a small, linear 950-kb chromosome with greater than 20 plasmids, on which many of its proteins are encoded. These range in size from 5 to 56 kb.[106] The *B. burgdorferi* genome contains the most individual plasmids of any known bacteria.[104] It has an estimated 150 lipoprotein genes,[107] and redundancy is extremely common.[104]

B. burgdorferi expresses six essential outer surface lipoproteins (Osps), named A through F.[104,106] These surface lipoproteins are variably expressed in response to changes in the local environment, such as temperature, pH, and nutrient and cell density.[106] OspC is not expressed while the bacteria are in the gut of the unfed tick. During the blood meal, shifting temperature and pH within the feeding tick upregulate transcription of OspC. The increased expression aids in the migration of the bacteria from the midgut to the tick's salivary glands and into the host. The lipoprotein OspA, which enables the bacterium to adhere to the inner wall of the tick gut, is modulated by these factors in a reverse manner; it is upregulated in the tick, and downregulated during feeding.[104,106,108,109]

B. Immune Evasion by *B. burgdorferi*

B. burgdorferi uses many molecular and genetic strategies to evade the host immune system, resulting in an increased inflammatory response from the host. *B. burgdorferi* inactivates the alternative complement pathway by commandeering inhibitors that destabilize complement factors. Complement regulator-acquiring surface proteins, called CRASPs, are lipoproteins expressed on the surface of the bacterium that directly bind these complement regulators. By binding the C-terminal ends of the regulators of complement, Factor H and FHL-1, CRASPs align these inhibitors so that they retain their complement inhibiting function on the membrane of the spirochete.[110-112] The surface lipoprotein OspE also functions like a CRASP by binding Factor H.[113]

B. burgdorferi also uses other proteins to avoid detection by the host immune response. The VlsE plasmid is required by *B. burgdorferi* to maintain infection within the host. During feeding, the bacterium recombines the VlsE expression sequence by the insertion of neighboring cassettes. This results in variation of the VlsE protein and enables individual spirochetes to express unique proteins, leading to antigenic variation within the population.[114,115] *B. burgdorferi* possesses two outer membrane proteins, P66 and *Borrelia* glycosaminoglycan-binding protein, that act as spirochetal adhesins. These proteins mediate the binding of the spirochete to decorin and fibronectin, which are major components of the host extracellular matrix. The binding of decorin and fibronectin could enable the bacterium to establish itself in joints and connective tissues to prevent clearance, thereby contributing to chronic inflammation.[116]

C. Pathology of Lyme Disease

Once *B. burgdorferi* enters a mammalian host, the immune response consists of a series of stages with different cytokines and leukocytic types present.[3,117] This infection can lead to Lyme disease, which in humans, is a multisystemic illness that affects the cardiovascular, neural, reticuloendothelial, and gastrointestinal systems, with varying degrees of tissue functional complications and damage.[1,3,117] The initial reaction to the bacterium in the skin of a human is an infiltrate comprising neutrophils, macrophages, eosinophils, and some mast and B cells. This infiltrate induces a rash called erythema migrans at the site of the tick bite.[2,5] *B. burgdorferi* may disseminate from the skin through the extracellular matrix and into the bloodstream where it can travel to new regions in the body, including joints, lymph nodes, spleen, bone marrow, and liver. After a period of several weeks, the acute response subsides, and myocarditis and sub-acute arthritis can develop. Perturbations of the function of the nervous system can also occur at this stage.[2,5,117]

In 60% of untreated patients, recurring arthritis develops.[118] Within the joint of patients, there is a nonspecific, hypertrophic synovitis with varying degrees of fibrosis and proliferation of blood vessels, as is observed in other chronic inflammatory diseases.[2,5,117] In the proliferating synovial tissue of infected joints, there is an accumulation of macrophages, T lymphocytes, plasma cells, and mast cells.[5] Neutrophils, on the other hand, are rarely seen in the synovial tissue.[2,5] In the synovial fluid, neutrophils are present during the chronic states. However, Th1 cells comprise the majority of lymphocytes observed.[119] These cells are responsible for the production of IFNγ and other pro-inflammatory cytokines, and their presence correlates with severity of Lyme arthritis.[119] Elevated levels of TNFα, IL-1β,

CXCL9, and CXCL10 are also present in the synovial fluid of patients with Lyme arthritis and can persist even after treatment.[120]

Susceptible strains of mice infected with *B. burgdorferi* exhibit signs of arthritis within 10 days,[121] which peaks in severity between 14 and 28 days.[122,123] In infected mice, arthritic lesions are intensely populated by neutrophils, with exudation of the leukocytes and fibrin into the lumina. Neutrophils are also present in the synovial space.[121,124] At sites of ligament and tendon attachments, there is increased fibroblastic proliferation.[121] In addition, the synovial lining of these joints begins to swell due to the proliferation of synovial cells that line the joint space.[121] Within arthritic joints, the concentrations of CXCL1 and CCL2 positively correlate with severity of arthritis.[125] Murine Lyme arthritis typically resolves after 90 days post-infection, but residual fibrosis and macrophages are still observed in the synovial space of some mice.[124]

In human Lyme carditis, cardiac lesions consist mostly of infiltrating mononuclear leukocytes and some neutrophils in the base of the heart and large vessels such as the aorta. During early stages of infection, neutrophils are detected along the endothelium of the aorta, in addition to mixed leukocytic populations migrating into vascular walls. As disease progresses, the majority of leukocytes present are mononuclear and are located in the root of the aorta, epicardium, endocardium, and periaortic adventitia.[121,124] Human Lyme carditis can lead to varying degrees of atrioventricular heart block and arrhythmia.[126] In mice, lesions of Lyme carditis contain mostly mononuclear leukocytes,[123] primarily macrophages.[127] Lymphocytes are also observed, but few neutrophils are noted. Lymphocytes, plasma cells, and monocytes/macrophages migrate into the layers of myocardium.[122,127,128] Additionally,

levels of IFNγ, TNFα, and IL-1β remain elevated during murine carditis from 7 to 42 days post-infection.[129]

The nervous system can be affected over the course of Lyme disease. Lyme neuroborreliosis can lead to cranial neuropathy, radiculopathy, meningitis, and inflammatory myopathy.[130] Inflammation consisting of lymphocytes and plasma cells results along the perineurium but is not restricted to a singular neural structure.[2] Leukocytes can be observed at the autonomic root and ganglia with an increase in the number of macrophages present. In addition to symptoms such as malaise and headache, bilateral Bell's palsy manifests in some patients.[5]

D. Effects of *B. burgdorferi* on Endothelium

In a human microvascular endothelial cell line, expression of mRNA encoding CCL2, CCL5, CXCL1, CXCL8, CXCL9, and CXCL10 is upregulated by *B. burgdorferi*. Additionally, transcripts of the adhesion molecules E-selectin, ICAM-1, and VCAM-1 are induced.[131] Surface expression of these adhesion molecules is also increased by incubation of primary human umbilical vein endothelial cells (HUVEC) with *B. burgdorferi*.[132] The lipidated surface proteins of *B. burgdoferi* are responsible for the increase in the expression of adhesion molecules.[133] Spirochetes also stimulate endothelium to release CXCL8[134] and CCL2.[135]

An *in vitro* model of the blood vessel wall, consisting of monolayers of HUVEC grown on acellular amniotic connective tissue,[136] has been used to demonstrate that *B. burgdorferi* acts on endothelium to promote the transmigration of neutrophils,[132,134] T lymphocytes,[137] and monocytes.[135] Upon further examination of the migrating T cell

population, transmigration assays revealed that transitional T cells preferentially migrate, as opposed to naïve or memory T cells. Phenotypically, populations of T cells migrating across endothelium activated by *B. burgdorferi* are also enriched for those that express the CD8 receptor.[137] Additionally, the populations of $CD4^+$ and $CD8^+$ T cells that traverse HUVEC stimulated with *B. burgdorferi* are enriched for those that produce IFNγ.[138]

E. Role of Leukocytes in Lyme Disease

1. Neutrophils

Neutrophils are present during the early stages of Lyme disease[2,5] and are necessary for the progression of arthritis in other inflammatory diseases such as collagen-induced arthritis[139] and adjuvant-induced arthritis.[140] Neutrophils are capable of killing *B. burgdorferi* with their phagocytic properties and antimicrobial agents.[141] In murine Lyme arthritis, neutrophils are the predominant cell type present during the acute phase,[123] and the production of the neutrophil attractant CXCL1 positively correlates with severity of arthritis.[125] In mice lacking CXCR2, the receptor for CXCL1, neutrophils remain confined within blood vessels and do not infiltrate the synovium.[125] In the absence of CXCL1, severity of murine Lyme arthritis and carditis is decreased, and there are fewer neutrophils present.[142] While neutrophils are implicated to control the colonization of *B. burgdorferi*,[143] the decreased presence of neutrophils does not alter spirochetal loads in mice.[142]

2. T lymphocytes

A predominance of pro-inflammatory Th1 cells is observed in patients with Lyme arthritis, and the severity of arthritis positively correlates with the ratio of Th1 to Th2 cells in

the synovial fluid.[119] T lymphocytes isolated from patients with chronic Lyme arthritis, which have clonally expanded due to *Borrelia* antigen, generate IL-2, TNFα, IFNγ, and GM-CSF[144,145] but not IL-4 and IL-5.[145] In agreement, isolated mononuclear cells from synovial fluid of patients with Lyme arthritis also demonstrate a Th1 response by producing high amounts of IFNγ and TNFα, with little IL-4, when stimulated with *Borrelia* antigen.[146] Expression of CXCR3 and CCR5 on the surface of T lymphocytes correlates with the Th1 response, and one or both of these receptors are present on 80% of T cells found in skin lesions of Lyme disease. [147]

With respect to mice, the incubation of murine synovial cells with sonicated *B. burgdorferi* induces the transcripts for chemokines and other IFN-inducible genes. This response is augmented by the presence of T lymphocytes.[148] In *Borrelia*-infected mice, the ratio of Th1 to Th2 cells also correlates with greater severity of arthritis. In these mice, $CD8^+$ T lymphocytes produce the majority of IFNγ.[149] Moreover, neutralization of IL-4 results in more severe Lyme arthritis, whereas neutralization of IFNγ reduces its severity.[150] T lymphocytes also play a role in resolution of infections with *B. burgdorferi*. Mice depleted in subsets of T cells revealed that $CD4^+$ T cells are needed to control infection, because the severity of arthritis and spirochetal load increase in joints of these animals.[151] These data suggest that Th1 cells, which secrete IFNγ, have a crucial role in the pathology of Lyme disease and potentially contribute to chronic Lyme disease.[150]

3. Monocyte/Macrophages

Macrophages are present in lesions of Lyme disease in both humans[5] and mice[121] and are activated by *B. burgdorferi* to secrete TNFα in a dose-dependent manner.[152] Significant

elevation of TNFα is found in the sera and synovial fluids of patients.[152] Macrophages phagocytose spirochetes and degrade the majority that are engulfed, but on rare occasions the engulfed bacterium may remain alive after 24 h.[153] Monocyte/macrophages are activated by the uptake of spirochetes and upregulate IFN-stimulated genes.[154] In addition, macrophages are activated by spirochetal antigens.[155,156] Monocyte/macrophages are also a primary source of pro-inflammatory cytokines in Lyme disease.[157] Macrophages are the most abundant cell type within murine Lyme carditis, and their presence appears to be driven by the production of CCL2 in inflammatory regions.[122] In the absence of CCR2, the receptor for CCL2, macrophages comprise the majority of the cellular infiltrate, but the population of neutrophils increases.[128] During the resolution of inflammation associated with Lyme disease, macrophages are quite prevalent.[123]

F. Role of IFNγ in Lyme Disease

IFNγ appears to play a role in the development of chronic Lyme disease in humans by promoting the cellular infiltrates and cytokine profile necessary for chronic inflammation. Serum levels of IFNγ correlate positively with severity of disease in individuals infected with *B. burgdorferi*.[147] In some instances, the levels of IFNγ in synovial fluid remain higher even after the infection is cleared.[120] IFNγ is also detected at elevated levels in blister fluids collected from the skin lesions of infected patients.[147]

In vitro data show that *B. burgdorferi* and IFNγ cooperate to enhance the migration of T cells across HUVEC-amnion cultures, while IFNγ diminishes migration of neutrophils across spirochete-activated endothelium. Microarray analysis demonstrates that *B. burgdorferi* and IFN*γ* synergistically upregulate transcription of various chemoattractants

involved with inflammation in endothelial cells. Seven of the thirty-three genes synergistically upregulated by concurrent incubation of HUVEC with IFNγ and *B. burgdorferi* encode chemokines. Six are attractants for mononuclear leukocytes (CCL7, CCL8, CX3CL1, CXCL9, CXCL10, and CXCL11); only one (CXCL2) is specific for neutrophils. Also, the six chemokines specific for mononuclear leukocytes are not induced when endothelium is stimulated with *B. burgdorferi* alone.[158] These *in vitro* observations suggest that IFNγ may influence recruitment of leukocytes to tissues infected with *B. burgdorferi*.

Investigations into the role of IFNγ using the murine model of Lyme disease have generated differing results. The blockade of IFNγ with antibodies reduces joint swelling in mice.[150,159] Additionally, neutralization of IL-4, which opposes the function of IFNγ by promoting the humoral immune response, exacerbates arthritis.[159] Splenocytes extracted from *B. burgdorferi*-infected mice produce increased levels of IFNγ.[159] From these data, it appears that IFNγ contributes to the progression of inflammation in Lyme disease. However, IFNγ-deficient and IFNγ receptor-deficient mice develop the same severity of Lyme arthritis as wild-type animals, which suggests that IFNγ is not required for progression of disease.[160,161]

The role of IFNγ in murine Lyme carditis has been investigated through indirect means using Stat1-deficient mice, which have defects in signaling pathways induced by IFNα, IFNβ, and IFNγ. IFNγ could play a protective in murine Lyme carditis, because there is an increase in the extent of carditis but not arthritis at 21 days post-infection in the Stat1-/- animals.[162] In contrast, mice deficient in IL-4, which produce abnormally high levels of IFNγ, develop more severe carditis after infection with *B. burgdorferi*, implying that IFNγ may exacerbate carditis.[163] Using IFNγ receptor-deficient mice, one study examined the role

of IFNγ directly. In these mice, the loss of the receptor produced a slight increase in severity of Lyme carditis at 14 days after infection.[164]

Aims of the Research

B. burgdorferi is the causative agent of Lyme disease, a multisystemic illness that can affect the cardiovascular system, peripheral nervous system, and joints, resulting in various levels of tissue damage. Over time, humans may develop a chronic phase of the disease, where the destructive inflammation becomes self-sustaining even after apparent eradication of infection. The pro-inflammatory cytokine IFNγ is an active mediator in the development of inflammation. Therefore, the potential role of IFNγ in the pathogenesis of Lyme disease was examined.

Our laboratory previously demonstrated that IFNγ alters the phenotype of endothelium exposed to *B. burgdorferi*. Incubation of HUVEC with IFNγ and *B. burgdorferi* synergistically increases the expression and secretion of seven chemokines. All but one of these chemokines attract T cells and monocytes. Stimulation of HUVEC-amnion cultures by both IFNγ and *B. burgdorferi* also increases transendothelial migration of T cells as compared to stimulation with either agent alone. In contrast, the migration of neutrophils across *B. burgdorferi*-activated HUVEC is decreased when IFNγ is added.[158] Given that T lymphocytes and monocytes typify chronic inflammation, whereas neutrophils and NK cells characteristically present in acute inflammatory lesions, these *in vitro* observations are consistent with the hypothesis that IFNγ mediates a switch from acute to chronic inflammation in human Lyme disease.

To investigate further the contribution of IFNγ to the development of chronic Lyme disease, its effects on the transendothelial migration of monocytes and NK cells were investigated *in vitro*. In addition, this dissertation research sought to elucidate the mechanisms by which IFNγ alters migration of leukocytes across spirochete-activated

endothelium by examining expression of adhesion molecules and whether a soluble factor was responsible. The ability of IFNγ to alter the expression of genes in human and murine macrophages exposed to *B. burgdorferi* was determined through the use of microarray analysis, real-time RT-PCR, and immunoassays. Lastly, the role of IFNγ in the development of murine Lyme carditis was assessed. Severity of murine Lyme carditis and the accumulation of specific subsets of leukocytes in the hearts of infected wild-type and IFNγ-deficient mice were compared using histology and immunofluorescent microscopy. Collectively, the results of this dissertation work support the conclusion that IFNγ promotes the development of chronic inflammation in Lyme disease.

Materials and Methods

I. Culture of *B. burgdorferi* for *In Vitro* Studies

B. burgdorferi strain HBD1[1] at passages 44-49 was cultured at 33°C in low-endotoxin Barbour-Stoenner-Kelly-H (BSK) medium[132] that contained 5% EX-CYTE Growth Enhancement Media Supplement (Millipore, Billerica, MA). Three to five days after passage, spirochetes were centrifuged at 5,000 × *g* for 20 min and resuspended in the appropriate experimental medium. Spirochetes were counted using dark-field microscopy and added to macrophages at a ratio of 10 spirochetes (sp) per cell.

II. Isolation of Human Monocytes and NK Cells

Human monocytes or NK cells were isolated from venous blood of healthy donors with informed consent as described previously.[158] Blood was collected in a syringe containing 0.12% EDTA and mixed with an equal volume of phosphate-buffered saline lacking Mg^{2+} and Ca^{2+} (PBS-). Peripheral blood mononuclear cells (PBMC) were obtained using Accu-Prep Lymphocytes density-gradient medium (Accurate Chemical & Scientific Corp., Westbury, NY). Monocytes or NK cells were then isolated from PBMCs through negative selection using the Monocyte Isolation Kit II or NK Cell Isolation Kit (Miltenyi Biotec Inc., Auburn, CA), respectively, according to the protocol of the manufacturer.[158] Flow cytometry was used to measure purity of the isolated cells using antibodies to detect CD14 (BD Biosciences, San Jose, CA) for monocytes or CD56 (BD Biosciences) for NK cells. Purity of these populations was consistently 90% or greater for monocytes and 96% or greater for NK cells.

III. Transendothelial Migration Assay

HUVEC were harvested with 0.35 mg/ml type II collagenase (Worthington Biochemical Corp., Lakewood, NJ) as previously described[136] and cultured in 60-mm dishes in Medium 199 (M199; Thermo Fisher Scientific, Waltham, MA) containing penicillin (100 U/ml), streptomycin (100 μg/ml), amphotericin B (2 μg/ml), and 20% fetal bovine serum (FBS; Thermo Fisher Scientific) for up to 5 days.

HUVEC were passaged onto acellular amniotic connective tissue attached to Teflon rings as described.[165] After 7 to 10 days, when transendothelial electrical resistances are maximal,[136] HUVEC-amnion cultures were washed and incubated with M199 plus 20% heat-inactivated FBS, *B. burgdorferi* (10 sp/cell), human recombinant IFNγ (R&D Systems Inc., Minneapolis, MN) (10 ng/ml), or *B. burgdorferi* and IFNγ together for 24 h. Alternatively, some HUVEC-amnion cultures were stimulated with 0.1 ng/ml of TNFα (R&D Systems) or 10 ng/ml of IFNγ and 0.1 ng/ml TNFα concurrently. Cultures were washed, and leukocytes were added to the apical sides at a concentration of 8×10^5 in 0.5 ml of M199 with 20% heat-inactivated FBS (assay medium). Monocytes and NK cells were allowed to migrate for 20 min and 4 h, respectively, at 37°C. The HUVEC-amnion cultures then were fixed with 10% buffered formalin and stained with Wright stain (Sigma-Aldrich Co., St. Louis, MO) for 6 to 8 min. The number of associated leukocytes was tallied from nine randomly chosen 400× fields using a bright-field microscope. The Wright-stained cultures then were dehydrated in ethanol and embedded in glycol methacrylate (Polysciences, Inc., Warrington, PA). Sections cut perpendicularly to the plane of the endothelial monolayer were stained with toluidine blue and viewed by bright-field microscopy. The position with respect to the HUVEC monolayer (above and below) was determined for a minimum of 100 leukocytes. Correction

for any loss of leukocytes from the apical surface of the endothelium during the embedding process was performed as previously described.[166]

IV. Isolation of Human Neutrophils

Neutrophils were isolated from venous blood of healthy donors with informed consent. Blood was collected in a syringe containing 0.12% EDTA. For every 10 ml of blood, 1.0 ml of 6% dextran in 0.87% NaCl was added to a tube and mixed with the blood by inverting. The blood mixture was allowed to sediment for 45 min if the blood was from a female or 60 min if from a male. The leukocyte-rich plasma was removed and centrifuged, and the pellet was resuspended in phosphate-buffered saline (PBS) with 0.2% glucose. Neutrophils were isolated from the suspension by layering over Accu-Prep Lymphocytes (Accurate Chemical), centrifuging, removing the PBMC at the interface, and resuspending the pellet.[132]

V. Chemotaxis of Neutrophils

HUVEC were isolated as above and plated at a concentration of 2.4×10^5 cells/ml. Once confluent, they were incubated for 24 h with assay medium, *B. burgdorferi* (10 sp/cell), IFNγ (10 ng/ml), or *B. burgdorferi* (10 sp/cell) and IFNγ (10 ng/ml) concurrently. Conditioned media were removed and centrifuged at 8000 × *g* for 10 min. Aliquots of freshly-isolated neutrophils were incubated for 25 min in one of the conditioned media samples. A 48-well Boyden chamber apparatus (Neuro Probe, Inc., Gaithersburg, MD) was arranged so that 20 nM of CXCL8 (R&D Systems) or M199 plus 10% FBS was added as the chemoattractant or control, respectively, in the bottom portion of the chamber. A 5-μm

cellulose nitrate filter (Neuro Probe) was placed between the two halves of the Boyden chamber. Pre-treated neutrophils in a volume of 50 µl, at no more than 4×10^6 cells/ml, were loaded into the top chamber and allowed to migrate for 15 min at 37°C. The filter was fixed in 100% 2-propanol, stained with Harris-type hematoxylin, clarified with xylene, and mounted for analysis. The distance that neutrophils traveled into the filter was measured using the leading-front method via bright-field microscopy.[135]

VI. Transendothelial Migration Assay Using CXCL8 as an Attractant

HUVEC-amnion cultures were prepared as described above. The cultures were washed with M199 containing 10% FBS and placed upon silicone rubber supports as described.[134] As a positive and negative control, respectively, 0.5 ml of 20 nM CXCL8 in M199 + 10% FBS or M199 + 10% FBS alone was placed beneath the cultures. Human neutrophils were isolated as described above and incubated for 25 min in conditioned medium from HUVEC stimulated with assay medium or both *B. burgdorferi* (10 sp/cell) and IFNγ (10 ng/ml). Neutrophils (8×10^5 in 0.4 ml) then were placed above each HUVEC-amnion culture and allowed to migrate for 30 min. The HUVEC-amnion cultures were fixed using 10% buffered formalin at 4°C and stained with Wright stain for 6 to 8 min. The number of migrated neutrophils was tallied from nine 400× fields using a bright-field microscope.

VII. Immunofluorescent Staining of Cell-Surface Adhesion Molecules

HUVEC were cultured on amnion as described above. Once confluent, they were treated with assay medium, *B. burgdorferi* (10 sp/cell), IFNγ (10 ng/ml), or *B. burgdorferi* (10 sp/cell) and IFNγ (10 ng/ml) concurrently for 24 h. Cultures were fixed in 3%

paraformaldehyde for 20 min and washed 3 times in 0.05% saponin in PBS. HUVEC-amnion cultures were incubated with 5 μg/ml of mouse anti-human PECAM (eBiosciences, Inc., San Diego, CA), 5 μg/ml of mouse anti-human CD99 (eBiosciences), or 10 μg/ml of mouse anti-human ESAM (R&D Systems) overnight at 4°C; all of these are monoclonal antibodies (mAb). Samples were washed with 0.05% saponin in PBS and then incubated for 3 h with a 1:300 dilution of Cy3-conjugated donkey anti-mouse IgG (Jackson Immuno Research, West Grove, PA). Cultures were washed, stained with 4',6-diamidino-2-phenylindole (DAPI) at 1 μg/ml in PBS for 5 min, and mounted for analysis on a Axiovert 200M deconvolution microscope or an Axioplan2 fluorescent microscope (both from Carl Zeiss Inc., Thornwood, NY).

VIII. Measurement of Cell-Surface Adhesion Molecules by Whole-Cell Enzyme-Linked Immunosorbent Assay (ELISA)

HUVEC were isolated as described above and seeded on 96-well plates at 2.3×10^5 cells/ml in a volume of 100 μl. The cells then were treated with M199 + 20% heat-inactivated FBS only, *B. burgdorferi* (10 sp/cell), IFNγ (10 ng/ml), or *B. burgdorferi* and IFNγ together for 24 h at 37°C. For the ELISA assay, the HUVEC were incubated with 1 μg/ml of R6.5 mouse mAb to human ICAM-1, 4B9 mouse mAb to human VCAM-1 (both from Biogen, Inc., Weston, MA), or mouse mAb to human PECAM (eBiosciences) for 1 h. Cells were washed with M199 + 5% heat-inactivated FBS and incubated with biotinylated goat anti-mouse antibodies (Pierce Biotechnology, Inc., Rockford, IL) at a 1:4000 dilution for 1 h. Avidin-horseradish peroxidase (Pierce) was added to the wells for 1 h before washing

again. O-phenylenediamine dihydrochloride substrate (Thermo Fisher Scientific) was added to the cultures for colorimetric detection at 490 nm.

IX. Microarray Analysis of Murine and Human Macrophages

To isolate murine macrophages, C57BL/6 mice at 8 weeks of age were euthanized using CO_2. Femurs and tibia were removed, and marrow was collected by washing the inside of each bone with Dulbecco modified Eagle medium (DMEM) (Invitrogen, Carlsbad, CA) containing 5% FBS, 100 U/ml of penicillin, and 100 µg/ml of streptomycin. Cells were plated in bone marrow medium-high (BMM_{high}), which consisted of DMEM with 2 mM L-glutamine, 1 mM sodium pyruvate (Invitrogen), 20% heat-inactivated FBS, and 30% medium conditioned by L929 cells.[167] On the fifth day, macrophages were detached by rinsing with PBS- and plated in BMM_{low}, which was composed of DMEM with 1 mM sodium pyruvate, 2 mM L-glutamine, 10% heat-inactivated FBS, and 15% L929 cell-conditioned medium.[100,168] For each experimental group, 8×10^6 macrophages were plated in BMM_{low} for 24 h at 37°C. Macrophages then were incubated for 8 h at 37°C with BMM_{low} only, *B. burgdorferi* (10 sp/cell), IFNγ (10 ng/ml), or *B. burgdorferi* and IFNγ together before collection of RNA.

Human monocytes were isolated from venous blood of healthy donors as described above. The monocytes were seeded in RPMI 1640 medium (Thermo Fisher Scientific) containing 10% heat-inactivated FBS and 50 ng/ml of recombinant human macrophage colony-stimulating factor (R&D Systems) for five days prior to stimulation. For each condition, 9.6×10^6 cells were incubated for 8 h at 37°C with RPMI 1640 medium alone, *B. burgdorferi* (10 spirochetes/cell), IFNγ (10 ng/ml), or *B. burgdorferi* and IFNγ together.

For both murine and human macrophages, the stimuli were removed after 8 h, and RNAlater (Applied Biosystems, Carlsbad, CA) was added at 4°C overnight. RNA was isolated using an RNeasy Mini Kit (Qiagen Inc., Valencia, CA) according to the manufacturer's protocol and stored at -80°C. Quality and concentration of RNA samples were measured using an Agilent 2100 Bioanalyzer Automated Analysis System (Agilent Technologies, Inc., Santa Clara, CA). Microarray analysis was performed by the Stony Brook University DNA Microarray Core Facility using the Affymetrix Mouse Expression Array 430 2.0 or Affymetrix Human U33 Expression Array Plus 2.0. Data were analyzed by the Affy and Limma packages for the open-source BioConductor project (BioConductor.org) run in the R statistical environment.

X. Measurement of Expression of Chemokines by Murine and Human Macrophages

Murine macrophages were isolated as described above and incubated with BMM_{low} only, *B. burgdorferi* (10 spirochetes/cell), IFNγ (10 ng/ml), or *B. burgdorferi* and IFNγ together for 8 h at 37°C. The stimuli were removed, and RNAlater was added at 4°C overnight. RNA was isolated using an RNeasy Mini Kit (Qiagen) according to the manufacturer's protocol and stored at -80°C. RNA was converted into cDNA using a Verso cDNA Kit (Thermo Fisher Scientific) as specified by the manufacturer. Solaris qPCR primer and probe pairs for cytokines of interest were used in conjunction with Solaris qPCR Gene Expression Low ROX Master Mix (Thermo Fisher Scientific) on an ABI 7500 Real Time PCR System (Applied Biosystems) in 96-well Thermo-Fast detection plates (Thermo Fisher Scientific) according to the manufacturer's protocol in a total volume of 25 µl. The *Gapdh* transcript was used as an endogenous control for all samples. Efficiency of each primer and

probe set was analyzed and within acceptable limits for fold-change calculation using the $\Delta\Delta C_T$ method as calculated by ABI System SDS software. To measure expression of chemokines at the protein level, murine or human macrophages were stimulated as above for 24 h at 37°C. Conditioned media were removed and centrifuged at 8000 × *g* for 10 min. Supernatants were analyzed for content of selected chemokines using ELISA kits, all from R&D Systems except that for human CXCL2 (Immuno-Biological Laboratories, Inc., Minneapolis, MN).

XI. Infection of Mice

Wild-type C57BL/6 and B6.129S7-*Ifng*^{tm1Ts}/J (IFNγ-deficient) mice were received from The Jackson Laboratory (Bar Harbor, ME) at 8 weeks of age. All procedures involving mice were approved by Stony Brook University's Institutional Animal Care and Use Committee. Low-passage *B. burgdorferi* N40 was grown in BSK medium (Sigma-Aldrich) supplemented with 6% rabbit serum (Sigma-Aldrich) for 5 to 7 days at 33°C. Spirochetes were counted using dark-field microscopy, and mice were inoculated intradermally with 2.5 × 10^5 bacteria in 100 µl of BSK medium or with 100 µl of BSK medium alone as a control. To confirm infection, bladders were collected at the time of sacrifice, and each was cultured separately in a tube containing 7 ml of BSK medium.[124] After 7 days, cultures were examined for spirochetes using dark-field microscopy. Results verified the infection of all mice that had been inoculated with spirochetes.

XII. Evaluation of Severity of Carditis

Five infected and two uninfected wild-type or IFNγ-deficient mice were sacrificed using CO_2 at 14, 21, and 28 days after inoculation. Hearts were collected, perfused with PBS, and bisected sagittally. Hearts were fixed in 10% neutral buffered formalin for 24 h at room temperature (RT), embedded in paraffin, sectioned at a thickness of 5 μm, and stained with hematoxylin and eosin. Severity of carditis was graded by two independent observers who were unaware of the origin of each section. Severity of inflammation within these sections was measured using the following criteria: Grade 0, no inflammation; Grade 1, minimal inflammation with fewer than two small foci of inflammation; Grade 2, moderate inflammation with two or more foci; and Grade 3, severe inflammation with focal and diffuse infiltration covering a large area.[162]

XIII. Identification of Leukocytic Subtypes in Cardiac Lesions

Five infected and two uninfected wild-type or IFNγ-deficient mice were sacrificed using CO_2 at 14 and 25 days after inoculation. Hearts were collected, perfused with PBS, and bisected sagittally. Hearts were flash-frozen in Optimal Cutting Temperature (OCT) embedding medium (Sakura Finetek USA, Inc., Torrance, CA) using isopentane cooled by liquid N_2. Frozen tissues were serially sectioned using a cryostat at a thickness of 5 μm and stored at -80°C until stained. This experiment was repeated using six infected and four uninfected wild-type or IFNγ-deficient mice at the 25-day time point only.

For immunofluorescent staining, sections were fixed in acetone for 5 min at -20°C, rehydrated in PBS-, blocked with 5% bovine serum albumin (BSA; Sigma-Aldrich) in PBS- for 1 h, and washed. Sections were incubated for 30 min at RT with conjugated primary

antibodies diluted in PBS-. Unconjugated primary antibodies were placed on sections overnight at 4°C. After washing, sections were incubated with conjugated secondary antibodies for 45 min at RT. All sections were mounted with VectaShield mounting medium containing DAPI (Vector Laboratories, Inc., Burlingame, CA). Additionally, some tissue sections were stained with hematoxylin and eosin to grade the severity of carditis as described above.

To identify T lymphocytes, fluorescein isothiocyanate (FITC)-conjugated rat anti-mouse CD3 (1:50) was used. NK cells were identified by FITC mouse anti-mouse NK1.1 (1:50). Alexa Fluor 647 rat anti-mouse B220 (1:50) and phycoerythrin (PE) rat anti-mouse IgM (1:50) were used simultaneously to identify B cells. To identify dendritic cells, FITC hamster anti-mouse CD11c (1:50) and Alexa Fluor 647 rat anti-mouse CD11b (1:50) were used simultaneously. All of these mAb were obtained from BD Biosciences. Unconjugated rat anti-mouse Gr-1 (1:100) (AbD Serotec, Raleigh, NC) and goat anti-mouse F4/80 (1:50) (Santa Cruz Biotechnology, Inc., Santa Cruz, CA) were used simultaneously to identify neutrophils and macrophages. Secondary antibodies for detection were Alexa Fluor 555 donkey anti-goat IgG (1:1000) (Invitrogen Corporation, Carlsbad, CA) followed by Alexa Fluor 488 goat anti-rat IgG (1:1000) (AbD Serotec). Fc Block™ (BD Biosciences) was used to prevent non-specific binding of antibodies to cell-surface Fc receptors. Matched antibodies to irrelevant antigens from the same manufacturers were used as negative controls. For comparison, negative controls were prepared in parallel with the positively-stained samples. The number of positively-stained leukocytes was counted by an observer using coded samples. DAPI staining of leukocytes was used to determine areas of inflammation within the atria and the base of the heart, where Lyme carditis is typically located.[127,128,162] Within

regions of inflammation, the number of stained leukocytes was tallied in ten randomly-selected fields. Whenever possible, fields were selected from two sections separated by an interval of at least 30 μm.

XIV. Measurement of Chemokines in Hearts of Mice

Five infected and five uninfected wild-type or IFNγ-deficient mice were sacrificed using CO_2 at 25 days after inoculation. Hearts were removed, perfused with PBS, blotted dry, and stored in RNAlater for 1 day at 4°C. RNA was isolated using a Fibrous Tissue RNA Kit (Qiagen) according to the manufacturer's protocol and stored at -80°C. RNA was converted into cDNA using a Verso cDNA Kit as specified by the manufacturer. Solaris qPCR primer and probe pairs for cytokines of interest were employed as described above.

XV. Assessment of *B. burgdorferi* Burden in Hearts of Mice

Five infected and two uninfected wild-type or IFNγ-deficient mice were sacrificed using CO_2 at 25 days after inoculation. Hearts were removed, perfused with PBS, blotted dry, and minced. DNA was isolated using a DNeasy Blood and Tissue Kit (Qiagen) according to the manufacturer's protocol and stored at -20°C. Primers were used to amplify the *B. burgdorferi recA* gene (Forward: 5'-GTG GAT CTA TTG TAT TAG ATG AGG CTC TCG-3' and Reverse: 5'-GCC AAA GTT CTG CAA CAT TAA CAC CTA AAG-3') and the mouse nidogen-1 gene (*Nid1*) (Forward: 5'-CCA GCC ACA GAA TAC CAT CC-3' and Reverse 5'-GGA CAT ACT CTG CTG CCA TC-3'). The amounts of *B. burgdorferi recA* DNA were analyzed relative to *Nid1* on an ABI 7500 Real Time PCR System in 96-well Thermo-Fast detection plates using the ABsolute Blue SYBR Green Low ROX Master Mix (Thermo

Fisher Scientific) according to the manufacturer's protocol in a total volume of 25 µl. Results are presented as the expression of *recA* in infected mice relative to uninfected mice as calculated by ABI System SDS software. Reactions were done in quadruplicate.

XVI. Statistics

Data assessing the degree of severity of Lyme carditis were analyzed by the Mann-Whitney test (two-tailed). All other data were analyzed using an unpaired analysis of variance followed by the Tukey-Kramer multiple-comparison test using InStat software (GraphPad, La Jolla, CA). A p value of < 0.05 was considered statistically significant.

Results

I. Effects of IFNγ on the Migration of Monocytes and NK cells Across Spirochete-activated Endothelium

Our laboratory previously investigated whether IFNγ alters leukocyte migration across endothelium exposed to *B. burgdorferi*. Concurrent stimulation of HUVEC-amnion cultures by IFNγ and *B. burgdorferi* increases transendothelial migration of T cells as compared to stimulation with either agent alone. In contrast, the migration of neutrophils across *B. burgdorferi*-activated HUVEC is decreased when IFNγ is added.[158]

Monocytes were examined to test further the hypothesis that the coaction of *B. burgdorferi* and IFNγ promotes the migration of cells typical of chronic inflammation. HUVEC-amnion cultures were stimulated with *B. burgdorferi*, IFNγ, or a combination of *B. burgdorferi* and IFNγ. Freshly isolated human peripheral blood monocytes were added to the apical surface of the HUVEC-amnion cultures. After 20 min, migration of the monocytes was significantly greater across IFNγ- or *B. burgdorferi*-treated endothelium than unstimulated endothelium ($p < 0.001$) (Figure 1). An additive increase in migration was observed when HUVEC were stimulated with both *B. burgdorferi* and IFNγ, compared to the single stimuli alone.

To assess the effect of *B. burgdorferi* and IFNγ on migration of NK cells, HUVEC-amnion cultures were similarly stimulated with *B. burgdorferi*, IFNγ, or a combination of *B. burgdorferi* and IFNγ. NK cells were isolated and allowed to migrate for 4 hours. HUVEC-amnion cultures activated by *B. burgdorferi* or IFNγ alone fostered an increase of NK cell adhesion to and migration across the monolayer, compared to unstimulated samples ($p < 0.001$) (Figure 2). When both *B. burgdorferi* and IFNγ were used

to stimulate HUVEC, adhesion of NK cells to the monolayer was increased compared to *B. burgdorferi* or IFNγ alone ($p < 0.001$). While adhesion was increased, migration of these NK cells was downregulated in comparison to HUVEC activated by *B. burgdorferi* or IFNγ alone.

A potential explanation for the observed decrease in the transmigration of NK cells (Figure 2) is that IFNγ reduces the rate at which NK cells traverse HUVEC stimulated by *B. burgdorferi*. To examine the possibility that NK cells are migrating at a slower rate, the previous 4-h NK cell transmigration experiment was repeated, but with an extended migration time of 24 h. As seen previously (Figure 2), the adhesion of NK cells was greater when HUVEC were treated with both IFNγ and *B. burgdorferi* compared to either stimulus alone (Figure 3). In addition, a similar reduction in the migration of NK cells across endothelium stimulated by both IFNγ and *B. burgdorferi* was still observed after 24 h. Thus, the impairment is not simply due to slower migration.

Figure 1. Stimulation of HUVEC with *B. burgdorferi* and IFNγ Increases Transmigration of Monocytes Compared with Either Agent Alone. HUVEC-amnion cultures were incubated with control medium (Unstim), *B. burgdorferi* (10 sp/ec), IFNγ (10 ng/ml), or a combination of *B. burgdorferi* (10 sp/ec) and IFNγ (10 ng/ml) for 24 h. Cultures were washed, and monocytes were added for 20 min at 37°C. Adhesion and migration were assessed microscopically. The upper, white portion of each bar indicates the percentage of monocytes adherent to the apical surface of the endothelium. The lower, solid portion indicates the percentage that migrated beneath the endothelial monolayer. Bars represent the means ± SD of 4 or 5 replicate samples. This experiment was repeated two more times with comparable results. ***, $p < 0.001$ compared with migration across cultures exposed to *B. burgdorferi* or IFNγ alone.

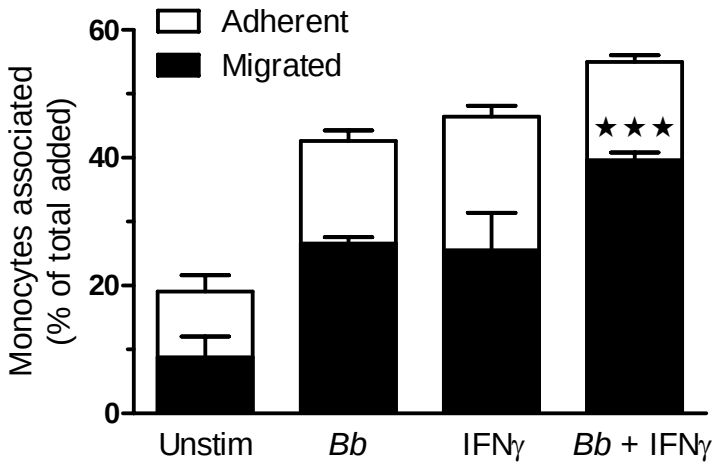
Adherent
Migrated
Monocytes associated
(% of total added)
60
40
20
0
★★★
Unstim
Bb
IFNγ
Bb + IFNγ

Figure 2. IFNγ Decreases Migration of NK cells Across HUVEC Stimulated with *B. burgdorferi* Compared with Either Agent Alone. HUVEC-amnion cultures were incubated with control medium (Unstim), *B. burgdorferi* (10 sp/ec), IFNγ (10 ng/ml), or a combination of *B. burgdorferi* (10 sp/ec) and IFNγ (10 ng/ml) for 24 h. Cultures were washed, and NK cells were added for 4 h at 37°C. Adhesion and migration were assessed microscopically. The upper, white portion of each bar indicates the percentage of NK cells adherent to the apical surface of the endothelium. The lower, solid portion indicates the percentage that migrated beneath the endothelial monolayer. Bars represent the means ± SD of 4 or 5 replicate samples. This result was seen in three separate experiments using NK cells from different donors. ***, $p < 0.001$ compared with migration across unstimulated cultures or cultures stimulated with *B. burgdorferi* and IFNγ together.

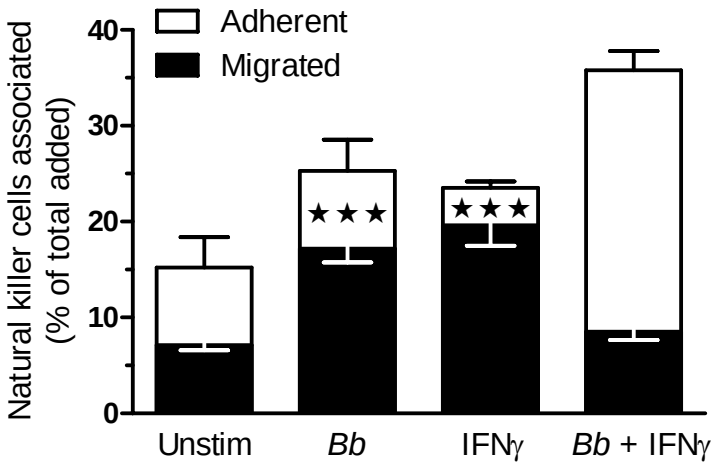
Adherent
Migrated
Natural killer cells associated
(% of total added)
40
30
20
10
0
★★★
★★★
Unstim
Bb
IFNγ
Bb + IFNγ

Figure 3. IFNγ Decreases Migration of NK cells Across HUVEC Stimulated with *B. burgdorferi* Compared with Either Agent Alone After 24 hours. HUVEC-amnion cultures were incubated with control medium (Unstim), *B. burgdorferi* (10 sp/ec), IFNγ (10 ng/ml), or a combination of *B. burgdorferi* (10 sp/ec) and IFNγ (10 ng/ml) for 24 h. Cultures were washed, and NK cells were added for 24 h at 37°C. Adhesion and migration were assessed microscopically. The upper, white portion of each bar indicates the percentage of NK cells adherent to the apical surface of the endothelium. The lower, solid portion indicates the percentage that migrated beneath the endothelial monolayer. Bars represent the means ± SD of 4 or 5 replicate samples. *, $p < 0.05$ compared with Unstim or *B. burgdorferi* and IFNγ migration.

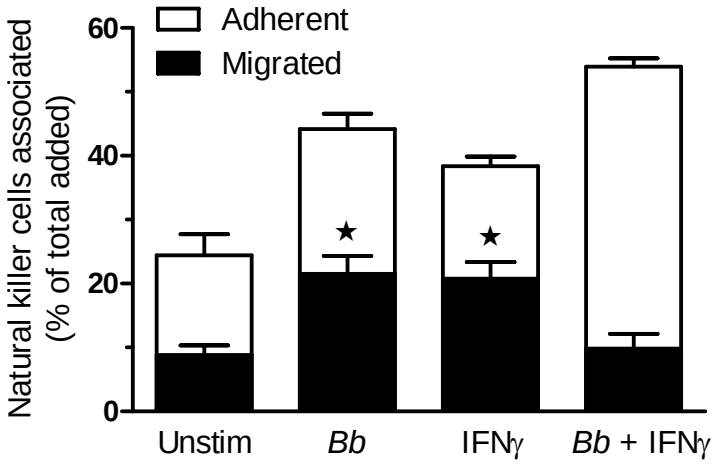
Adherent
Migrated
Natural killer cells associated
(% of total added)
60
40
20
0
★
★
Unstim
Bb
IFNγ
Bb + IFNγ

II. Examination of Mechanisms by Which IFNγ Alters Migration of Leukocytes Across Endothelium Stimulated with *B. burgdorferi*

A. Soluble Factor

Although *B. burgdorferi* and IFNγ increase the transendothelial migration of T cells[158] and monocytes (Figure 1), migration of neutrophils[158] and NK cells (Figures 2 and 3) is suppressed. Chemotaxis assays were used to determine whether the two stimuli together induce endothelium to secrete a soluble factor that inhibits the migration of neutrophils and NK cells. As a first approach, Boyden chambers were used to determine whether soluble components could prevent migration of neutrophils into nitrocellulose filters in response to CXCL8, a chemoattractant for neutrophils. Conditioned media were collected from HUVEC-amnion cultures that had been stimulated with *B. burgdorferi*, IFNγ, or *B. burgdorferi* and IFNγ for 24 hours. Aliquots of freshly isolated human neutrophils were incubated with the various conditioned media for 25 min and then placed in the Boyden chamber. All neutrophils migrated towards CXCL8 more avidly than to control medium (Figure 4). However, the pre-incubation of neutrophils with the various conditioned media had no effect on their migration towards CXCL8.

Secondly, to mimic our laboratory's previous neutrophil migration experiments, the HUVEC-amnion model was used to determine if a soluble factor secreted by endothelium could inhibit migration of neutrophils and NK cells. Instead of using the Boyden chamber, HUVEC-amnion cultures were set on top of wells in which the chemoattractant CXCL8 was placed. Once again, purified human neutrophils were pre-incubated with conditioned media and then allowed to migrate across the HUVEC-amnion cultures. No decrease in migration of neutrophils in response to CXCL8 was observed when they were incubated with conditioned

medium from HUVEC stimulated with both *B. burgdorferi* and IFNγ (Figure 5). In fact, neutrophils in all samples migrated towards CXCL8 in equal numbers. These data suggest that the decrease in migration of neutrophils across HUVEC activated with *B. burgdorferi* and IFNγ is not mediated by a soluble factor.

B. Adhesion Molecules

Rival et al.[169] have demonstrated that neutrophils increase their adhesion to endothelial cell monolayers activated by both IFNγ and TNFα, compared to either stimulus alone. However, there is a decrease in migration of the neutrophils across these monolayers. This pattern of increased adhesion and decreased migration is comparable to the pattern of migration of NK cells across HUVEC incubated with *B. burgdorferi* and IFNγ (Figures 2 and 3). In the case of neutrophils, it is hypothesized that cell-surface adhesion proteins are responsible for their increased adhesion and decreased transmigration when endothelial monolayers are treated with IFNγ and TNFα.[169] Endothelium activated by IFNγ and TNFα concurrently shows disrupted cell junctions and dispersal of PECAM away from the junctional area.[169] We therefore considered the possibility that *B. burgdorferi* and IFNγ foster alterations in adhesion molecules, which could result in the observed decrease in migration of neutrophils[158] and NK cells (Figures 2 and 3).

The experiments of Rival et al.[169] were carried out using HUVEC cultured to confluence on gelatin-coated porous membranes with a pore size of 8 μm. To determine whether TNFα cooperates with IFNγ similarly to *B. burgdorferi* using the HUVEC-amnion system, cultures were incubated with IFNγ, TNFα, or both TNFα and IFNγ for 24 hours. As performed previously, NK cells were allowed to migrate for 4 hours. HUVEC activated by

TNFα ($p < 0.01$) or IFNγ ($p < 0.001$) promoted an increase in the migration of NK cells (Figure 6). In contrast, migration of NK cells was downregulated when HUVEC were co-activated with TNFα and IFNγ. In addition, the adhesion of NK cells was greater when HUVEC were treated with the two stimuli together, compared to either alone. In total, these observations were similar to the effects of *B. burgdorferi* and IFNγ together (Figure 2).

The reduction in the transmigration of neutrophils across HUVEC stimulated by IFNγ and TNFα is hypothesized to be the result of altered endothelial junctional adhesion molecules.[169] It is possible that IFNγ and *B. burgdoferi* together might also disrupt normal junctions, which could be responsible for the decrease in the migration of NK cell and neutrophils. Therefore, the distribution of the adhesion molecules PECAM, CD99, and ESAM was examined by immunofluorescent microscopy on HUVEC-amnion cultures stimulated with *B. burgdorferi*, IFNγ, or a combination of *B. burgdorferi* and IFNγ. Expression of PECAM,[170] CD99,[171] and ESAM[67] is normally localized to junctional borders between neighboring endothelial cells. Accordingly, indirect immunofluorescent staining of unstimulated HUVEC for PECAM revealed a distinct band that outlined the border of each cell. Little to no change from this pattern was observed when comparing HUVEC that were incubated with IFNγ or *B. burgdorferi* (Figure 7A). However, when cultures were activated by IFNγ and *B. burgdorferi* together, there was a pronounced disruption of staining for PECAM in the junctions between endothelial cells. In most fields, cells had punctate staining throughout the whole cell, with a loss of fluorescent intensity in the junctional areas. Unlike PECAM, CD99 (Figure 7B) and ESAM (Figure 7C) were not markedly changed in distribution or overall expression when HUVEC-amnion cultures were incubated with IFNγ and *B. burgdorferi* singly or together.

To gain further insight into whether IFNγ and *B. burgdorferi* cooperate to alter expression of endothelial adhesion molecules, the surface expression of ICAM-1, VCAM-1, and PECAM was quantified by whole-cell ELISA. These studies revealed that incubation of HUVEC with IFNγ or *B. burgdorferi* increases the expression of ICAM-1 (Figure 8A) and VCAM-1 (Figure 8B) compared to unstimulated cells. However, expression of PECAM did not change with either stimulus (Figure 8C). The incubation of HUVEC with both IFNγ and *B. burgdorferi* resulted in an increase in the expression of ICAM-1 (Figure 8A) and VCAM-1 (Figure 8B) above each stimulus alone. This increase was significant in two of three experiments measuring ICAM-1 and both of two experiments assessing VCAM-1. In contrast, there was no change in the expression of PECAM when HUVEC were activated by IFNγ and *B. burgdorferi* singly or together (Figure 8C).

Figure 4. Conditioned Medium from HUVEC Stimulated with IFNγ and *B. burgdorferi* Does Not Inhibit Chemotaxis of Neutrophils. Conditioned media were collected from HUVEC-amnion cultures incubated with control medium (Unstim), *B. burgdorferi* (10 sp/ec), IFNγ (10 ng/ml), or *B. burgdorferi* (10 sp/ec) and IFNγ (10 ng/ml) for 24 h. Neutrophils were pre-incubated for 25 min with these conditioned media or in M199 + 10% FBS for Control and Medium samples. Neutrophils, still in the conditioned media, then were placed on top of 5-μm nitrocellulose filters for 15 min at 37°C. Migration was towards 20 nM CXCL8 for all samples except Control, which was toward M199 + 10% FBS. Filters were stained and analyzed microscopically, and data reflect how far the neutrophils migrated into the filters. Bars represent the means ± SD of 3 replicate filters (5 fields each). ***, $p < 0.001$ compared with all other samples

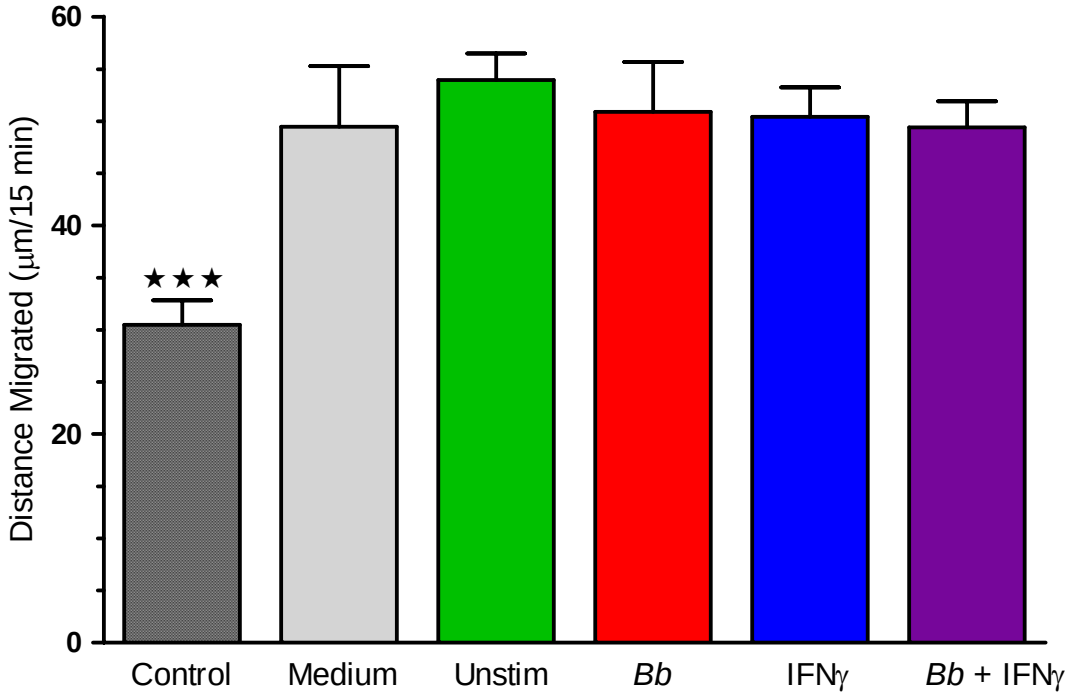
60
40
20
0
Distance Migrated (μm/15 min)
★★★
Control
Medium
Unstim
Bb
IFNγ
Bb + IFNγ

Figure 5. Conditioned Medium from HUVEC Stimulated with IFNγ and *B. burgdorferi* Does Not Inhibit Transendothelial Migration of Neutrophils Toward CXCL8.

Conditioned media were collected from HUVEC-amnion cultures incubated with control medium (Unstim) or *B. burgdorferi* (10 sp/ec) and IFNγ (10 ng/ml) together for 24 h. Neutrophils were pre-incubated with these conditioned media or with M199 + 10% FBS (Control and Medium samples) for 25 min. HUVEC-amnion cultures were placed upon silicone rubber supports with 20 nM CXCL8 or M199 + 10% FBS (Control and Medium samples only) below. Neutrophils, still in the conditioned media, then were added to the cultures for 30 min. Migration was analyzed microscopically. Bars represent the means ± SD of 3 or 5 replicate samples. ***, $p < 0.001$ compared with all other samples.

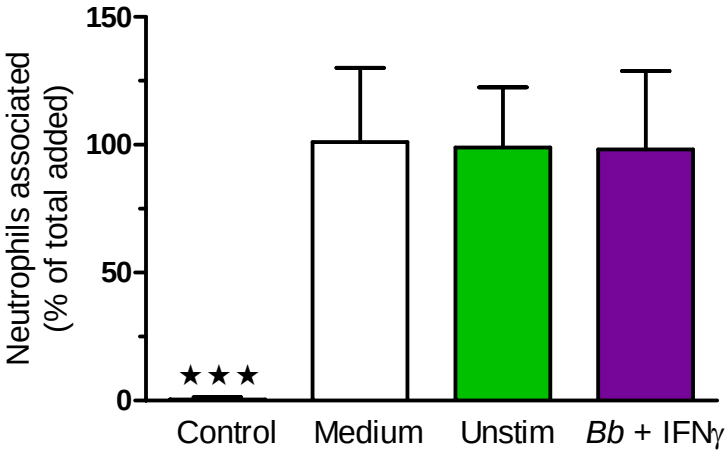
150
100
50
0
Neutrophils associated
(% of total added)
★★★
Control
Medium
Unstim
Bb + IFNγ

Figure 6. IFNγ Decreases Migration of NK Cells Across HUVEC Exposed to TNFα. HUVEC-amnion cultures were treated with control medium (Unstim), TNFα (0.1 ng/ml), IFNγ (10 ng/ml), or a combination of TNFα (0.1 ng/ml) and IFNγ (10 ng/ml) for 24 h. Cultures were washed, and NK cells were added for 4 h at 37°C. Adhesion and migration were assessed microscopically. The upper, white portion of each bar indicates the percentage of NK cells adherent to the apical surface of the endothelium. The lower, solid portion indicates the percentage that migrated beneath the endothelial monolayer. Bars represent the means ± SD of 4 or 5 replicate samples. *, $p < 0.05$ compared with TNFα + IFNγ migration. **, $p < 0.01$ compared with compared with TNFα + IFNγ migration.

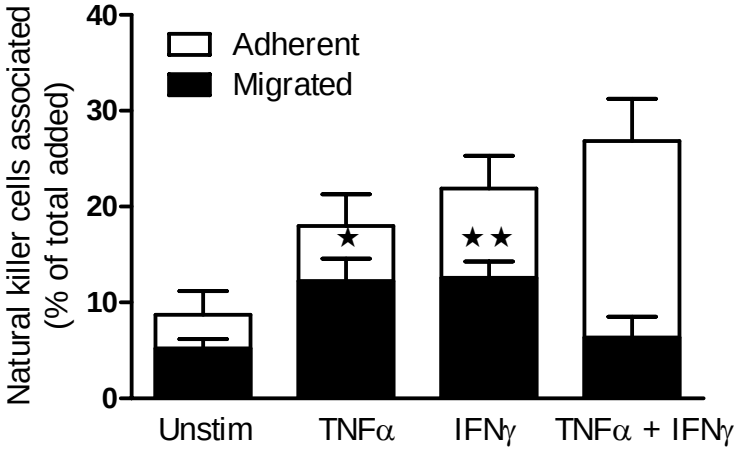
Natural killer cells associated
(% of total added)
40
30
20
10
0
Adherent
Migrated
★
★★
Unstim
TNFα
IFNγ
TNFα + IFNγ

Figure 7. Stimulation of HUVEC with *B. burgdorferi* and IFNγ Concurrently Alters the Pattern of Expression of PECAM but Not CD99 or ESAM. HUVEC-amnion cultures were incubated with medium only (Unstim), *B. burgdorferi* (10 sp/ec), IFNγ (10 ng/ml), or a combination of *B. burgdorferi* (10 sp/ec) and IFNγ (10 ng/ml) for 24 h. Cultures were washed, fixed, and incubated overnight with mouse anti-human PECAM (A), mouse anti-human CD99 (B), or mouse anti-human ESAM (C). Samples were washed and incubated for 3 h with Cy3-conjugated donkey anti-mouse IgG. Cultures were treated with DAPI stain (A and C only) and mounted for analysis by fluorescence microscopy at 200× magnification (A) or deconvolution microscopy at 630× magnification (B and C).

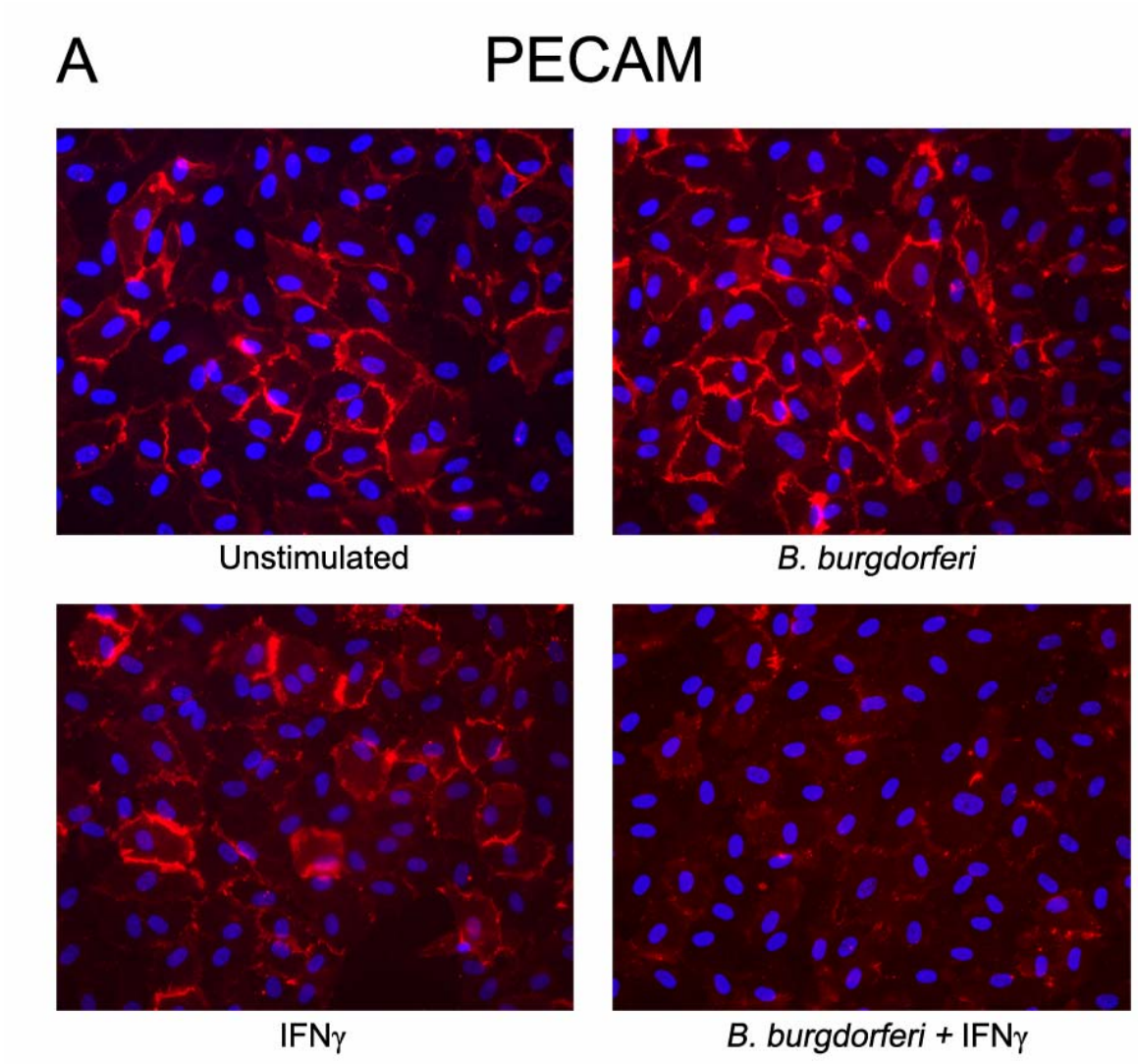
A
PECAM
Unstimulated
B. burgdorferi
IFNγ
B. burgdorferi + IFNγ

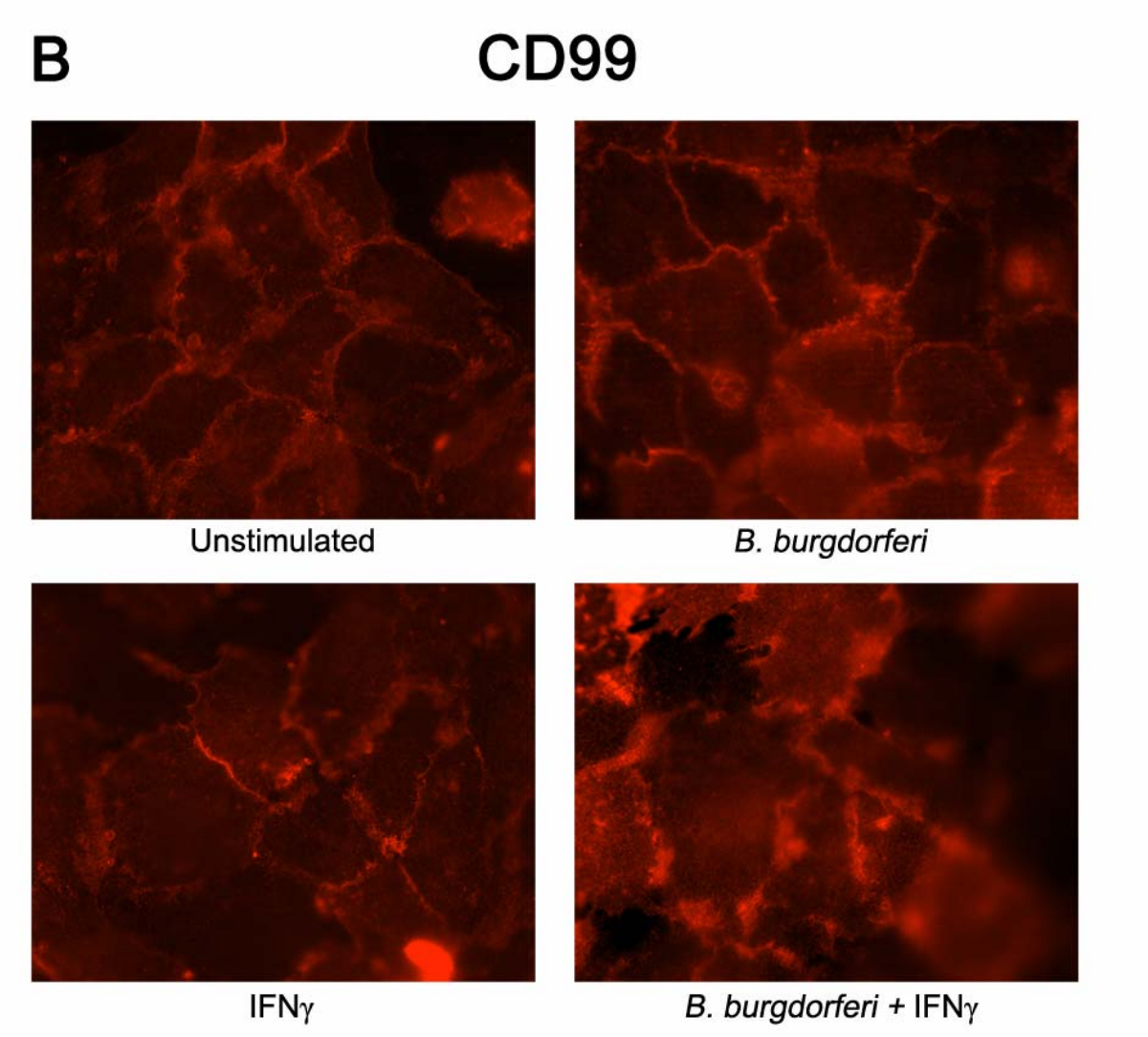
B
CD99
Unstimulated
B. burgdorferi
IFNγ
B. burgdorferi + IFNγ

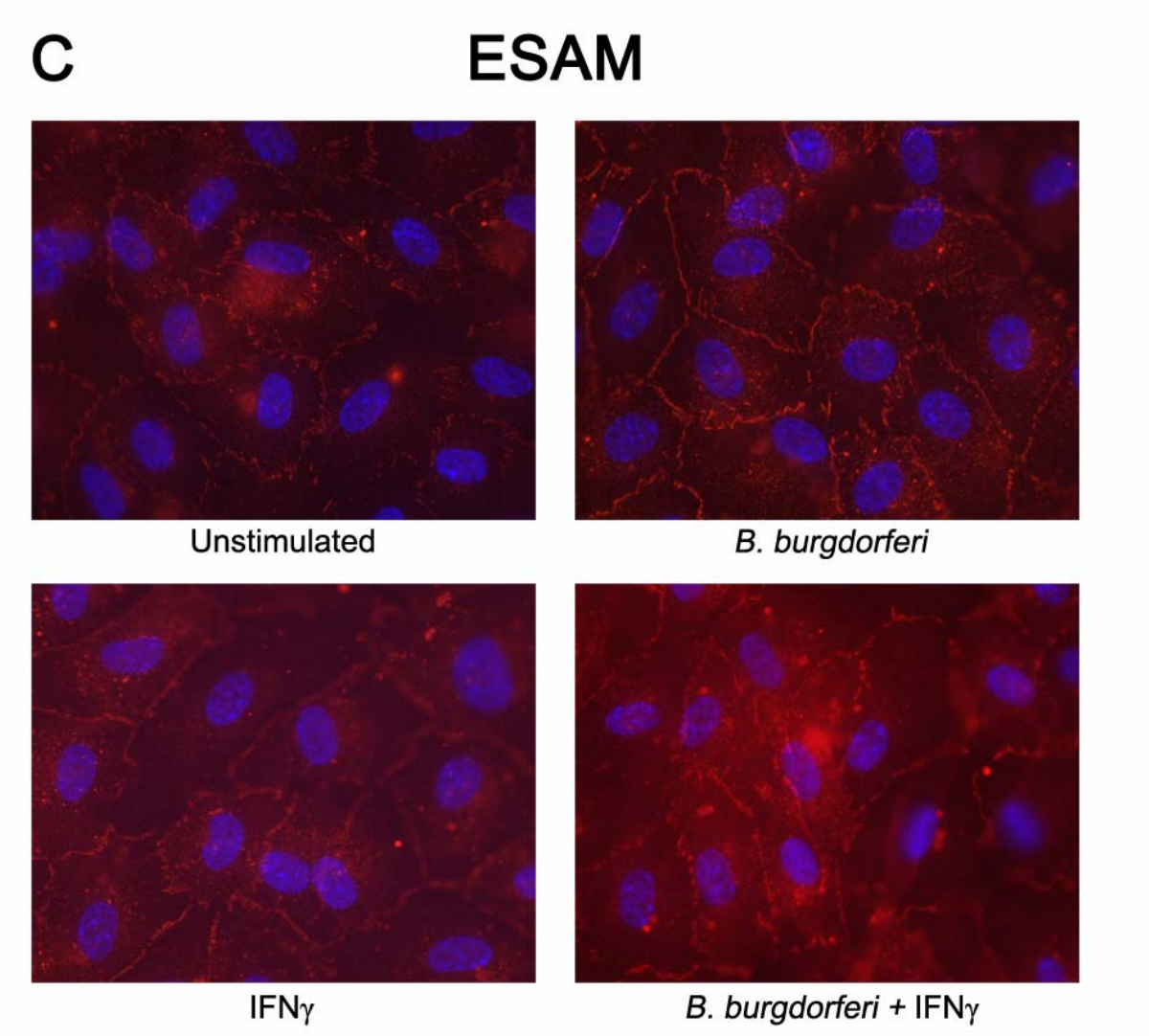
C
ESAM
Unstimulated
B. burgdorferi
IFNγ
B. burgdorferi + IFNγ

Figure 8. Stimulation of HUVEC with *B. burgdorferi* and IFNγ Concurrently Increases Surface Expression of ICAM-1 and VCAM-1 but Not PECAM. HUVEC were incubated with control medium (Unstim), *B. burgdorferi* (10 sp/cell), IFNγ (10 ng/ml), or *B. burgdorferi* (10 sp/cell) and IFNγ (10 ng/ml) together for 24 h at 37°C. Expression of ICAM-1 (A), VCAM-1 (B), and PECAM (C) was measured by whole-cell ELISA. Bars indicate the means ± SD of 4 or 5 replicate samples. ICAM-1 and PECAM experiments were repeated once and twice, respectively, with similar results. **, $p < 0.01$ compared with *B. burgdorferi* + IFNγ together. ***, $p < 0.001$ compared with *B. burgdorferi* + IFNγ together.

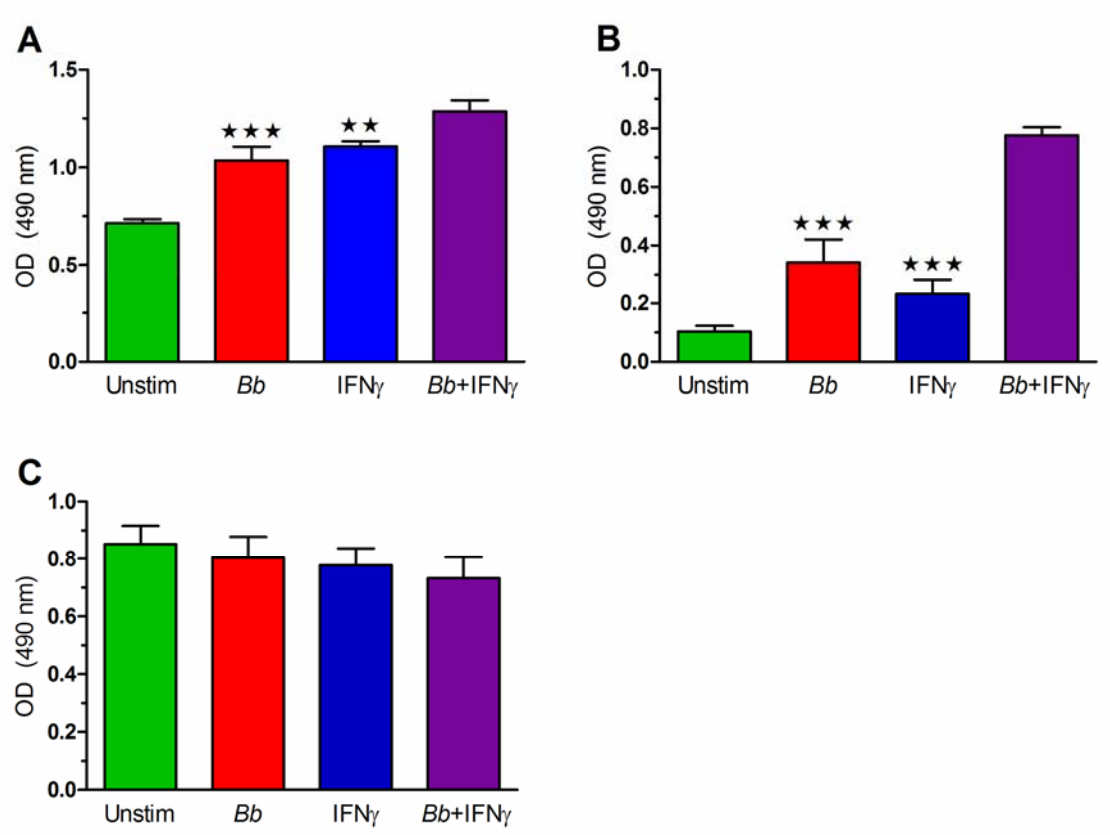
A
OD (490 nm)
1.5
1.0
0.5
0.0
★★★
★★
Unstim
Bb
IFNγ
Bb+IFNγ
B
OD (490 nm)
1.0
0.8
0.6
0.4
0.2
0.0
★★★
★★★
Unstim
Bb
IFNγ
Bb+IFNγ
C
OD (490 nm)
1.0
0.8
0.6
0.4
0.2
0.0
Unstim
Bb
IFNγ
Bb+IFNγ

III. Effects of IFNγ on the Expression of Genes in Macrophages Exposed to *B. burgdorferi*

A. Murine Macrophages

Like endothelial cells, macrophages when activated secrete various pro-inflammatory cytokines, which may recruit additional leukocytes to areas of infection. Furthermore, macrophages are present in lesions of Lyme disease in both humans[172] and mice[124,127] and are activated by *B. burgdorferi in vitro*.[155,156] We therefore hypothesized that as for HUVEC,[158] IFNγ could be acting as a switch to promote the production by *B. burgdorferi*-stimulated macrophages of chemokines that attract leukocytes associated with chronic inflammation.

To determine if IFNγ alters the expression of chemokine genes in murine macrophages exposed to spirochetes, microarray analysis was performed. Murine macrophages were stimulated with *B. burgdorferi*, IFNγ, or *B. burgdorferi* and IFNγ concurrently for 8 h. Concurrent activation of murine macrophages by IFNγ and *B. burgdorferi* resulted in the synergistic upregulation of 404 annotated and unannotated genes and a synergistic downregulation of 571 annotated and unannotated genes as measured using Affymetrix microarrays. The 125 most highly upregulated and downregulated genes are listed in Table 1 and Table 2, respectively. Genes encoding the chemokines CXCL9, CXCL11, CXCL16, and CCL12 were synergistically upregulated by *B. burgdorferi* and IFNγ, whereas those for CXCL1, CXCL3, and CXCL5 were synergistically downregulated. In addition to the listed chemokines, four other pro-inflammatory cytokines or their subunits were synergistically upregulated (IL-1β, IL-12a, IL-12b, and IL-15), as defined by a synergy score greater than 1.25. A positive synergy score was calculated by dividing the expression of a gene activated by IFNγ and *B. burgdorferi* together by the sum of the gene inductions by

either stimulus alone. The upregulated genes of chemokines all encode attractants for mononuclear cells, while the downregulated ones encode neutrophil chemoattractants.[26]

The classification of genes of murine macrophages according to function was performed using the database for annotation, visualization and integrated discovery (DAVID) v6.7. Gene ontology clustering of genes that were synergistically induced linked many genes to the positive regulation of the immune system, leukocyte activation and proliferation, and the response to viral infection. Examination of biological pathways placed many of these genes as having roles in the signaling between macrophages and T cells through cell-cell contact and cytokines and their receptors. The genes that were synergistically downregulated are primarily involved in mitosis and the cell cycle. Those cytoskeletal genes synergistically downregulated were those that function during cellular division.

Six of the chemokines that were synergistically affected were chosen for further analysis using real-time RT-PCR (Figure 9). Transcripts of chemokines that typically attract neutrophils were highly upregulated by *B. burgdorferi* alone compared to cells activated by IFNγ alone. Conversely, genes encoding chemokines that attract mononuclear cells were upregulated by stimulation with IFNγ, while *B. burgdorferi* alone had little effect. The response of macrophages to IFNγ and *B. burgdorferi* combined also differed between the two categories of chemokines. The addition of both stimuli to macrophages resulted in the reduced expression of genes encoding chemokines that attract neutrophils, compared to *B. burgdorferi*-stimulated cells (Figure 9, A and B). On the contrary, incubation of macrophages with *B. burgdorferi* and IFNγ concurrently promoted an increased level of expression of genes encoding chemokines that attract mononuclear leukocytes, compared to macrophages stimulated with IFNγ alone (Figure 9, C-F).

Transcripts for CXCL10 and CXCL2 were synergistically upregulated by *B. burgdorferi* and IFNγ in HUVEC[158] but not in murine macrophages, as measured by microarray analysis. Nonetheless, we examined the transcription of these chemokine genes in the macrophages using real-time RT-PCR. When macrophages were activated by *B. burgdorferi* alone, expression of CXCL2, a chemokine that recruits neutrophils, was increased. As was the case for other neutrophil chemoattractants, a decrease in gene expression was observed with the further addition of IFNγ (compare Figure 9G with Figure 9, A and B). Expression of CXCL10, an attractant for mononuclear cells, was increased by stimulation of macrophages with IFNγ alone, and incubation with *B. burgdorferi* and IFNγ concurrently did not further increase the level of transcripts (Figure 9H).

Secretion of CXCL1, CXCL2, CXCL9, and CXCL10 from stimulated macrophages was measured by ELISA. In agreement with the RT-PCR results, the production of CXCL1 and CXCL2 was decreased when macrophages were incubated concurrently with IFNγ and *B. burgdorferi* compared to *B. burgdorferi* alone (Figure 10, A and B). In contrast, amounts of CXCL9 were increased by the two stimuli together compared to either stimulus alone (Figure 10C). Although transcripts for CXCL10 in macrophages incubated with IFNγ were not further increased when *B. burgdorferi* was added (Figure 9H), the secretion of this chemokine was synergistically elevated by the two stimuli together (Figure 10D). Within macrophages activated by *B. burgdorferi*, IFNγ thus promotes the production of chemokines that attract mononuclear leukocytes but suppresses that of chemokines that recruit neutrophils.

B. Human Macrophages

As assessed by microarrays, concurrent activation of human macrophages by IFNγ and *B. burgdorferi* resulted in the synergistic upregulation of 1515 annotated and unannotated genes and the synergistic downregulation of 416 annotated and unannotated genes. The 125 genes exhibiting the greatest positive synergy or negative synergy are shown in Tables 3 and 4, respectively. Of these genes, four encode chemokines that attract mononuclear leukocytes (CCL19, CCL1, CCL5, and CCL15). In addition to the listed chemokines, nine other pro-inflammatory cytokines or their subunits were synergistically upregulated (IL-12a, TNFSF15, IL-12b, IL-23a, TNFSF9, IL-32, IL-27, TNFα, and TNFSF7). Similar to their effects on murine macrophages, IFNγ and *B. burgdorferi* synergistically downregulated several chemoattractants for neutrophils (CXCL2, CXCL5, and CXCL6).

The classification of genes of human macrophages according was function was also performed using DAVID. Gene ontology sorted the synergistically upregulated genes into three primary clusters: induction and regulation of apoptosis, inflammatory response, and leukocyte activation and proliferation. Further investigation showed positive induction of genes encoding members of the NF-κB pathway. In addition, the majority of cell adhesion molecules that are important for interactions between macrophages and T cells were synergistically upregulated. Gene ontology analysis of the genes of human macrophages that were synergistically downregulated clustered them into two prominent groups those responsible for cell cycle and mitosis and those encoding cytoskeletal proteins such as kinesins.

Table 1: Synergistically Upregulated Genes in Murine Macrophages Stimulated With *B. burgdorferi* and IFNγ Together

Name[a]	Symbol	*Bb*[b]	IFNγ[b]	*Bb* + IFNγ[b]	Synergy Score[c]
heat shock protein 1A	Hspa1a	2.16	1.07	42.94	13.30
chemokine (C-C motif) receptor 7	Ccr7	1.31	1.28	34.13	13.16
follistatin	Fst	2.92	-1.10	44.26	11.55
CD200 antigen	Cd200	1.53	-1.04	25.38	10.19
nitric oxide synthase 2 inducible	Nos2	2.79	1.31	40.59	9.90
cDNA sequence BC037703	BC037703	-1.03	1.02	17.65	8.86
heat shock protein 1B	Hspa1b	4.00	-1.18	37.55	7.75
heat shock protein 1B	Hspa1b	6.53	1.30	56.49	7.22
heat shock protein 1B	Hspa1b	6.47	1.18	53.88	7.04
LIM homeobox protein 2	Lhx2	-1.06	3.73	30.64	6.55
cytohesin 1 interacting protein	Cytip	-9.45	-1.36	5.12	6.08
interleukin 12b	Il12b	82.08	1.28	505.66	6.07
cytohesin 1 interacting protein	Cytip	-7.96	-1.42	4.69	5.64
GLI pathogenesis-related 2	Glipr2	1.75	3.21	27.92	5.62
serine (or cysteine) peptidase inhibitor clade B member 1a	Serpinb1a	-1.07	7.09	41.01	5.11
transmembrane and tetratricopeptide repeat containing 2	Tmtc2	2.26	1.22	17.65	5.06
solute carrier family 40 (iron-regulated transporter) member 1	Slc40a1	-4.42	-6.10	1.96	5.02
BCL2-like 14 (apoptosis facilitator)	Bcl2l14	-1.10	2.53	16.57	4.81
nuclear receptor subfamily 4 group A member 2	Nr4a2	-1.11	1.90	12.04	4.30
serine (or cysteine) peptidase inhibitor clade B member 1a	Serpinb1a	1.04	1.16	8.92	4.06
solute carrier family 40 (iron-regulated transporter) member 1	Slc40a1	-3.71	-5.97	1.74	3.97
special AT-rich sequence binding protein 1	Satb1	-1.22	1.17	7.74	3.89
SLAM family member 7	Slamf7	8.27	13.15	80.44	3.76
ubiquitin D	Ubd	1.35	2.34	13.42	3.64
fucosyltransferase 8	Fut8	-1.87	1.03	5.56	3.54
RIKEN cDNA 1110032F04 gene	1110032F04Rik	1.31	1.04	7.98	3.40
GLI pathogenesis-related 2	Glipr2	1.22	1.60	9.32	3.31
inhibitor of DNA binding 2	Id2	1.31	1.38	8.88	3.30

Name[a]	Symbol	*Bb*[b]	IFNγ[b]	*Bb* + IFNγ[b]	Synergy Score[c]
RIKEN cDNA 4930518C04 gene	4930518C04Rik	-1.01	-1.08	6.32	3.28
July 2007 (NCBI Build 37)	chr5:115373291-115387707 (+) // 89.2 // qF	2.35	13.87	52.67	3.25
family with sequence similarity 129 member A	Fam129a	-2.73	-1.56	3.25	3.23
BCL2-like 14 (apoptosis facilitator)	Bcl2l14	1.10	2.05	10.12	3.21
cytohesin 1 interacting protein	Cytip	-1.72	-1.24	4.42	3.18
phorbol-12-myristate-13-acetate-induced protein 1	Pmaip1	-1.95	2.42	8.93	3.05
MAX dimerization protein 1	Mxd1	1.53	2.56	12.45	3.04
follistatin	Fst	1.39	1.05	7.42	3.03
sorbin and SH3 domain containing 1	Sorbs1	-1.10	-1.34	4.96	3.00
structural maintenance of chromosomes 5	Smc5	-1.37	-1.09	4.93	2.99
signaling lymphocytic activation molecule family member 1	Slamf1	5.29	-1.08	18.49	2.98
GRB2-related adaptor protein	Grap	-1.01	-1.21	5.33	2.94
signal transducer and activator of transcription 4	Stat4	-1.26	-1.24	4.65	2.91
---	---	2.07	2.71	13.75	2.88
aldehyde dehydrogenase 1 family member B1	Aldh1b1	1.20	2.16	9.65	2.87
DnaJ (Hsp40) homolog subfamily B member 4	Dnajb4	-1.25	-1.98	3.72	2.85
---	---	1.38	-1.21	6.20	2.81
deoxyribonuclease 1-like 3	Dnase1l3	1.01	2.21	9.01	2.80
MAX dimerization protein 1	Mxd1	1.54	2.82	12.20	2.80
expressed sequence AI848100	AI848100	2.03	1.17	8.93	2.79
schlafen 4	Slfn4	4.20	6.46	29.42	2.76
oligonucleotide/oligosaccharide-binding fold containing 2A	Obfc2a	-1.19	1.28	5.84	2.75
special AT-rich sequence binding protein 1	Satb1	1.12	1.16	6.22	2.72
expressed sequence AI848100	AI848100	1.68	1.02	7.28	2.71
cytidine monophosphate (UMP-CMP) kinase 2 mitochondrial	Cmpk2	3.56	10.34	37.58	2.70
cystatin F (leukocystatin)	Cst7	1.24	3.12	11.70	2.68
DnaJ (Hsp40) homolog subfamily B member 4	Dnajb4	-1.41	-2.38	3.02	2.67

Name[a]	Symbol	*Bb*[b]	IFNγ[b]	*Bb* + IFNγ[b]	Synergy Score[c]
---	---	2.36	-1.16	8.57	2.66
sorbin and SH3 domain containing 1	Sorbs1	-1.48	-1.27	3.86	2.63
ataxin 7-like 1	Atxn7l1	-1.44	1.34	5.32	2.61
RIKEN cDNA A630072M18 gene	A630072M18Rik	1.09	4.71	14.88	2.57
syndecan binding protein (syntenin) 2	Sdcbp2	-1.05	1.23	5.55	2.54
chemokine (C-X-C motif) ligand 9	Cxcl9	-1.02	60.12	154.85	2.53
carbonic anhydrase 2	Car2	2.07	1.23	8.31	2.52
---	---	1.07	1.05	5.31	2.50
cDNA sequence BC006779	BC006779	4.32	6.52	27.09	2.50
NEDD4 binding protein 2-like 1	N4bp2l1	-10.41	-1.73	1.68	2.49
nuclear receptor subfamily 4 group A member 2	Nr4a2	1.03	1.47	6.20	2.48
RIKEN cDNA 1200016E24 gene	1200016E24Rik	8.38	3.64	29.68	2.47
fibroblast growth factor binding protein 3	Fgfbp3	-2.09	1.08	3.82	2.45
N-acyl phosphatidylethanolamine phospholipase D	Napepld	1.21	-1.21	4.95	2.43
chr2:122506966-122528232 (-) // 98.37 // qE5	solute carrier family 30 (zinc transporter) member 4	1.10	1.10	5.31	2.41
signaling lymphocytic activation molecule family member 1	Slamf1	5.86	1.20	16.94	2.40
---	---	1.17	1.56	6.46	2.36
structural maintenance of chromosomes 5	Smc5	-1.09	-1.03	4.44	2.36
cDNA sequence AB182283 /// similar to receptor activity modifying protein 3 /// receptor (calcitonin) activity modifying protein 3	AB182283 /// LOC100046186 /// Ramp3	1.43	-1.02	5.69	2.36
myeloid differentiation primary response gene 116	Myd116	4.25	1.30	13.08	2.36
interleukin 12b	Il12b	142.49	1.17	337.42	2.35
sulfiredoxin 1 homolog (S. cerevisiae)	Srxn1	2.62	-1.75	7.47	2.34
myxovirus (influenza virus) resistance 2	Mx2	1.44	1.92	7.85	2.33
radical S-adenosyl methionine domain containing 2	Rsad2	7.58	15.86	54.61	2.33
expressed sequence AI848100	AI848100	1.99	1.05	7.06	2.32

Name[a]	Symbol	*Bb*[b]	IFNγ[b]	*Bb* + IFNγ[b]	Synergy Score[c]
ADP-ribosylation factor-like 5B	Arl5b	1.68	1.11	6.47	2.32
cyclin D2	Ccnd2	-1.78	4.20	11.02	2.31
radical S-adenosyl methionine domain containing 2	Rsad2	8.99	17.60	61.33	2.31
CD40 antigen	Cd40	19.96	19.59	91.03	2.30
pleiomorphic adenoma gene-like 1	Plagl1	1.21	1.78	6.88	2.30
GRAM domain containing 3	Gramd3	1.15	1.13	5.23	2.29
pituitary tumor-transforming gene 1	Pttg1	-1.26	1.39	4.97	2.28
glutamate-cysteine ligase catalytic subunit	Gclc	-1.08	-3.42	2.77	2.28
runt related transcription factor 3	Runx3	1.08	1.68	6.26	2.27
cyclin D2	Ccnd2	-2.07	4.21	10.63	2.26
---	---	2.10	-1.98	5.89	2.26
RAB33A member of RAS oncogene family	Rab33a	1.20	-1.05	4.87	2.26
ataxin 7-like 1	Atxn7l1	-1.10	1.51	5.36	2.21
c-mer proto-oncogene tyrosine kinase	Mertk	-5.05	-1.00	2.64	2.21
CD69 antigen	Cd69	42.26	54.21	210.61	2.18
vascular cell adhesion molecule 1	Vcam1	11.25	6.53	38.59	2.17
activated leukocyte cell adhesion molecule	Alcam	1.67	1.33	6.47	2.16
family with sequence similarity 129 member A	Fam129a	-4.35	-2.01	1.56	2.14
transmembrane and coiled coil domains 3	Tmcc3	-1.52	3.04	7.86	2.13
cytidine monophosphate (UMP-CMP) kinase 2 mitochondrial	Cmpk2	4.24	13.89	38.43	2.12
lysophosphatidic acid receptor 1	Lpar1	2.74	2.22	10.50	2.12
zinc finger protein 800	Zfp800	2.53	3.28	12.24	2.10
chr2:164881182-164897055 (+) // 93.08 // qH3	CD40 antigen	14.07	12.85	56.27	2.09
ganglioside-induced differentiation-associated-protein 10	Gdap10	5.27	14.77	41.86	2.09
GRAM domain containing 3	Gramd3	-1.00	1.06	4.29	2.09
myxovirus (influenza virus) resistance 1	Mx1	5.62	39.03	92.96	2.08
interferon induced with helicase C domain 1	Ifih1	1.84	4.04	12.22	2.08
chemokine (C motif) receptor 1	Xcr1	1.30	1.32	5.42	2.07
plakophilin 4	Pkp4	1.10	1.59	5.55	2.06
sulfiredoxin 1 homolog	Srxn1	2.75	-1.70	6.86	2.05

Name[a]	Symbol	*Bb*[b]	IFNγ[b]	*Bb* + IFNγ[b]	Synergy Score[c]
---	---	1.47	7.38	18.10	2.05
---	---	-1.07	-1.12	3.73	2.04
prostaglandin E receptor 4 (subtype EP4)	Ptger4	1.41	1.45	5.81	2.03
CD83 antigen	Cd83	2.86	5.31	16.60	2.03
actin filament associated protein 1	Afap1	-1.57	2.06	5.47	2.02
serine (or cysteine) peptidase inhibitor clade G member 1	Serping1	1.08	1.12	4.46	2.02
sulfiredoxin 1 homolog (S. cerevisiae)	Srxn1	2.57	-2.29	6.08	2.02
protein tyrosine phosphatase receptor-type F interacting protein binding protein 2	Ppfibp2	3.90	-2.33	8.70	2.01
---	---	1.47	1.17	5.29	2.00
nuclear factor of kappa light polypeptide gene enhancer in B-cells inhibitor epsilon	Nfkbie	7.99	3.67	23.32	2.00
---	---	1.04	2.04	6.14	1.99
ladinin	Lad1	4.96	-1.34	11.34	1.99
kinase insert domain protein receptor	Kdr	-1.16	-1.03	3.63	1.97
zinc finger protein 800	Zfp800	2.29	2.65	9.71	1.97

[a] Annotated and unannoted genes of the Affymetrix Mouse Expression Array 430 2.0

[b] Fold change in expression level of genes of macrophages stimulated by the corresponding agent compared to untreated macrophages.

[c] The synergy score is equal to the levels of gene expression from macrophages stimulated with IFNγ and *B. burgdorferi* together, divided by the sum of the levels of gene expression from macrophages treated with either stimulus alone.

Table 2: Synergistically Downregulated Genes in Murine Macrophages Stimulated With *B. burgdorferi* and IFNγ Together

Name[a]	Symbol	*Bb*[b]	IFNγ[b]	*Bb* + IFNγ[b]	Synergy Score[c]
NUF2 NDC80 kinetochore complex component homolog (S. cerevisiae)	Nuf2	-3.45	-1.46	-31.23	-6.35
protein regulator of cytokinesis 1	Prc1	-1.77	-1.61	-20.40	-6.04
disabled homolog 2 (Drosophila)	Dab2	-4.09	-3.28	-43.66	-5.93
Rac GTPase-activating protein 1	Racgap1	-2.81	-1.32	-19.89	-4.81
topoisomerase (DNA) II alpha	Top2a	-2.53	-1.42	-18.42	-4.66
RIKEN cDNA C330027C09 gene	C330027C09Rik	-2.46	-1.61	-18.34	-4.51
glucosaminyl (N-acetyl) transferase 1 core 2	Gcnt1	-22.86	-2.91	-115.72	-4.49
budding uninhibited by benzimidazoles 1 homolog (S. cerevisiae)	Bub1	-1.87	-1.79	-16.41	-4.48
arginase liver	Arg1	15.86	2.05	-2.46	-4.46
antigen identified by monoclonal antibody Ki 67	Mki67	-1.53	-1.95	-15.49	-4.45
chr1:97484258-97564171 (-) // 79.31 // qD	ST8 alpha-N-acetyl-neuraminide alpha-2	-1.21	-2.64	-16.87	-4.39
lamin B receptor	Lbr	-2.93	-2.09	-21.96	-4.38
cyclin B1 /// predicted gene EG434175 /// predicted gene EG667005	Ccnb1 /// EG434175 /// EG667005	-1.48	-1.13	-11.41	-4.37
dyskeratosis congenita 1 dyskerin homolog (human)	Dkc1	-2.61	1.15	-15.17	-4.36
centrosomal protein 55	Cep55	-2.81	-1.79	-19.58	-4.25
ceramide kinase /// similar to Ceramide kinase (Acylsphingosine kinase) (mCERK)	Cerk /// LOC676420	-3.72	-3.98	-31.49	-4.09
cell division cycle 20 homolog (S. cerevisiae)	Cdc20	-1.94	-1.48	-13.61	-3.98
ribonucleotide reductase M2	Rrm2	-12.35	-2.58	-59.15	-3.96
fatty acid binding protein 7 brain	Fabp7	1.31	1.10	-6.46	-3.86
---	---	1.18	-1.14	-7.67	-3.86
kinesin family member 2C	Kif2c	-2.64	-1.78	-16.87	-3.82
Nfat activating molecule with ITAM motif 1	Nfam1	-1.27	-1.58	-10.79	-3.79
PDZ binding kinase	Pbk	-3.68	-1.98	-20.87	-3.69
mitogen-activated protein kinase 14	Mapk14	-1.01	-1.96	-10.90	-3.67
formin-like 3	Fmnl3	-1.28	-1.33	-9.56	-3.67
centromere protein A	Cenpa	-2.25	-1.28	-12.88	-3.64

Name[a]	Symbol	*Bb*[b]	IFNγ[b]	*Bb* + IFNγ[b]	Synergy Score[c]
anillin actin binding protein	Anln	-3.45	-1.84	-18.97	-3.59
cysteinyl leukotriene receptor 1	Cysltr1	-1.01	-1.15	-7.75	-3.58
RIKEN cDNA 2810417H13 gene	2810417H13Rik	-5.49	-2.21	-27.39	-3.56
potassium channel tetramerisation domain containing 12	Kctd12	2.43	-1.26	-5.94	-3.55
Ras association (RalGDS/AF-6) domain family member 2	Rassf2	-1.52	-1.22	-9.61	-3.50
ubiquitin-conjugating enzyme E2C	Ube2c	-1.29	-1.30	-8.97	-3.47
cell division cycle associated 8	Cdca8	-2.09	-1.43	-11.69	-3.32
cyclin B1	Ccnb1	-1.57	-1.24	-9.26	-3.30
dual specificity phosphatase 6	Dusp6	-6.01	-5.08	-36.21	-3.26
baculoviral IAP repeat-containing 5	Birc5	-2.32	-1.39	-12.07	-3.26
influenza virus NS1A binding protein	Ivns1abp	-7.23	-2.11	-29.96	-3.21
cell division cycle associated 8	Cdca8	-1.95	-1.50	-11.09	-3.21
histone cluster 1 H2ab /// histone cluster 1 H2ac /// histone cluster 1 H2ad /// histone cluster 1 H2ae /// histone cluster 1 H2ag /// histone cluster 1 H2ai /// histone cluster 1 H2an /// histone cluster 1 H2ao /// similar to histone 2a	Hist1h2ab /// Hist1h2ac /// Hist1h2ad /// Hist1h2ae /// Hist1h2ag /// Hist1h2ai /// Hist1h2an /// Hist1h2ao /// RP23-480B19.10	-1.13	1.34	-6.02	-3.21
mitogen-activated protein kinase 14	Mapk14	-1.32	-2.09	-10.89	-3.19
ribonucleotide reductase M2	Rrm2	-10.21	-2.20	-38.23	-3.08
influenza virus NS1A binding protein	Ivns1abp	-6.26	-1.95	-24.55	-2.99
metastasis suppressor 1	Mtss1	-12.74	-2.94	-46.27	-2.95
ect2 oncogene	Ect2	-3.53	-1.67	-15.19	-2.92
Jun oncogene	Jun	-1.31	1.60	-5.64	-2.92
kinesin family member 11	Kif11	-3.40	-1.60	-14.10	-2.82
non-SMC condensin I complex subunit D2	Ncapd2	-4.27	-1.94	-17.44	-2.81
on-SMC condensin I complex subunit G	Ncapg	-3.68	-1.76	-15.01	-2.76
RRS1 ribosome biogenesis regulator homolog (S. cerevisiae)	Rrs1	1.44	-1.15	-4.99	-2.70
aurora kinase B	Aurkb	-2.82	-1.56	-11.80	-2.69
chr10:62407408-62409250 (+) // 81.76 // qB4	solute carrier family 25 (mitochondrial carrier Graves disease autoantigen) member 16	-1.82	-1.37	-8.25	-2.59

Name[a]	Symbol	*Bb*[b]	IFNγ[b]	*Bb* + IFNγ[b]	Synergy Score[c]
polo-like kinase 1 (Drosophila)	Plk1	-2.40	-1.47	-9.99	-2.58
Friend leukemia integration 1	Fli1	-4.45	-3.38	-20.06	-2.56
regulator of G-protein signaling 18	Rgs18	-13.70	-3.70	-44.51	-2.56
cell division cycle associated 8	Cdca8	-2.00	-1.25	-8.25	-2.54
disabled homolog 2 (Drosophila)	Dab2	-3.30	-3.13	-16.28	-2.53
v-maf musculoaponeurotic fibrosarcoma oncogene family protein B (avian)	Mafb	-2.91	-1.29	-10.49	-2.50
kinesin family member 20A	Kif20a	-2.96	-2.12	-12.68	-2.50
PDZ and LIM domain 2	Pdlim2	-3.19	-1.49	-11.61	-2.48
cell division cycle 2 homolog A (S. pombe)	Cdc2a	-2.05	-1.81	-9.52	-2.47
maternal embryonic leucine zipper kinase	Melk	-3.30	-1.60	-12.00	-2.45
proliferation-associated 2G4	Pa2g4	-1.87	-1.29	-7.72	-2.45
disabled homolog 2 (Drosophila)	Dab2	-2.13	-2.01	-10.05	-2.43
v-maf musculoaponeurotic fibrosarcoma oncogene family protein B (avian)	Mafb	-2.26	-1.02	-7.93	-2.42
cyclin B1	Ccnb1	-1.47	-1.16	-6.35	-2.41
guanine nucleotide binding protein (G protein) gamma transducing activity polypeptide 2	Gngt2	1.18	-2.74	-8.64	-2.40
cyclin B2	Ccnb2	-2.15	-1.21	-8.04	-2.39
transforming growth factor beta induced	Tgfbi	-1.03	-1.75	-6.61	-2.38
transforming growth factor beta induced	Tgfbi	-1.00	-1.64	-6.28	-2.38
transforming growth factor beta induced	Tgfbi	-1.06	-1.58	-6.24	-2.37
kinesin family member 20B	Kif20b	-3.25	-1.74	-11.82	-2.37
kinesin family member 22	Kif22	-2.96	-1.46	-10.48	-2.37
transforming growth factor beta induced	Tgfbi	-1.07	-1.59	-6.30	-2.36
kinesin family member 23	Kif23	-3.24	-1.59	-11.40	-2.36
DNA segment Chr 17 human D6S56E 5	D17H6S56E-5	-2.10	1.60	-6.42	-2.35
adrenergic receptor beta 2	Adrb2	-6.47	-2.56	-21.25	-2.35
dedicator of cytokinesis 8	Dock8	-3.53	-2.09	-13.23	-2.35
similar to Sesn1 protein /// sestrin 1	LOC100047324 /// Sesn1	-30.79	-5.05	-84.01	-2.34
cysteinyl leukotriene receptor 1	Cysltr1	-1.14	-1.26	-5.54	-2.31
proliferation-associated 2G4	Pa2g4	-1.83	-1.31	-7.23	-2.30
NIMA (never in mitosis gene a)-related expressed kinase 2	Nek2	-1.89	-1.67	-8.19	-2.30
Jun oncogene	Jun	-1.16	1.58	-4.10	-2.29
adenylate cyclase 9	Adcy9	-2.90	-5.81	-19.80	-2.27

Name[a]	Symbol	*Bb*[b]	IFNγ[b]	*Bb* + IFNγ[b]	Synergy Score[c]
pre B-cell leukemia transcription factor 3	Pbx3	-3.77	-2.72	-14.76	-2.27
GRAM domain containing 1B	Gramd1b	-2.29	-1.44	-8.45	-2.27
RRS1 ribosome biogenesis regulator homolog (S. cerevisiae)	Rrs1	1.44	-1.15	-4.17	-2.26
C-type lectin domain family 4 member a3	Clec4a3	2.49	-2.89	-7.42	-2.25
DNA segment Chr 17 human D6S56E 5	D17H6S56E-5	-2.14	1.33	-6.50	-2.25
kinetochore associated 1	Kntc1	-2.45	-1.58	-8.97	-2.22
ATPase family AAA domain containing 3A	Atad3a	-1.31	-1.15	-5.47	-2.22
retinoic acid induced 14	Rai14	1.68	1.17	-3.21	-2.21
sperm associated antigen 5	Spag5	-2.29	-1.85	-9.17	-2.21
ArfGAP with RhoGAP domain ankyrin repeat and PH domain 3	Arap3	-1.82	-6.15	-17.52	-2.20
similar to Sesn1 protein /// sestrin 1	LOC100047324 /// Sesn1	-23.36	-6.01	-64.48	-2.20
WD repeat domain 77	Wdr77	-1.41	-1.22	-5.78	-2.19
RAD51 associated protein 1	Rad51ap1	-6.44	-1.57	-17.55	-2.19
centromere protein F	Cenpf	-2.64	-1.70	-9.46	-2.18
nucleolar and spindle associated protein 1	Nusap1	-2.09	-1.47	-7.74	-2.17
Nfat activating molecule with ITAM motif 1	Nfam1	-1.49	-1.72	-6.96	-2.17
Kruppel-like factor 7 (ubiquitous)	Klf7	5.13	-1.27	-3.18	-2.17
kinesin family member 13A	Kif13a	1.28	-1.61	-5.17	-2.16
aurora kinase B	Aurkb	-3.70	-1.47	-11.15	-2.15
mago-nashi homolog B (Drosophila)	Magohb	3.04	2.39	-1.61	-2.15
centromere protein Q	Cenpq	-2.12	-1.59	-7.96	-2.15
guanine nucleotide binding protein (G protein) gamma 2	Gng2	-4.92	-1.16	-13.02	-2.14
chromobox homolog 3 (Drosophila HP1 gamma)	Cbx3	-2.95	-1.40	-9.29	-2.14
cyclin A2	Ccna2	-2.94	-1.53	-9.54	-2.13
cyclin H	Ccnh	-1.94	-1.09	-6.46	-2.13
transmembrane protein 48	Tmem48	-1.57	-1.57	-6.69	-2.13
RAD51 associated protein 1	Rad51ap1	-5.34	-1.58	-14.60	-2.11
disabled homolog 2 (Drosophila)	Dab2	-2.52	-2.47	-10.40	-2.08
caveolin 2	Cav2	-2.23	-4.44	-13.87	-2.08
cyclin H	Ccnh	-1.98	-1.09	-6.37	-2.07
cyclin A2	Ccna2	-3.02	-1.41	-9.14	-2.07
CDC23 (cell division cycle 23 yeast homolog)	Cdc23	-1.87	-1.80	-7.56	-2.06

Name[a]	Symbol	*Bb*[b]	IFNγ[b]	*Bb* + IFNγ[b]	Synergy Score[c]
poly (ADP-ribose) polymerase family member 1	Parp1	-3.68	-2.32	-12.35	-2.06
thioredoxin interacting protein	Txnip	-2.53	-1.05	-7.36	-2.06
cell division cycle 25 homolog B (S. pombe)	Cdc25b	-2.74	-1.98	-9.67	-2.05
solute carrier family 20 member 1	Slc20a1	1.61	-1.25	-3.83	-2.05
general transcription factor II I	Gtf2i	-3.05	-1.50	-9.31	-2.05
cell division cycle associated 5	Cdca5	-4.09	-1.66	-11.77	-2.05
structural maintenance of chromosomes 2	Smc2	-3.02	-1.71	-9.62	-2.04
NudC domain containing 2	Nudcd2	-1.76	-1.58	-6.78	-2.03
olfactomedin 1	Olfm1	-1.64	-1.20	-5.72	-2.02

[a] Annotated and unannoted genes of the Affymetrix Mouse Expression Array 430 2.0

[b] Fold change in expression level of genes of macrophages stimulated by the corresponding agent compared to untreated macrophages.

[c] The synergy score is equal to the inverse of the levels of gene expression from macrophages stimulated with both IFNγ and *B. burgdorferi* together divided by the sum of the inverses of the levels of gene expression from macrophages treated with either stimulus alone; this number is multiplied by -1 to represent the negative value of the synergy score.

Table 3: Synergistically Upregulated Genes in Human Macrophages Stimulated With *B. burgdorferi* and IFNγ Together

Name[a]	Symbol	*Bb*[b]	IFNγ[b]	*Bb* + IFNγ[b]	Synergy Score[c]
CASP8 and FADD-like apoptosis regulator	CFLAR	-12.13	-9.11	6.29	32.72
UDP-Gal:betaGlcNAc beta 14-galactosyltransferase polypeptide 5	B4GALT5	-3.98	-3.54	11.99	22.48
inhibin beta A (activin A activin AB alpha polypeptide)	INHBA	5.15	1.22	123.50	19.39
interleukin 12A (natural killer cell stimulatory factor 1 cytotoxic lymphocyte maturation factor 1 p35)	IL12A	1.33	1.24	45.80	17.81
plasminogen activator tissue	PLAT	3.28	1.01	73.61	17.18
CD38 antigen (p45)	CD38	1.09	-1.05	33.07	16.23
bromodomain adjacent to zinc finger domain 1A	BAZ1A	-7.87	-3.62	6.37	15.82
chemokine (C-C motif) receptor 7	CCR7	3.74	2.06	91.29	15.74
RAB7 member RAS oncogene family-like 1	RAB7L1	-10.18	-3.07	6.66	15.71
NA	NA	-2.62	-3.73	9.87	15.19
kinesin family member 5B	KIF5B	-30.13	-13.81	1.57	14.82
chromosome 3 open reading frame 1	C3orf1	1.32	1.74	41.82	13.63
NA	LOC162073	-4.95	-5.77	4.66	12.41
muscleblind-like (Drosophila)	MBNL1	-22.63	-13.42	1.44	12.09
NA	NA	1.55	1.19	32.87	12.00
v-rel reticuloendotheliosis viral oncogene homolog (avian)	REL	-5.48	-7.83	3.69	11.91
ubiquitin-conjugating enzyme E2D 3 (UBC4/5 homolog yeast)	UBE2D3	-7.06	-5.95	3.58	11.57
tumor necrosis factor (ligand) superfamily member 15	TNFSF15	1.15	-1.34	21.19	11.19
Rap guanine nucleotide exchange factor (GEF) 2	RAPGEF2	-2.17	-1.77	11.44	11.15
myosin IG	MYO1G	-1.83	-1.87	12.00	11.12
KIAA1618	KIAA1618	-20.57	-6.45	2.22	10.88
NA	NA	-7.95	-5.10	3.27	10.16
NA	NA	-13.10	-9.80	1.75	9.80
dual specificity phosphatase 4	DUSP4	1.20	1.03	21.37	9.56
kinectin 1 (kinesin receptor)	KTN1	-19.08	-13.11	1.23	9.55
Wilms tumor 1 associated protein	WTAP	-2.74	-3.64	6.10	9.53
CDC42 small effector 2	CDC42SE2	-2.52	-2.83	7.06	9.41
interleukin 7 receptor	IL7R	-1.14	-1.78	13.48	9.37
interleukin 12B (natural killer cell stimulatory factor 2 cytotoxic lymphocyte maturation factor 2 p40)	IL12B	80.78	1.43	759.02	9.23

Name[a]	Symbol	*Bb*[b]	IFNγ[b]	*Bb* + IFNγ[b]	Synergy Score[c]
solute carrier family 25 member 37	SLC25A37	-3.59	-3.47	5.18	9.14
CD44 antigen (homing function and Indian blood group system)	CD44	-1.70	-3.32	7.74	8.69
ring finger protein 19	RNF19	-1.62	-2.07	9.49	8.63
CDP-diacylglycerol synthase (phosphatidate cytidylyltransferase) 1	CDS1	-1.15	-1.30	14.15	8.60
pre-B-cell colony enhancing factor 1	PBEF1	1.28	-2.23	14.35	8.31
leukocyte immunoglobulin-like receptor subfamily A (with TM domain) member 5	LILRA5	-1.04	-1.14	15.19	8.23
NA	NA	-3.80	-1.70	6.89	8.10
NA	NA	1.64	1.57	25.85	8.07
POU domain class 2 transcription factor 2	POU2F2	-1.06	-1.31	13.71	8.02
LIM domain kinase 2	LIMK2	1.54	1.32	22.91	8.01
Dicer1 Dcr-1 homolog (Drosophila)	DICER1	-10.22	-8.29	1.68	7.69
activating transcription factor 5	ATF5	-5.97	-2.85	3.98	7.67
NA	NA	-4.16	-4.87	3.38	7.59
chromosome 17 open reading frame 27	C17orf27	-2.51	-2.54	5.94	7.50
fascin homolog 1 actin-bundling protein (Strongylocentrotus purpuratus)	FSCN1	-1.37	-2.14	8.74	7.29
chemokine (C-C motif) ligand 19	CCL19	1.86	1.04	21.12	7.28
AKT1 substrate 1 (proline-rich)	AKT1S1	-10.67	-5.97	1.90	7.26
NA	NA	-4.45	-4.00	3.43	7.22
G protein-coupled receptor 54	GPR54	1.09	1.08	15.53	7.14
baculoviral IAP repeat-containing 4	BIRC4	-6.17	-7.89	2.06	7.12
ATPase Class I type 8B member 1	ATP8B1	-2.89	-3.10	4.62	6.91
cathepsin S	CTSS	-12.62	-9.97	1.24	6.89
baculoviral IAP repeat-containing 4	BIRC4	-5.40	-5.33	2.54	6.83
SON DNA binding protein	SON	-40.77	-9.17	-1.10	6.78
KIAA1533	KIAA1533	-1.15	-1.45	10.50	6.74
serine/threonine kinase 4	STK4	-4.44	-3.82	3.28	6.74
splicing factor arginine/serine-rich 4	SFRS4	-6.05	-5.07	2.44	6.72
transcription factor 7-like 2 (T-cell specific HMG-box)	TCF7L2	-3.05	-3.72	3.89	6.51
apolipoprotein L 6	APOL6	1.04	2.09	20.04	6.40
Kruppel-like factor 6	KLF6	-4.59	-2.09	4.39	6.31
poly (ADP-ribose) polymerase family member 14	PARP14	-6.90	1.11	7.88	6.29
cyclin A1	CCNA1	2.11	2.17	26.84	6.27
ATPase Na+/K+ transporting beta 1 polypeptide	ATP1B1	-16.11	-2.23	3.18	6.23
G protein-coupled receptor 157	GPR157	-1.08	-1.97	8.87	6.18
golgi associated gamma adaptin ear containing ARF binding protein 1	GGA1	-28.14	-22.79	-2.05	6.15

Name[a]	Symbol	*Bb*[b]	IFNγ[b]	*Bb* + IFNγ[b]	Synergy Score[c]
FYVE RhoGEF and PH domain containing 2	FGD2	-2.30	-1.16	7.90	6.08
leukocyte immunoglobulin-like receptor subfamily A (with TM domain) member 5	LILRA5	1.67	-1.19	15.17	6.05
carboxypeptidase M	CPM	-1.16	-7.81	5.99	6.05
runt-related transcription factor 1 (acute myeloid leukemia 1	RUNX1	-1.75	-2.08	6.36	6.04
ubiquitin-conjugating enzyme E2D 3 (UBC4/5 homolog yeast)	UBE2D3	-7.06	-4.48	2.11	5.80
bromodomain containing 2	BRD2	-20.28	-13.62	-1.43	5.68
carboxypeptidase M	CPM	-1.37	-2.46	6.47	5.68
succinate receptor 1	SUCNR1	-2.42	1.50	10.77	5.64
syndecan 4 (amphiglycan ryudocan)	SDC4	1.05	-1.26	10.31	5.58
nuclear factor of kappa light polypeptide gene enhancer in B-cells 1 (p105)	NFKB1	-2.26	-1.94	5.28	5.52
interleukin 6 receptor	IL6R	-8.01	-10.71	1.17	5.37
heterogeneous nuclear ribonucleoprotein L-like	HNRPLL	-5.03	-2.64	3.07	5.31
NA	NA	-10.37	-7.03	1.27	5.30
microtubule-actin crosslinking factor 1	MACF1	-2.80	-1.92	4.64	5.28
serologically defined colon cancer antigen 1	SDCCAG1	-17.56	-10.90	-1.29	5.22
NA	MGC20235	-2.52	-2.12	4.42	5.09
zinc finger homeobox 1b	ZFHX1B	-7.78	-8.77	1.21	4.97
NA	LOC440668	-6.40	-3.43	2.21	4.94
transmembrane 7 superfamily member 1 (upregulated in kidney)	TM7SF1	-1.40	-1.40	7.05	4.94
NA	LOC348162	-2.84	-3.19	3.22	4.83
phosphodiesterase 4D interacting protein (myomegalin)	PDE4DIP	-6.62	-7.91	1.33	4.81
NA	NA	-6.98	-4.43	1.77	4.80
A kinase (PRKA) anchor protein 13	AKAP13	-4.33	-3.74	2.37	4.75
NA	TPARL	-6.60	-4.74	1.70	4.70
CASP8 and FADD-like apoptosis regulator	CFLAR	-1.21	-1.92	6.31	4.68
zinc finger protein 207	ZNF207	-3.85	-3.82	2.43	4.65
BAT2 domain containing 1	BAT2D1	-1.44	-1.78	5.79	4.62
tumor necrosis factor receptor superfamily member 9	TNFRSF9	-1.78	-2.98	4.15	4.61
mitogen-activated protein kinase kinase kinase 8	MAP3K8	-2.86	-3.31	3.00	4.61
catenin (cadherin-associated protein) beta 1 88kDa	CTNNB1	-2.77	-2.77	3.31	4.59
interleukin 23 alpha subunit p19	IL23A	3.48	1.29	21.66	4.54

Name[a]	Symbol	*Bb*[b]	IFNγ[b]	*Bb* + IFNγ[b]	Synergy Score[c]
interferon alpha-inducible protein 27	IFI27	3.91	9.63	61.14	4.52
NA	FLJ31951	-5.45	-8.72	1.33	4.45
NA	NA	-14.03	-11.55	-1.43	4.44
NA	LOC439964	-4.92	-5.01	1.79	4.43
serum/glucocorticoid regulated kinase family member 3	SGK3	-12.87	-5.29	1.17	4.39
synaptopodin 2	SYNPO2	2.43	2.30	20.68	4.38
NA	NA	-3.76	-2.34	3.03	4.37
NA	FLJ42393	-2.06	-2.20	4.09	4.36
NA	FLJ20054	-1.02	-1.55	7.05	4.34
nuclear receptor subfamily 3 group C member 1 (glucocorticoid receptor)	NR3C1	-6.93	-7.58	1.20	4.33
pallidin homolog (mouse)	PLDN	-10.09	-4.84	1.32	4.31
NA	NA	-2.16	-1.19	5.51	4.23
stromal antigen 2	STAG2	-6.66	-7.41	1.20	4.21
1-acylglycerol-3-phosphate O-acyltransferase 3	AGPAT3	-5.61	-2.47	2.45	4.21
leukocyte immunoglobulin-like receptor subfamily A (without TM domain) member 3	LILRA3	3.47	1.18	19.45	4.19
Kruppel-like factor 6	KLF6	-3.41	-3.31	2.49	4.19
metal-regulatory transcription factor 1	MTF1	-2.27	-1.99	3.93	4.17
lysosomal-associated membrane protein 3	LAMP3	18.27	5.39	98.53	4.17
RAS p21 protein activator 4	RASA4	-7.81	-6.66	1.16	4.16
interleukin 2 receptor alpha	IL2RA	6.46	1.77	34.25	4.16
phospholipid scramblase 1	PLSCR1	-1.55	-1.65	5.20	4.16
echinoderm microtubule associated protein like 4	EML4	-3.04	-2.83	2.81	4.12
protein phosphatase 1K (PP2C domain containing)	PPM1K	1.29	-1.01	9.36	4.10
phosphodiesterase 4B cAMP-specific (phosphodiesterase E4 dunce homolog Drosophila)	PDE4B	2.81	1.68	18.31	4.08
jumonji domain containing 1C	JMJD1C	-2.73	-2.10	3.41	4.05
t-complex-associated-testis-expressed 1-like 1	TCTEL1	-2.74	-2.50	3.08	4.03
zinc finger CCHC domain containing 7	ZCCHC7	-4.72	-5.03	1.65	4.02

[a] Annotated and unannoted genes of the Affymetrix Human U33 Expression Array Plus 2.0

[b] Fold change in expression level of genes of macrophages stimulated by the appropriate agent compared to untreated macrophages.

[c] The synergy score is equal to the levels of gene expression from macrophages stimulated with both IFNγ and *B. burgdorferi* together divided by the sum of the levels of gene expression from macrophages treated with either stimulus alone.

Table 4: Synergistically Downregulated Genes in Human Macrophages Stimulated With *B. burgdorferi* and IFNγ Together

Name[a]	Symbol	*Bb*[b]	IFNγ[b]	*Bb* + IFNγ[b]	Synergy Score[c]
anillin actin binding protein (scraps homolog Drosophila)	ANLN	-1.76	-2.49	-29.33	-6.89
CDC5 cell division cycle 5-like (S. pombe)	CDC5L	5.35	4.64	-2.63	-6.53
topoisomerase (DNA) II alpha 170kDa	TOP2A	-1.68	-2.56	-24.44	-5.76
kinetochore associated 2	KNTC2	-1.14	-1.57	-11.78	-4.35
asp (abnormal spindle)-like microcephaly associated (Drosophila)	ASPM	-1.68	-2.10	-16.46	-4.35
NIMA (never in mitosis gene a)-related kinase 2	NEK2	-1.17	-1.60	-11.63	-4.19
cyclin-dependent kinase inhibitor 2C (p18 inhibits CDK4)	CDKN2C	-1.61	-1.96	-14.64	-4.09
ankyrin repeat domain 17	ANKRD17	3.65	3.44	-2.23	-3.96
caspase 2 apoptosis-related cysteine peptidase (neural precursor cell expressed developmentally down-regulated 2)	CASP2	2.45	2.23	-3.32	-3.87
ankyrin repeat domain 20B	ANKRD20B	8.92	5.30	-1.16	-3.85
kinesin family member 11	KIF11	-1.44	-2.10	-13.59	-3.84
kinesin family member 14	KIF14	-1.21	-1.87	-11.62	-3.78
oncoprotein induced transcript 3	OIT3	3.68	3.72	-2.01	-3.72
prickle-like 1 (Drosophila)	PRICKLE1	3.42	3.81	-2.01	-3.63
nucleolar and spindle associated protein 1	NUSAP1	-1.60	-2.05	-13.08	-3.58
cell division cycle 2 G1 to S and G2 to M	CDC2	1.49	-1.47	-7.42	-3.47
high-mobility group box 2	HMGB2	1.09	-1.37	-7.62	-3.32
discs large homolog 7 (Drosophila)	DLG7	-1.55	-1.99	-11.63	-3.29
metastasis suppressor 1	MTSS1	-2.98	-2.19	-16.68	-3.23
PRKC apoptosis WT1 regulator	PAWR	6.65	4.40	-1.20	-3.17
NA	NA	4.40	5.73	-1.26	-3.13
ankyrin repeat domain 20 family member A1	ANKRD20A1	6.11	4.02	-1.29	-3.13
NA	PRO1268	4.11	4.26	-1.49	-3.12
BUB1 budding uninhibited by benzimidazoles 1 homolog beta (yeast)	BUB1B	-1.58	-1.97	-10.89	-3.06
growth arrest-specific 2 like 3	GAS2L3	-1.98	-1.50	-10.38	-2.99
MAD2 mitotic arrest deficient-like 1 (yeast)	MAD2L1	1.07	-1.67	-7.75	-2.97
cell division cycle associated 1	CDCA1	1.21	-1.99	-8.35	-2.96
NA	FLJ12975	4.09	4.28	-1.41	-2.95

Name[a]	Symbol	*Bb*[b]	IFNγ[b]	*Bb* + IFNγ[b]	Synergy Score[c]
hyaluronan-mediated motility receptor (RHAMM)	HMMR	-1.02	-1.57	-7.63	-2.95
NA	LOC440546	5.48	3.63	-1.34	-2.93
NA	LOC283027	6.58	4.35	-1.07	-2.82
NA	DKFZp547E087	3.93	3.20	-1.57	-2.77
v-maf musculoaponeurotic fibrosarcoma oncogene homolog (avian)	MAF	-1.18	-1.57	-7.52	-2.73
NA	AD7C-NTP	4.13	4.11	-1.30	-2.68
zinc finger protein 528	ZNF528	3.49	3.33	-1.56	-2.67
chromosome 10 open reading frame 3	C10orf3	-1.39	-1.51	-7.62	-2.63
cyclin B1	CCNB1	1.01	-1.34	-6.09	-2.61
ribonucleotide reductase M2 polypeptide	RRM2	1.58	-1.21	-4.78	-2.60
C-type lectin domain family 4 member A	CLEC4A	1.25	-1.56	-6.09	-2.58
NA	LOC401131	4.43	3.27	-1.37	-2.58
astrotactin 2	ASTN2	3.99	2.68	-1.60	-2.57
small nuclear ribonucleoprotein polypeptide N	SNRPN	3.18	2.25	-1.93	-2.55
phosphodiesterase 3B cGMP-inhibited	PDE3B	3.47	3.48	-1.45	-2.52
FYN binding protein (FYB-120/130)	FYB	-1.11	1.44	-4.51	-2.49
v-maf musculoaponeurotic fibrosarcoma oncogene homolog (avian)	MAF	-1.56	-2.17	-9.22	-2.48
RAD51 associated protein 1	RAD51AP1	-1.40	-1.81	-7.91	-2.47
NA	FKSG14	1.05	-1.10	-4.99	-2.43
NA	LOC441014	4.04	2.26	-1.67	-2.42
cell division cycle 2 G1 to S and G2 to M	CDC2	1.15	-2.06	-7.07	-2.42
NA	HCAP-G	1.21	-1.59	-5.78	-2.40
NA	NA	1.84	1.29	-3.13	-2.37
NA	DKFZp434L142	-1.13	-1.07	-5.18	-2.35
NA	NA	4.85	4.26	-1.04	-2.35
olfactomedin-like 2B	OLFML2B	-3.61	-3.01	-15.50	-2.34
NA	BC37295_3	3.50	3.40	-1.35	-2.33
cathepsin Z	CTSZ	-1.86	1.86	-5.56	-2.32
zinc finger protein 33A	ZNF33A	4.06	3.48	-1.24	-2.32
NA	NA	5.11	4.45	1.04	-2.29
cytoskeleton associated protein 2	CKAP2	-1.51	-1.55	-6.97	-2.27
glucocorticoid induced transcript 1	GLCCI1	-3.23	-1.62	-10.98	-2.27
ubiquitin-like containing PHD and RING finger domains 1	UHRF1	-1.14	-1.68	-6.39	-2.26

Name[a]	Symbol	*Bb*[b]	IFNγ[b]	*Bb* + IFNγ[b]	Synergy Score[c]
DEP domain containing 1	DEPDC1	1.29	-1.50	-5.09	-2.24
BUB1 budding uninhibited by benzimidazoles 1 homolog (yeast)	BUB1	-1.08	-1.77	-6.38	-2.23
KIAA2010	KIAA2010	3.48	3.50	-1.28	-2.23
Mediterranean fever	MEFV	3.29	3.34	-1.34	-2.22
regulator of G-protein signalling 18	RGS18	-6.55	-4.76	-25.13	-2.22
shugoshin-like 2 (S. pombe)	SGOL2	1.25	-1.51	-5.11	-2.22
adiponectin C1Q and collagen domain containing	ADIPOQ	2.92	2.89	-1.49	-2.17
LUC7-like 2 (S. cerevisiae)	LUC7L2	3.23	2.34	-1.60	-2.17
protein tyrosine phosphatase non-receptor type 22 (lymphoid)	PTPN22	-2.08	1.60	-5.83	-2.15
NA	KIAA1467	-1.44	-1.16	-5.55	-2.14
NA	NA	4.77	3.31	-1.09	-2.14
NA	HCAP-G	-1.25	-2.12	-7.19	-2.13
C-type lectin domain family 4 member A	CLEC4A	-1.10	-2.28	-7.18	-2.12
centromere protein A 17kDa	CENPA	-1.22	-1.73	-6.22	-2.11
kinesin family member 15	KIF15	-1.13	-1.74	-6.04	-2.10
SH3-domain GRB2-like 3	SH3GL3	3.97	2.86	-1.25	-2.08
kelch-like 24 (Drosophila)	KLHL24	-3.51	-1.27	-9.86	-2.06
ZW10 interactor	ZWINT	-1.16	-1.36	-5.16	-2.05
transforming growth factor beta receptor II (70/80kDa)	TGFBR2	-2.78	-2.32	-10.43	-2.05
NA	LOC441014	3.19	2.14	-1.59	-2.04
NA	MGC21675	2.58	2.47	-1.61	-2.03
zinc finger protein 492	ZNF492	3.46	2.78	-1.32	-2.03
kinesin family member 23	KIF23	-1.32	-1.59	-5.87	-2.02
NA	FLJ11000	2.25	1.96	-1.92	-2.01
DEP domain containing 1	DEPDC1	-1.07	-1.98	-6.09	-2.00
spindle pole body component 25 homolog (S. cerevisiae)	SPBC25	-1.24	-2.47	-7.37	-1.99
Rac GTPase activating protein 1	RACGAP1	-1.10	-1.56	-5.28	-1.98
B melanoma antigen	BAGE	4.37	3.24	-1.06	-1.98
NA	NA	1.96	3.30	-1.61	-1.97
NA	NA	3.54	2.46	-1.35	-1.96
NA	NA	3.71	4.22	1.01	-1.95
pro-platelet basic protein (chemokine (C-X-C motif) ligand 7)	PPBP	7.88	12.70	2.50	-1.95
NA	MGC14289	1.57	-1.11	-3.39	-1.95
chromosome 1 open reading frame 181	C1orf181	3.64	3.22	-1.13	-1.93
myelodysplasia syndrome 1	MDS1	3.64	2.52	-1.30	-1.93
NA	DKFZp434L142	-6.43	-6.59	-25.03	-1.92
NA	NA	3.56	4.07	-1.01	-1.92
centromere protein F 350/400ka	CENPF	-2.06	-2.64	-9.00	-1.92

Name[a]	Symbol	*Bb*[b]	IFNγ[b]	*Bb* + IFNγ[b]	Synergy Score[c]
serine peptidase inhibitor-like with Kunitz and WAP domains 1 (eppin)	SPINLW1	4.70	3.78	1.09	-1.92
NA	NA	3.19	2.98	-1.24	-1.91
Rho GTPase activating protein 18	ARHGAP18	-1.41	-1.10	-4.77	-1.90
v-maf musculoaponeurotic fibrosarcoma oncogene homolog (avian)	MAF	-1.19	-1.67	-5.45	-1.90
pyruvate dehydrogenase kinase isoenzyme 4	PDK4	-25.74	-11.27	-70.33	-1.90
NA	NA	3.49	3.01	-1.18	-1.90
tumor necrosis factor receptor superfamily member 11a NFKB activator	TNFRSF11A	-5.95	-3.76	-18.45	-1.90
c-mer proto-oncogene tyrosine kinase	MERTK	-3.83	-9.44	-25.05	-1.89
histamine N-methyltransferase	HNMT	-1.25	-1.23	-4.66	-1.88
ribonucleotide reductase M2 polypeptide	RRM2	-1.81	-2.51	-8.14	-1.88
aryl hydrocarbon receptor	AHR	1.21	-1.33	-4.06	-1.88
NA	LOC401131	3.76	2.10	-1.39	-1.88
transmembrane protein 55A	TMEM55A	-1.20	1.36	-3.61	-1.86
SMC2 structural maintenance of chromosomes 2-like 1 (yeast)	SMC2L1	-1.65	-2.00	-6.79	-1.86
NA	NA	2.90	2.70	-1.32	-1.85
MCM3 minichromosome maintenance deficient 3 (S. cerevisiae) associated protein	MCM3AP	3.06	3.04	-1.21	-1.85
NA	NA	1.61	1.36	-2.50	-1.84
NA	NA	3.05	3.15	-1.19	-1.84
NA	DKFZp434K2435	-1.24	1.72	-3.33	-1.83
NA	NA	3.84	3.03	-1.08	-1.82
TPX2 microtubule-associated homolog (Xenopus laevis)	TPX2	-1.76	-2.39	-7.54	-1.82
protein regulator of cytokinesis 1	PRC1	-1.86	-2.68	-8.25	-1.82
NA	FLJ90036	3.45	3.90	1.01	-1.81
cancer susceptibility candidate 5	CASC5	-1.07	-1.46	-4.59	-1.81
ATPase family AAA domain containing 2	ATAD2	1.17	-1.02	-3.40	-1.81
lactamase beta 2	LACTB2	-1.33	1.73	-3.45	-1.81

[a] Annotated and unannoted genes of the Affymetrix Human U33 Expression Array Plus 2.0

[b] Fold change in expression level of genes of macrophages stimulated by the appropriate agent compared to untreated macrophages.

[c] The synergy score is equal to the inverse of the levels of gene expression from macrophages stimulated with both IFNγ and *B. burgdorferi* together divided by the sum of the inverses of the levels of gene expression from macrophages treated with either stimulus alone; this number is multiplied by -1 to represent the negative value of the synergy score.

Figure 9. Incubation of Murine Macrophages with *B. burgdorferi* and IFNγ Alters the Expression of Chemokine Genes. Murine macrophages were incubated with medium alone, *B. burgdorferi*, IFNγ, or *B. burgdorferi* and IFNγ concurrently for 8 h. RNA was extracted from cells and analyzed using real-time RT-PCR for the following transcripts: CXCL1 (A), CXCL3 (B), CXCL9 (C), CXCL11 (D), CXCL16 (E), CCL12 (F), CXCL2 (G), and CXCL10 (H). Fold changes are relative to the level of transcripts in macrophages incubated with medium alone.

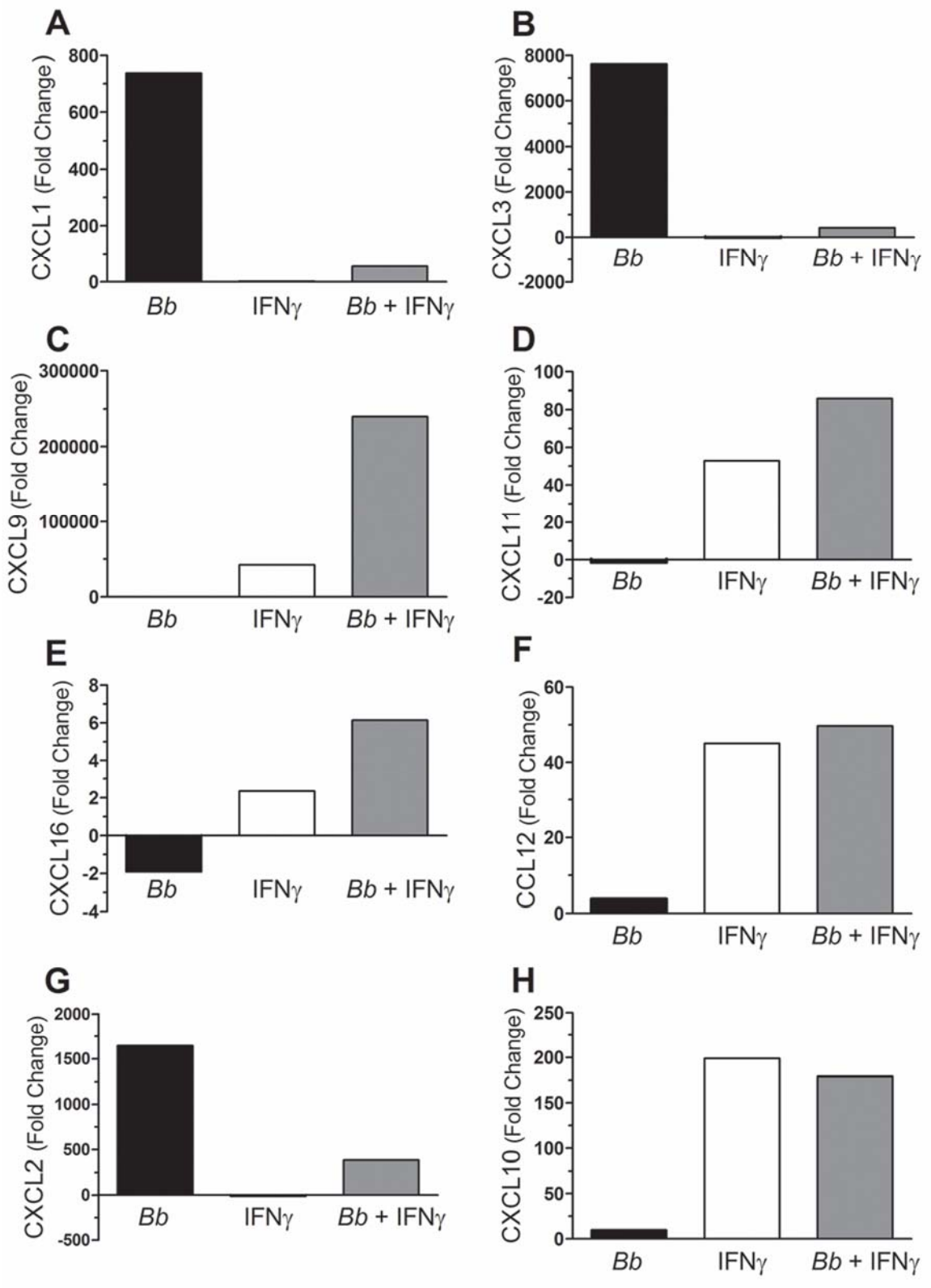
A
CXCL1 (Fold Change)
800
600
400
200
0
Bb
IFNγ
Bb + IFNγ
B
CXCL3 (Fold Change)
8000
6000
4000
2000
0
-2000
Bb
IFNγ
Bb + IFNγ
C
CXCL9 (Fold Change)
300000
200000
100000
0
Bb
IFNγ
Bb + IFNγ
D
CXCL11 (Fold Change)
100
80
60
40
20
0
-20
Bb
IFNγ
Bb + IFNγ
E
CXCL16 (Fold Change)
8
6
4
2
0
-2
-4
Bb
IFNγ
Bb + IFNγ
F
CCL12 (Fold Change)
60
40
20
0
Bb
IFNγ
Bb + IFNγ
G
CXCL2 (Fold Change)
2000
1500
1000
500
0
-500
Bb
IFNγ
Bb + IFNγ
H
CXCL10 (Fold Change)
250
200
150
100
50
0
Bb
IFNγ
Bb + IFNγ

Figure 10. IFNγ Alters the Pattern of Chemokines Secreted by *B. burgdorferi*-stimulated Macrophages. Murine macrophages were incubated with medium alone, *B. burgdorferi*, IFNγ, or *B. burgdorferi* and IFNγ concurrently for 24 h. Conditioned media were assessed by ELISA for the concentrations of CXCL1 (A), CXCL2 (B), CXCL9 (C), and CXCL10 (D). Data represent the means ± SD of triplicate samples. This experiment was repeated two more times with similar results. *** $p < 0.001$ compared to *B. burgdorferi* or IFNγ alone.

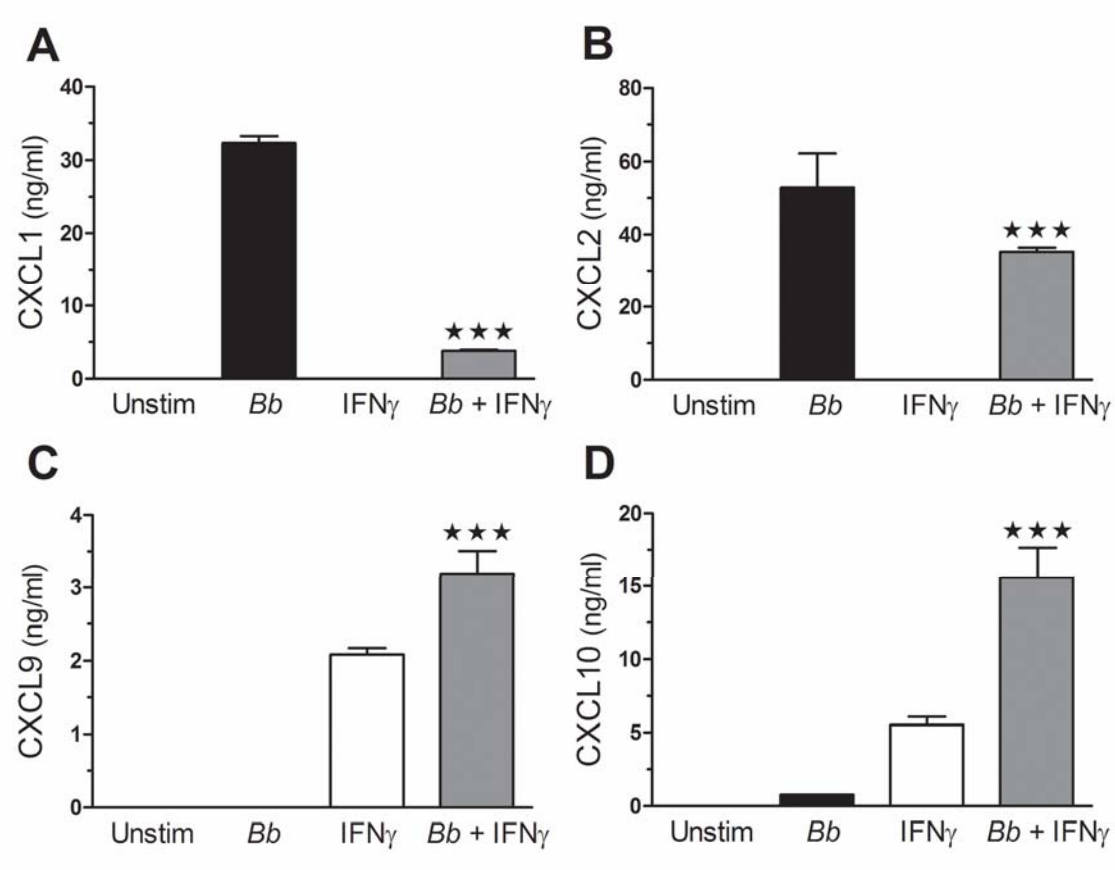
A
CXCL1 (ng/ml)
40
30
20
10
0
★★★
Unstim
Bb
IFNγ
Bb + IFNγ
B
CXCL2 (ng/ml)
80
60
40
20
0
★★★
Unstim
Bb
IFNγ
Bb + IFNγ
C
CXCL9 (ng/ml)
4
3
2
1
0
★★★
Unstim
Bb
IFNγ
Bb + IFNγ
D
CXCL10 (ng/ml)
20
15
10
5
0
★★★
Unstim
Bb
IFNγ
Bb + IFNγ

IV. The Role of IFNγ in the Development of Murine Lyme Carditis

To determine the role of IFNγ in the development of Lyme carditis in mice, wild-type and IFNγ-deficient C57BL/6 animals were injected intradermally with the pathogenic *B. burgdorferi* strain N40. Three individual experiments were conducted to compare the severity of carditis in the two types of mice at times ranging from 14 to 28 days post-infection. Lesions consisting of infiltrated leukocytes were seen in all infected mice (Figure 11, A-D) but not in sham-inoculated animals (Figure 11E). Histological examination of sections stained with hematoxylin and eosin revealed that the majority of infiltrating leukocytes were located at the base of the heart and root of the aorta, consistent with previous reports.[127,128,162] Mononuclear leukocytes were the predominate type of cell and were observed along the endocardium and in the myocardium (Figure 11, A-D). The severity of carditis in wild-type and IFNγ-deficient mice was assessed semi-quantitatively using a previously established scale of 0 to 3.[162] An initial study examined hearts harvested from mice 14, 21, and 28 days post-infection, and severity scores did not differ between wild-type and IFNγ-deficient mice at any of these times (Figure 12A). A second study measured severity of carditis at 14 and 25 days post-infection, and a third was performed at 25 days only. The combined results of these two studies are shown in Figure 12B. Consistent with the initial experiment, there was no difference in the severity of carditis assessed by histological staining between wild-type and IFNγ-deficient mice at 14 days or 25 days post-infection. Overall, the size and density of lesions within hearts of infected wild-type and IFNγ-deficient were comparable at all times examined.

Although the absence of IFNγ did not alter the severity of murine Lyme carditis, we investigated the possibility that IFNγ affects the composition of leukocytic infiltrates within

these cardiac lesions. This possibility is supported by our *in vitro* studies, wherein IFNγ increases the migration of T cells[158] and monocytes (Figure 1), but decreases that of neutrophils[158] and NK cells (Figure 2 and 3), across endothelium activated by *B. burgdorferi*. Moreover, while most infiltrating leukocytes were mononuclear, many neutrophils were apparent in hearts of IFNγ-deficient, but not wild-type, mice after 25 days of infection (compare Figure 11, B and D). Therefore, we employed immunofluorescent microscopy to analyze the leukocytic subtypes that constitute the lesions of Lyme carditis in wild-type and IFNγ-deficient mice. The numbers of B cells, NK cells, dendritic cells, T cells, neutrophils, and macrophages were counted in regions of inflammation using frozen sections prepared from the same hearts that were graded for severity of carditis in Figure 12B. B lymphocytes were not detected in lesions of Lyme carditis of wild-type or IFNγ-deficient mice at either 14 or 25 days post-infection (not shown). Additionally, NK cells (Figure 13, A and B) and dendritic cells (Figure 13, C and D) were rarely seen at these time points in either type of mouse. T cells were more prevalent within lesions than dendritic cells and NK cells, but they were still in the minority in both wild-type (Figure 13E) and IFNγ-deficient (Figure 13F) mice. Simultaneous staining for neutrophils and macrophages revealed that both were present within lesions of carditis in the two strains of mice, but macrophages predominated (Figure 13, G and H).

Quantitative analysis of the immunostained sections determined that there was an increase in the number of $CD3^+$ T cells in hearts of infected wild-type mice at 25 days post-inoculation relative to uninfected mice ($p < 0.001$) (Figure 14A). Gr-1^+ neutrophils were increased relative to sham-inoculated controls in both strains of mice at 14 days post-infection ($p < 0.01$), but only in IFNγ-deficient mice at 25 days ($p < 0.001$) (Figure 14B).

F4/80$^+$ macrophages were elevated in both strains of mice after infection for either 14 or 25 days ($p < 0.001$) (Figure 14C).

When amounts of T lymphocytes, neutrophils, and macrophages were compared between wild-type and IFNγ-deficient mice, there were no significant differences at 14 days post-infection. However, at 25 days post-infection, a shift in subtypes of leukocytes within lesions of Lyme carditis was observed. In the hearts of infected IFNγ-deficient mice, there was a decrease in the number of T cells compared to infected wild-type mice (Figure 14A). In contrast, there was an increase in the number of neutrophils in IFNγ-deficient mice relative to wild-type mice (Figure 14B). The population of F4/80$^+$ macrophages was increased in infected mice, but differences in genotype had no influence on amounts (Figure 14C). During the counting of neutrophils and macrophages, cells that were positively stained for both Gr-1 and F4/80 were observed. This lineage of myeloid cell[96] was present to some degree in all mice. However, the total number of Gr-1$^+$ F4/80$^+$ cells was greatly increased in the cardiac lesions of infected IFNγ-deficient mice compared to infected wild-type mice at both 14 and 25 days (Figure 14D).

The shift in the populations of neutrophils and T cells within IFNγ-deficient mice at 25 days could be the result of an altered number of spirochetes within the heart. Therefore, it was important to compare the spirochetal load in the hearts of infected wild-type and IFNγ-deficient mice. Through the use of quantitative real-time PCR, it was determined that hearts of wild-type and IFNγ-deficient mice contained comparable numbers of *B. burgdorferi* (Figure 15). From these data, it is evident that alterations in the composition of leukocytic infiltrates in the absence of IFNγ are not simply due to a change in spirochetal burden.

The differing types of leukocytes present in the hearts of wild-type and IFNγ-deficient mice could be due to differences in the chemokine profile found in lesions of carditis. Therefore, quantitative real-time RT-PCR was performed to measure levels of CXCL1, CXCL2, CXCL3, CXCL9, CXCL10, CXCL11, CXCL16, and CCL12 in heart tissues of uninfected or infected wild-type and IFNγ-deficient animals. However, no differences in levels of transcripts were seen among the groups (data not shown).

Figure 11. The Histopathology of Lyme carditis is Similar in Wild-type and IFNγ-deficient Mice. Wild-type (WT) and IFNγ-deficient (KO) mice were infected with *B. burgdorferi* N40 or inoculated with BSK medium as uninfected (UI) controls. Representative sections stained with hematoxylin and eosin from hearts of infected WT (A and B), infected KO (C and D) mice, and UI WT (E) at 25 days post-infection are shown. Boxed regions in panels A and C are magnified in panels B and D, respectively. Bars = 100 μm for panels A, C, and E, and 50 μm for panels B and D. V, base of ventricle; Ao, aorta; At, atrium.

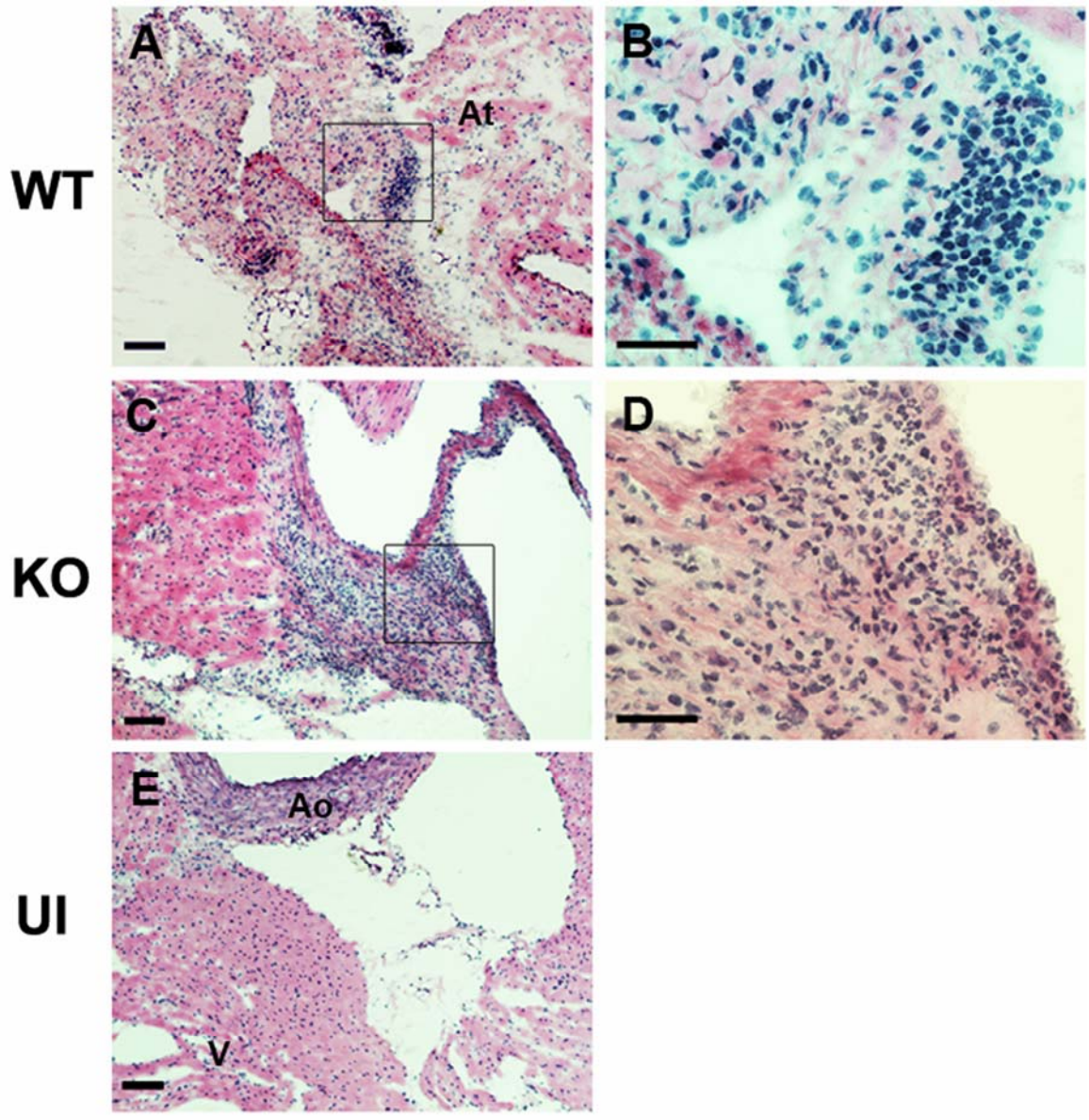
WT
KO
UI
A
At
B
C
D
E
Ao
V

Figure 12. IFNγ-deficient Mice Do Not Exhibit a Change in Severity of Carditis Compared to Wild-type Mice When Infected With *B. burgdorferi*. Wild-type and IFNγ-deficient mice were infected with *B. burgdorferi* N40. Five mice of each type were sacrificed at 14, 21, and 28 days (A) or 14 and 25 days (B) post-infection. Two mice of each strain inoculated with BSK medium only were sacrificed at the same time points. The severity of carditis was assessed by two independent observers as described in Materials and Methods. Horizontal bars indicate the mean score of carditis severity. Each data point represents the averaged severity score of an individual mouse. Data from uninfected mice at the various time points were combined. In Panel B, data from mice infected for 25 days were combined from two separate experiments.

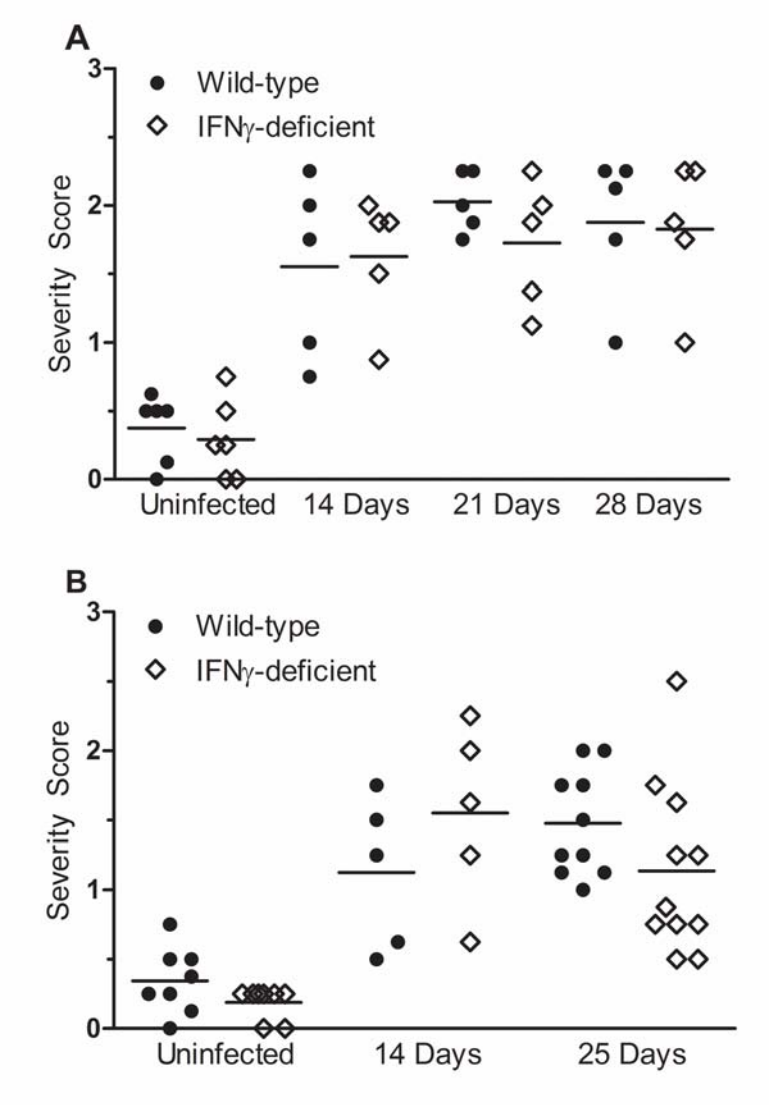
A
Wild-type
IFNγ-deficient
Severity Score
3
2
1
0
Uninfected
14 Days
21 Days
28 Days
B
Wild-type
IFNγ-deficient
Severity Score
3
2
1
0
Uninfected
14 Days
25 Days

Figure 13. The Composition of Leukocytic Infiltrates Differs in Hearts of Wild-type and IFNγ-deficient Mice Infected With *B. burgdorferi*. Wild-type (WT) and IFNγ-deficient (KO) mice were infected with *B. burgdorferi* N40. Representative sections from hearts of wild-type (A, C, E, and G) and IFNγ-deficient (B, D, F, and H) mice at 25 days post-infection are shown. Sections were stained with anti-NK1.1 (Green) to detect natural killer cells (A and B). To distinguish dendritic cells, anti-CD11c (Green) and anti-CD11b (Pink) were used concurrently (C and D). Anti-CD3 (Green) was used to detect T cells (E and F). Samples were incubated with anti-Gr-1 (Green) and anti-F4/80 (Red) concurrently to detect neutrophils and macrophages, respectively (G and H). Arrows point out examples of positively stained cells. Dendritic cells expressing both CD11c and CD11b are indicated by white staining (C). Arrowheads indicate examples of cells expressing both Gr-1 and F4/80 (H). Bars = 20 μm for all panels.

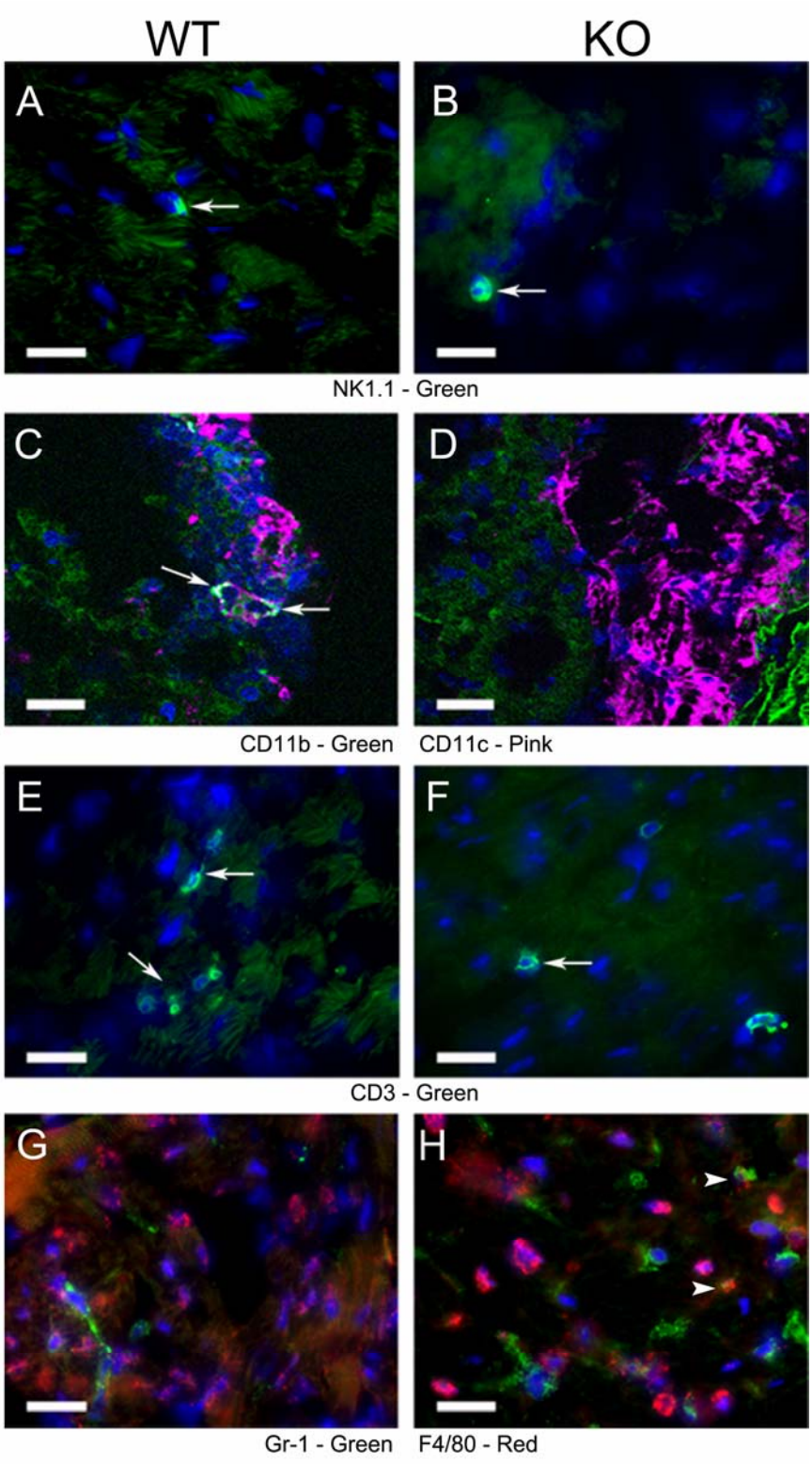
WT
KO
A
B
NK1.1 - Green
C
D
CD11b - Green
CD11c - Pink
E
F
CD3 - Green
G
H
Gr-1 - Green
F4/80 - Red

Figure 14. IFNγ Increases T cells and Decreases Neutrophils Within Lesions of Murine Lyme Carditis. Wild-type and IFNγ-deficient mice were infected with *B. burgdorferi* N40 or inoculated with BSK medium as uninfected controls. Hearts were collected at 14 and 25 days post-infection, sectioned, and stained with fluorescent antibodies against CD3 or both Gr-1 and F4/80 concurrently. Results show the total number of cells in ten 630× fields (mean ± SD) expressing CD3 (A), Gr-1 (B), F4/80 (C), or both Gr-1 and F4/80 (D). There was no difference between controls at 14 and 25 days post-infection, so data from the two time points were combined. Uninfected groups: n = 8 from two independent experiments; 14 Day groups: n = 5 from one experiment; 25 Day groups: n = 11 from two experiments. *** $p <$ 0.001 compared to wild-type at the same time point.

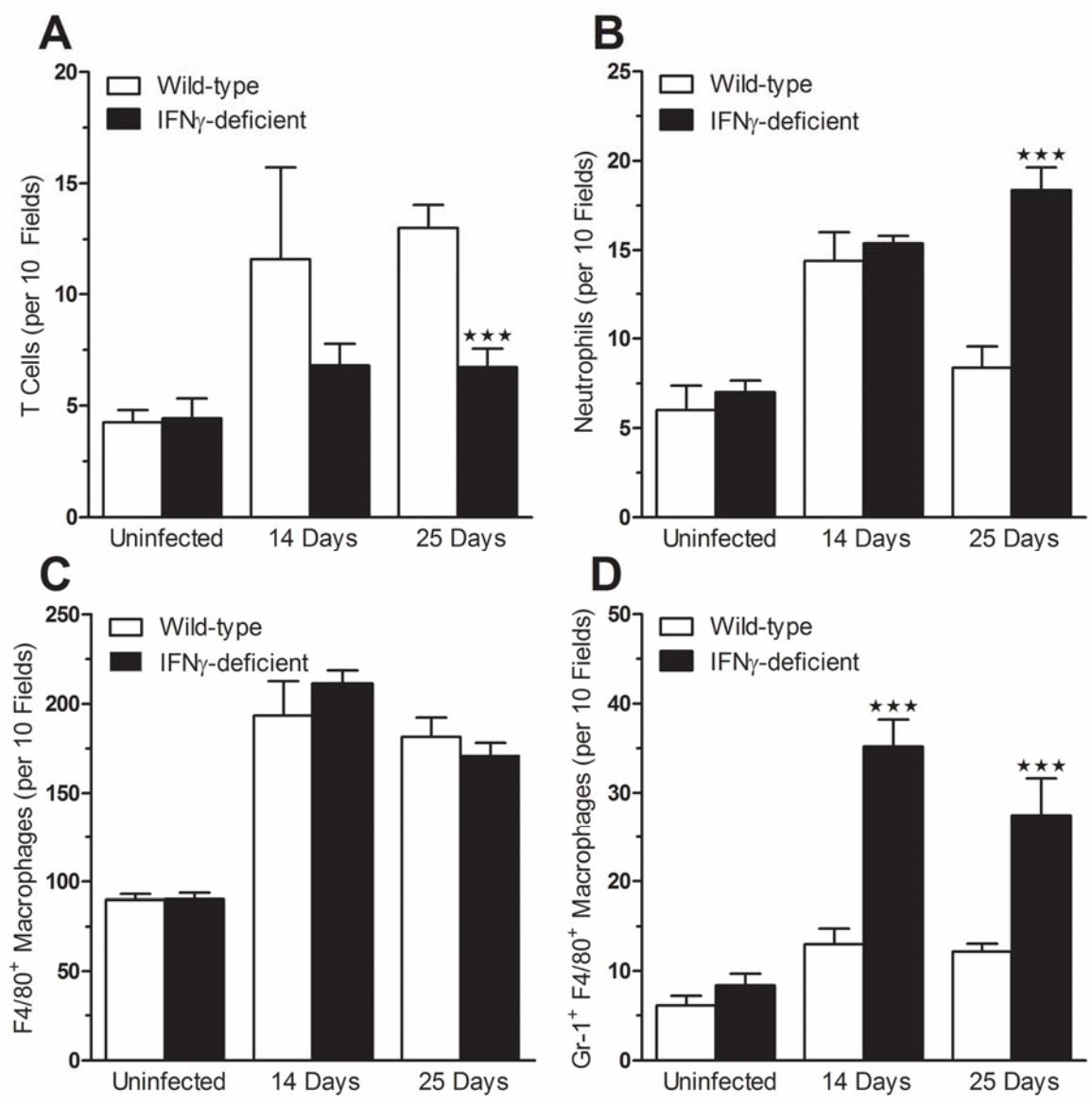
A
Wild-type
IFNγ-deficient
T Cells (per 10 Fields)
20
15
10
5
0
★★★
Uninfected
14 Days
25 Days
B
Wild-type
IFNγ-deficient
Neutrophils (per 10 Fields)
25
20
15
10
5
0
★★★
Uninfected
14 Days
25 Days
C
Wild-type
IFNγ-deficient
F4/80+ Macrophages (per 10 Fields)
250
200
150
100
50
0
Uninfected
14 Days
25 Days
D
Wild-type
IFNγ-deficient
Gr-1+ F4/80+ Macrophages (per 10 Fields)
50
40
30
20
10
0
★★★
★★★
Uninfected
14 Days
25 Days

Figure 15. Deficiency of IFNγ Does Not Alter Spirochetal Burden in Hearts of Infected Mice. Wild-type and IFNγ-deficient mice were infected with *B. burgdorferi* N40 or inoculated with BSK medium as uninfected controls. Hearts were collected at 25 days post-infection. DNA was extracted from the tissue and assessed using real-time PCR. The gene *recA* was used to measure the presence of *B. burgdorferi*. Samples were normalized to mouse *Nid1*, and data were plotted as means ± SD relative to uninfected controls of the same genotype. Wild-type group: n = 4; IFNγ-deficient group: n = 5.

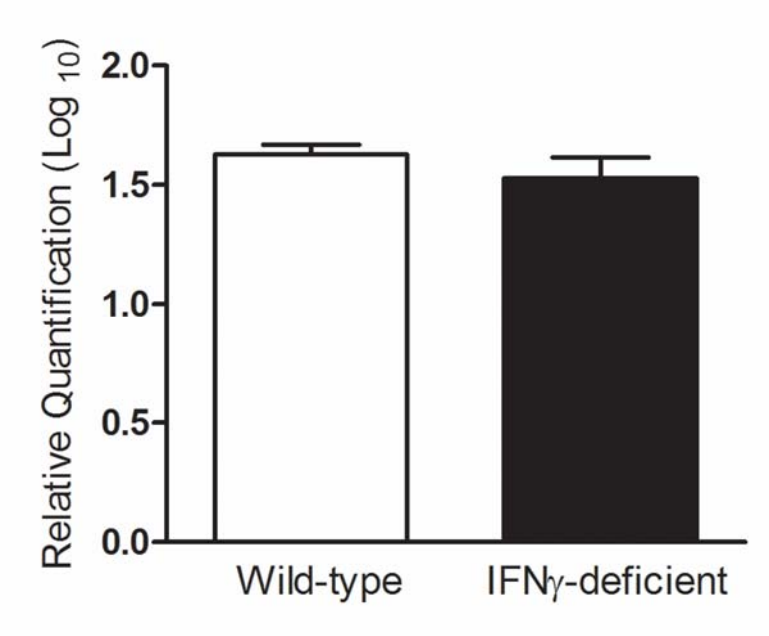
Relative Quantification (Log 10)
2.0
1.5
1.0
0.5
0.0
Wild-type
IFNγ-deficient

Discussion

I. IFNγ Alters the Migration of Monocytes and NK Cells Across Spirochete-stimulated Endothelium

A previous study showed that IFNγ synergizes with *B. burgdorferi* to promote secretion of seven chemokines from human endothelial cells. Six of the seven chemokines, CCL7, CCL8, CXCL9, CXCL10, CXCL11, and CX3CL1, attract leukocytes typical of chronic inflammation. The other, CXCL2, attracts cells of acute inflammation. Moreover, the addition of IFNγ to *B. burgdorferi*-activated HUVEC increases the migration of T cells and decreases that of neutrophils, which typify chronic and acute inflammation, respectively.[158] From these *in vitro* observations, it was reasoned that IFNγ may promote the development of chronic inflammation in Lyme disease. Monocytes are also present in lesions of chronic inflammation[10] and Lyme disease.[5,127] Therefore, it was predicted that IFNγ would positively influence recruitment of these cells across HUVEC activated by *B. burgdorferi*. Our data were in agreement with this hypothesis, and migration of monocytes was greater when HUVEC were incubated with both IFNγ and *B. burgdorferi* than with either stimulus alone (Figure 1).

Chemokines secreted by activated HUVEC are important for the transmigration of leukocytes. The addition of anti-CCL2 neutralizing antibodies diminishes the migration of monocytes across unstimulated HUVEC. However, the migration of monocytes across HUVEC treated with *B. burgdorferi* is blocked only partially by the anti-CCL2 antibodies.[135] The incomplete blockage of the migration of monocytes alludes to the idea that a single chemokine or factor may not be solely responsible for the migration of leukocytes typical of chronic inflammation into *B. burgdorferi*-infected tissues. The co-stimulation of HUVEC

with IFNγ and *B. burgdorferi* synergistically increases the production of chemoattractants for mononuclear cells that are not strongly secreted from endothelium activated by *B. burgdoferi* alone.[158] The increased diversity and amounts of chemokines for mononuclear cells are likely to be major factors in the increased migration of monocytes across HUVEC treated with IFNγ and *B. burgdorferi* together. However, the degree of importance of each chemokine during migration of monocytes *in vitro* and *in vivo* remains to be determined.

NK cells are typically found at sites of infection during the early stages of acute inflammation. Neutrophils are also present during acute inflammation, and their migration across *B. burgdorferi*-stimulated HUVEC is decreased with the addition of IFNγ.[158] Therefore, it might be predicted that the migration of NK cells would be decreased in a similar manner. However, the synergistic production of chemokines by HUVEC co-incubated with IFNγ and *B. burgdorferi* encompasses some that are attractants for NK cells, such as CXCL2, CXCL10, CXCL11, and CX3CL1.[173] We therefore tested whether IFNγ decreases or stimulates migration of NK cells across spirochete-stimulated HUVEC. The transmigration of NK cells was increased when HUVEC were treated with either IFNγ or *B. burgdorferi* alone. When the two stimuli were combined, a unique pattern emerged. Similar to that of neutrophils, the migration of NK cells was diminished when IFNγ was added to HUVEC activated by *B. burgdorferi*. However, the adhesion of NK cells to HUVEC was increased with the two stimuli together compared to either alone (Figure 2). In contrast, IFNγ had no effect on adhesion of neutrophils to spirochete-activated endothelium.[158]

The migration of neutrophils across *B. burgdorferi*-stimulated HUVEC is dependent on CXCL8.[134] However, the decrease in the transmigration of neutrophils due to the addition of IFNγ is not the result of a reduction in the secretion of CXCL8 from HUVEC.[158] In fact,

the two stimuli together synergistically increase transcripts encoding CXCL2, a potent chemoattractant of neutrophils.[158] Therefore, it is unlikely that the impaired migration of leukocytes typical of acute inflammation *in vitro* is the result of diminished chemokine production by endothelial cells.

NK cells are a heterogeneous population divided by the differential expression of CD56 and CD16. $CD56^{bright}$ $CD16^{-}$ NK cells express high levels of CXCR3, CCR5 and CCR7 and exhibit a strong attraction to CXCL10 and CXCL11. They lack or minimally express CXCR1 and CXCR2, which are the receptors for the neutrophil chemoattractants CXCL1, CXCL2, and CXCL8.[173] $CD56^{bright}$ $CD16^{-}$ NK cells also account for the vast majority of NK cells in lesions of inflammatory diseases and are responsible for the secretion of IFNγ and other pro-inflammatory cytokines.[174] $CD56^{dim}$ $CD16^{+}$ NK cells represent 90% of the circulating population of NK cells in the blood and express CXCR1, CXCR2, and CX3CR1. $CD56^{dim}$ $CD16^{+}$ NK cells rapidly respond to CX3CL1. The action of CXCL1 and CXCL8 on these NK cells also has been reported, but there are conflicts in the literature.[173]

Both of these populations of NK cells were isolated from the peripheral blood for the migration studies reported herein. The increase in the migration of NK cells across HUVEC activated by *B. burgdorferi* (Figure 2) is likely to be due to the more abundant $CD56^{dim}$ $CD16^{+}$ NK cells. This assumption is based on the fact that such HUVEC secrete chemokines that would be expected to predominantly attract the $CD56^{dim}$ $CD16^{+}$ NK cell subtype, namely CX3CL1, CXCL2, and CXCL8.[173] IFNγ increases the transmigration of $CD56^{bright}$ NK cells compared to $CD56^{dim}$ NK cells.[175] Furthermore, when IFNγ alone is added to HUVEC, there is an increase in the secretion of CXCL10 and CXCL11, which are attractants for $CD56^{bright}$ $CD16^{-}$ NK cells.[173] Therefore, although either *B. burgdorferi* or IFNγ promoted the

transmigration of NK cells (Figure 2), it is possible that the subtypes that responded were different. The coaction of IFNγ and *B. burgdorferi* on HUVEC resulted in a decrease in the migration of NK cells but an increase in their adhesion to the activated endothelium (Figure 2). As discussed above, the two subtypes of NK cells possess different properties, and it would be of interest to determine the identity of those NK cells that migrate and those that remain adherent when HUVEC are activated by both agents.

The reduction in the migration of neutrophils and NK cells across endothelium exposed to both IFNγ and *B. burgdorferi* could be the result of a secreted, soluble factor. Soluble GAGs bind to a range of chemokines and disrupt the formation of chemotactic gradients. These receptors can be secreted by pathogens as a means of dampening the immune response.[176] However, it is unlikely that *B. burgdorferi* are releasing abundant GAGs, because neutrophils and NK cells migrate across HUVEC stimulated by spirochetes alone. MMPs are secreted by endothelium, and MMP9 is found in skin lesions of patients with Lyme disease.[177] It is also possible for MMPs to inactivate chemokines, such as CXCL8,[178] through proteolysis.[176] To test whether such a soluble factor might be suppressive in our system, conditioned medium was collected from HUVEC treated with IFNγ and *B. burgdorferi* together and incubated with neutrophils before allowing the leukocytes to migrate in response to CXCL8. Using both chemotaxis (Figure 4) and HUVEC-amnion cultures (Figure 5) as means of assessment, the conditioned medium from cultures activated with both IFNγ and *B. burgdorferi* did not inhibit migration. Therefore, the suppressed transmigration of neutrophils and NK cells is not likely due to a soluble factor. However, the involvement of an unstable soluble factor cannot be dismissed.

II. Alterations in Adhesion Molecules by IFNγ May Affect Migration of Leukocytes Across Spirochete-activated Endothelium

HUVEC stimulated by both IFNγ and *B. burgdorferi* have a synergistic gene induction of VCAM-1[158] and increased surface expression of ICAM-1 and VCAM-1 (Figure 8, A and B). Monocytes are able to use both ICAM-1 and VCAM-1 as a means of migration across endothelium.[179] Integrins CD11/CD18 and VLA-4 bind to ICAM-1 and VCAM-1, respectively, and are found on monocytes and NK cells. The blockage of VLA-4 alone does not have a profound effect on migration of monocytes across *B. burgdorferi*-stimulated HUVEC, while blockage of CD18 reduces migration by 35%. However, the combination of the two blocking antibodies suppresses the migration of monocytes nearly completely.[135] Likewise, a severely diminished migration of neutrophils across spirochete-activated endothelium is observed when CD18 is inhibited.[132] Due to the importance of ICAM-1 and VCAM-1 to the migration of monocytes, the increased expression of these adhesion molecules could be promoting the increase in traversal of these leukocytes across HUVEC activated by IFNγ and *B. burgdorferi*. Seemingly arguing against this possibility is that migration of neutrophils across the doubly-activated HUVEC is reduced,[158] despite their dependence on ICAM-1. However, the two stimuli together caused a more dramatic increase in the expression of VCAM-1 than ICAM-1 (compare Figure 8A to 8B). Since neutrophils do not bind to VCAM-1, it is possible that it is the increase in VCAM-1 alone that is driving the enhanced migration of the monocytes.

The reduction in the migration of NK cells when HUVEC were treated with IFNγ and *B. burgdorferi* could have been due to a slower rate of migration. However, a 24-h migration yielded similar results as a 4-h migration (Figure 3). Therefore, the suppression of migration

of NK cells across these HUVEC-amnion cultures appears to be a true blockade. The increased adhesion of NK cells to HUVEC treated with both IFNγ and *B. burgdorferi* could be arresting their subsequent migration. The adhesion of NK cells to VCAM-1 is three times higher than that of T cells,[180] and one could reason that the increased adhesion to the doubly-activated HUVEC is due to the increase in expression of VCAM-1. However, as discussed above, monocytes also interact with VCAM-1, and their migration is actually enhanced when IFNγ and *B. burgdoferi* are both added to HUVEC (Figure 1). Further studies are required to resolve this apparent paradox and determine whether augmented expression of ICAM-1 and/or VCAM-1 contributes to the observed alterations in patterns of transmigration.

Many adhesion molecules are expressed at the junctions of endothelial cells, such as PECAM, CD99, ICAM-2, junctional adhesion molecule family members, and ESAM, and they play an important role in the migration of leukocytes.[47] Mice deficient in these adhesion molecules demonstrate that the transmigration of neutrophils through the endothelial junction occurs in distinct and sequential steps.[181] Rival et al.[169] showed that the adhesion of neutrophils to endothelium is increased with the co-treatment of IFNγ and TNFα, resulting in a decrease in the transmigration of these leukocytes. It was concluded that the two stimuli disrupt the localization of PECAM to the junctional borders of endothelial cells, thereby impairing movement of the neutrophils through the junctions.[169] Likewise, the addition of either polyclonal or monoclonal antibodies against PECAM increases the adhesion of NK cells to endothelial cells by as much as three-fold. These antibodies block equally the migration of $CD56^{bright}$ $CD16^{-}$ and $CD56^{dim}$ $CD16^{+}$ NK cells across unstimulated endothelium. However, when the endothelium is activated, the transmigration of $CD56^{bright}$

CD16$^-$ NK cells is not inhibited by anti-PECAM.[175] The experiments investigating PECAM were performed using artificial membranes as a substrate for culture of HUVEC.[169] Therefore, we examined the effects of IFNγ and TNFα on the migration of NK cells across HUVEC-amnion cultures to see if our system would yield similar results. The migration of NK cells across HUVEC-amnion cultures activated by TNFα was increased, similar to the effects of *B. burgdorferi* (Figure 6). Likewise, the addition of both IFNγ and TNFα to HUVEC resulted in a similar migration and adhesion pattern as observed when HUVEC were stimulated simultaneously with IFNγ and *B. burgdorferi*. Moreover, since these observations mirrored those of Rival et al.,[169] we reasoned that activation by IFNγ and *B. burgdorferi* together might be disrupting endothelial junctional molecules.

Consequently, we examined the surface expression of PECAM, ESAM, and CD99 on HUVEC-amnion cultures treated with IFNγ and/or *B. burgdorferi* using immunofluorescent microscopy. The expression of CD99, which acts downstream of PECAM and is required for the migration of both monocytes and neutrophils,[171] was unchanged (Figure 7B). The inhibition of ESAM *in vivo* reduces the migration of neutrophils in response to chemically induced inflammation in mice without preventing the migration of lymphocytes. In addition, the absence of ESAM does not affect the rolling and adhesion of leukocytes *in vivo* as assessed by intravital microscopy.[67] These data make the disruption of ESAM a plausible cause for the suppressed migration of NK cells and neutrophils across HUVEC stimulated with IFNγ and *B. burgdorferi*. However, the expression of ESAM was also unchanged under those conditions (Figure 7C). In contrast, PECAM was dispersed from the junctional borders on HUVEC activated by both IFNγ and *B. burgdorferi* (Figure 7A). However, the total surface expression was not reduced by co-incubation of the HUVEC compared to either

stimulus alone (Figure 6C). This alteration in localization may remove PECAM available for interactions with NK cells at the lateral border of endothelial cells, resulting in reduced efficiency of NK cell transmigration. While the amount of surface PECAM remained consistent regardless of stimuli, co-incubation of HUVEC with IFNγ and *B. burgdorferi* clearly altered its spatial distribution. A previous publication using TNFα and IFNγ together also reports changes in localization of PECAM, while gene transcription remains constant.[182]

Whereas the PECAM is required for the transendothelial migration of monocytes,[170] there is evidence that different domains of PECAM interact with monocytes during select stages of this process.[170] In the presence of anti-PECAM antibodies, the directed recycling of PECAM to lateral borders is disrupted. However, intracellular stores of PECAM may still promote the migration of leukocytes through the body of an endothelial cell rather than through the junctions.[183] It is possible that in our system monocytes, but not NK cells, are able to migrate across doubly-stimulated endothelium in a manner that does not depend on the presence of PECAM in the junctions. However, this scenario remains to be proven.

III. IFNγ Affects the Expression and Secretion of Chemokines by Macrophages Exposed to *B. burgdorferi*

The ability of IFNγ and *B. burgdorferi* to synergistically induce macrophages, like endothelium,[158] to produce chemokines that attract cells typical of chronic inflammation was examined. A synergistic induction of genes encoding chemokines that attract mononuclear leukocytes (*Cxcl9*, *Cxcl11*, *Cxcl16* and *Ccl12*) was observed when murine macrophages were stimulated with both IFNγ and *B. burgdorferi* (Figure 9). Additionally, the secretion of CXCL9 and CXCL10 from murine macrophages activated by the two stimuli was

synergistically increased (Figure 10). Likewise, the secretion of CXCL9 and CXCL10 is increased when murine cardiac endothelial cells (MCEC) are treated with IFNγ and *B. burgdorferi* together (S. C. McAllister and M. B. Furie, unpublished results).

In contrast, the addition of IFNγ to murine macrophages stimulated by *B. burgdorferi* synergistically decreased the levels of transcripts for CXCL1, CXCL2, and CXCL3, which are potent attractants for neutrophils. This decrease was confirmed at the protein level for CXCL1 and CXCL2 (Figure 10), whose receptor, CXCR2, is required for the migration of neutrophils into joints during murine Lyme arthritis.[125] CXCL1 also regulates the infiltration of neutrophils into lesions of murine Lyme carditis.[142] However, the addition of IFNγ did not reduce the secretion of the neutrophil attractants CXCL1 and CXCL2 in MCEC activated by *B. burgdorferi* (S. C. McAllister and M. B. Furie, unpublished results). Therefore, it appears that murine macrophages and endothelial cells respond to the coaction of IFNγ and *B. burgdorferi* differently.

The specific chemokines expressed by human macrophages differed from those induced in HUVEC in response to IFNγ and *B. burgdorferi* together. CXCL9, CXCL10, CXCL11 are synergistically upregulated when human endothelium is activated by IFNγ and *B. burgdorferi* together.[158] Notably, both CXCL9 and CXCL10 are observed in the synovial fluid of patients with chronic Lyme disease[120] and septic arthritis,[184,185] while CXCL9 is present in autoimmune arthritis.[186] However, no chemokines synergistically upregulated by the activation of human macrophages with IFNγ and *B. burgdorferi* matched those synergistically increased in HUVEC. Although CXCL9, CXCL10, and CXCL11 were highly induced in human macrophages activated by IFNγ and *B. burgdorferi*, the increase was not synergistic. Nonetheless, the chemokines synergistically upregulated in macrophages, as a

whole, would be expected to promote the influx of mononuclear cells typical of chronic inflammation. Stimulation of human macrophages with IFNγ and *B. burgdorferi* did synergistically reduce the expression of genes encoding the neutrophil chemoattractants CXCL2, CXCL5, and CXCL6. However, IFNγ does not reduce secretion of CXCL8 by HUVEC activated with *B. burgdorferi*. Moreover, levels of transcripts for CXCL2 in HUVEC are synergistically induced by the two stimuli.[158]

Collectively, these results raise the possibility that chemokines secreted by macrophages play a more important role in recruitment of neutrophils into lesions of Lyme disease than those produced by endothelial cells. Moreover, IFNγ dampens migration of neutrophils across spirochete-stimulated HUVEC *in vitro*, despite the fact that expression of chemokines important for their recruitment is not decreased.[158] Perhaps, then, alterations in other factors necessary for extravasation, such as endothelial cell adhesion molecules, also are involved in the mechanism by which IFNγ down-modulates the migration of neutrophils.

IV. IFNγ and *B. burgdorferi* Activate Similar Pathways in Murine and Human Macrophages

The effect of IFNγ and *B. burgdorferi* together on human and murine macrophages compared to either stimulus alone was not markedly species-specific. While the number of genes synergistically upregulated in human macrophages was much greater than in mice, the pathways involved were quite similar. Genes encoding adhesion molecules involved in antigen presentation and cell-cell signaling were induced in both species. Moreover, expression of many genes playing roles in apoptosis and cytotoxicity was increased. In addition, IFNβ was synergistically upregulated in both species; this cytokine was recently

linked to the development of early murine Lyme arthritis.[187] Also, the effect of IFNγ and *B. burgdorferi* together on human and murine macrophages compared to either stimulus alone was not species-specific in respect to synergistically downregulated genes. As a whole, both species of macrophages downregulated genes involved in the cell cycle and DNA replication.

The response of human and murine macrophages differed in the specific genes of chemokines that were synergistically upregulated. Genes of CC chemokines were induced in human macrophages, while murine macrophages increased the expression of CXC chemokines that attract mononuclear leukocytes. Both groups of synergistically-upregulated chemokines, however, act specifically on mononuclear leukocytes. One striking difference between the two species was the comprehensive induction of genes for the TNF superfamily and their corresponding receptors by human macrophages. In addition, upregulated genes involved in the NF-κB pathway were more numerous in human cells than in mouse macrophages. Despite these differences, the responses of human and murine macrophages to co-stimulation with IFNγ and *B. burgdorferi* are globally similar.

While no other group has published a report examining the response of macrophages to both IFNγ and *B. burgdorferi* together, there are studies measuring the response of monocytes to live spirochetes alone. As observed in our microarray analysis of macrophages, *B. burgdorferi* increases the expression by monocytes of pro-inflammatory cytokines, such as IL-1β and TNFα, and induces components of the NF-κB pathway.[188] IFNβ and Slamf7, which functions in NK cell activation, are also highly induced in monocytes exposed to live spirochetes. Similar to our microarray data, expression of genes involved in cytoskeletal architecture is greatly reduced.[154]

V. IFNγ Alters the Composition of Leukocytes in Murine Lyme Carditis

The presence of IFNγ positively correlates with severity of Lyme disease in humans.[147] However, studies of the role of IFNγ in murine Lyme arthritis have reached conflicting conclusions. Treatment of infected mice with anti-IFNγ antibodies reduces joint swelling.[150,159] Additionally, neutralization of IL-4, which opposes the function of IFNγ, exacerbates arthritis.[159] These data support the notion that IFNγ contributes to the evolution of inflammation. In contrast, IFNγ-deficient and IFNγ receptor-deficient mice develop the same severity of Lyme arthritis as wild-type animals, which suggests that IFNγ is not required for progression of disease.[160,161]

The role of IFNγ in murine Lyme carditis has been previously investigated through indirect means. Stat1-deficient mice, which have defects in signaling pathways induced by IFNα, IFNβ, and IFNγ, show an increase in the extent of carditis but not arthritis at 21 days post-infection.[162] This observation suggests that IFNγ may play a protective role in murine Lyme carditis. In contrast, mice deficient in IL-4 develop more severe carditis after infection with *B. burgdorferi*. These mice produce abnormally high levels of IFNγ, which implys that IFNγ may exacerbate carditis.[163] In both instances, spirochetal loads are similar in hearts of wild-type and knockout animals, even though the severity of carditis differs. To examine the effects of IFNγ on the progression of murine Lyme carditis directly, we infected mice that were incapable of producing IFNγ with *B. burgdorferi*. Hearts were scored for severity of carditis, and no difference between wild-type and IFNγ-deficient strains was measured at any time (Figure 12). Similar to the previous reports,[162,163] spirochetal burdens in hearts of the two strains of mice were the same (Figure 15). One previous publication also directly examined the role of IFNγ in Lyme carditis using IFNγ receptor-deficient mice. In contrast to

our results, these authors observed that loss of the receptor produced a slight increase in severity, as well as a greater spirochetal load in the heart, at 14 days after infection.[164] The differences in strain of mouse, strain of *B. burgdorferi*, and route of inoculation might account for the disparity.

Although IFNγ did not alter the severity of murine carditis in our study (Figures 11 and 12), we speculated that it might still be influencing the types of leukocytes that infiltrate cardiac lesions. Identification of leukocytes in hearts of infected wild-type or IFNγ-deficient mice showed very few natural killer cells, B cells, or dendritic cells at 14 or 25 days post-infection. While stimulation of HUVEC with both IFNγ and *B. burgdorferi* causes a reduction in the migration of NK cells (Figure 2), the lack of NK cells was even observed in IFNγ-deficient mice. NK cells respond early to sites of infection, and it is possible that the rarity of NK cells in murine Lyme carditis of wild-type and IFNγ-deficient mice was due to timing. By 14 days, carditis may have progressed past the time when NK cells are present. There could be a species differences as well. NK cells of mice do not express CD56. While a recent study has divided murine NK cells into two subtypes that resemble human $CD56^{bright}$ $CD16^{-}$ and $CD56^{dim}$ $CD16^{+}$ NK cells, their receptors and function are not identical to those of human NK cells.[189] Therefore, NK cells of humans and mice could react differently to the mediators that control the development of Lyme disease.

The predominant leukocyte observed in the hearts of both wild-type and IFNγ-deficient infected mice was the macrophage (Figure 13), which is consistent with other publications.[122,128,162] There was no difference in the populations of leukocytes in wild-type and IFNγ-deficient mice at 14 days post-infection. However, when the two strains were compared at 25 days after infection, IFNγ-deficient mice had more neutrophils in lesions of

carditis, whereas the number of T cells was decreased (Figure 14, A and B). It is likely that the larger population of neutrophils observed in IFNγ-deficient mice is due to an enhanced recruitment of the leukocytes, since they are short-lived cells in tissues.[74] This shift in the profile of leukocytes demonstrates an integral role for IFNγ in the progression of murine Lyme carditis.

Unlike T cells and neutrophils, F4/80$^+$ macrophages were found in similar numbers in infected IFNγ-deficient and wild-type mice at both time points examined. F4/80 is not highly expressed on all macrophages,[190] so it is possible that some of these leukocytes were not counted in our analysis. Strikingly, there was an increase in the amount of F4/80$^+$ cells that also expressed Gr-1 in the lesions of IFNγ-deficient mice at both 14 and 25 days (Figures C and D). IFNγ is required for macrophages to mature into inflammatory M1 macrophages. This subset of mature macrophages is a prominent secretor of pro-inflammatory cytokines.[96] The Gr-1$^+$ F4/80$^+$ macrophages that were observed are likely to be myeloid-derived suppressor cells, which are immature cells that can exhibit both monocyte-like and neutrophil-like properties. These cells typically play a role in wound healing within the heart.[96] Gr-1$^+$ F4/80$^+$ macrophages, however, were not prevalent in infected wild-type mice in our study. Therefore, they are unlikely to play a major role in the progression of Lyme disease. Our results indicate that IFNγ indeed influences the composition of leukocytic infiltrates in hearts of infected mice, since lesions in IFNγ-deficient animals have more neutrophils and fewer T cells than those in wild-type mice.

This dissertation research and published *in vitro* observations[158] support the idea that chemokines derived from murine macrophages and endothelial cells shape the composition of leukocytic infiltrates in murine Lyme carditis. In hearts of infected mice, IFNγ promoted

the accumulation of T lymphocytes. Likewise, IFNγ enhanced the production of attractants for T cells by endothelial cells[158] and macrophages exposed to *B. burgdorferi*. IFNγ also suppressed recruitment of neutrophils into lesions of Lyme carditis, and it reduced production of chemoattractants for neutrophils by spirochete-stimulated macrophages. These data support the hypothesis that IFNγ is fostering a shift from acute to chronic inflammation in human Lyme disease.

VI. IFNγ Promotes Chronic Inflammation in Illnesses Other Than Lyme Disease

B. burgdorferi elicits inflammatory responses that mirror other forms of chronic inflammation. Arthritic lesions in Lyme disease and rheumatoid arthritis have similar pathology, and both contain T cells, which are primarily T helper cells, distributed throughout the affected tissue.[191] As with *B. burgdorferi*, IFNγ synergizes with ligands of Toll-like receptors, such as peptidoglycan, dsRNA, flagellin, and lipopolysaccharide, to increase the secretion of CXCL9 and CXCL11 from fibroblasts[184] and CXCL9, CXCL10, and CXCL11 from human microvascular endothelial cells.[186] In our study, IFNγ was required for an influx of T cells and disappearance of neutrophils as Lyme carditis progressed, and it controls a shift in the profile of infiltrating leukocytes in other inflammatory conditions as well. In cardiac allografts in IFNγ-deficient mice, T cells and other mononuclear leukocytes that normally accumulate are replaced by large numbers of neutrophils.[192] Additionally, the absence of IFNγ results in an increased proportion of neutrophils infiltrating into the central nervous system of mice during experimental autoimmune encephalomyelitis.[193] As we observed in murine Lyme carditis, IFNγ is altering the composition of leukocytic populations in these instances by promoting the infiltration of mononuclear cells and suppressing that of

neutrophils. These results support the premise that IFNγ is acting a molecular switch in the progression of acute to chronic inflammation not only in Lyme disease, but in other inflammatory conditions as well.

Future Directions

Further investigation is required to uncover the role of adhesion molecules in migration of leukocytes across HUVEC stimulated by both IFNγ and *B. burgdorferi*. CD99 antigen like-2 (CD99L2) is required for the transendothelial migration of neutrophils, but as with ESAM, its absence does not diminish the migration of T lymphocytes.[194,195] In mice, CD99L2 and CD99 are required for the migration of neutrophils and can act independently from PECAM under certain conditions of stimulation.[196] The use of blocking antibodies against these surface adhesion molecules during transmigration of leukocytes may help to decipher the mechanism by which IFNγ suppresses the migration of NK cells and neutrophils across spirochete-stimulated endothelium. Showing that a specific adhesion molecule is required for movement of neutrophils or NK cells across HUVEC stimulated by spirochetes alone would buttress the argument that its loss in doubly-activated cells contributes to reduced transmigration. However, if the expression of an essential adhesion molecule is being reduced by the coaction of IFNγ and *B. burgdorferi*, directly proving that the loss is responsible for the suppressed migration of neutrophils or NK cells will be difficult due to the negative phenotype.

Select chemokines that were synergistically induced in murine macrophages activated by IFNγ and *B. burgdorferi* together were analyzed at both the transcript and protein levels. However, confirmation of the synergistic increases and decreases in the expression of chemokines by human macrophages, as measured by microarray, has not yet been completed. Extending this analysis would expand the knowledge of species-specific responses of macrophages to *B. burgdorferi* and IFNγ. A thorough analysis of the responses of MCEC to IFNγ and/or *B. burgdorferi* through the use of microarray or cytokine array may provide

insights on why there is a difference between the leukocytes present in lesions of human arthritis and those in murine Lyme arthritis. It would also aid in understanding the differences in the immune responses of humans and mice to *B. burgdorferi* in terms of pro- and anti-inflammatory cytokines and adhesion molecules. Likewise, it would enable further comparison between the functions of macrophages and endothelium in Lyme disease.

In vivo analysis of the cytokines and chemokines present in lesions of murine Lyme carditis would also help to illuminate the factors causing the shift in the profile of leukocytes in hearts of wild-type and IFNγ-deficient mice. In addition, measuring the proportion of cells within lesions of carditis that secrete IFNγ and chemoattractants would help specify the responsibilities of leukocytic subtypes during the development and progression of disease. Our attempted analysis of the chemokines found within lesions of Lyme carditis by real-time RT-PCR did not reveal differences between uninfected and infected mice. This failure could be due to the limited size and severity of the carditis in the mouse strain used (C57BL/6). Therefore, it may be beneficial to use C3H/HeN mice, which develop much greater pathology.[127] Alternatively, it might be possible to overcome this technical issue through the use of *in situ* immunohistochemistry.[197] This method would allow for the semi-quantitative detection of chemokines and cytokines in lesions of Lyme carditis by microscopic examination.

Reference List

1. Benach JL, Bosler EM, Hanrahan JP, Coleman JL, Habicht GS, Bast TF, Cameron DJ, Ziegler JL, Barbour AG, Burgdorfer W, Edelman R, Kaslow RA: Spirochetes isolated from the blood of two patients with Lyme disease. N Engl J Med 1983, 308:740-742

2. Duray PH: Histopathology of clinical phases of human Lyme disease. Rheum Dis Clin North Am 1989, 15:691-710

3. Steere AC, Glickstein L: Elucidation of Lyme arthritis. Nat Rev Immunol 2004, 4:143-152

4. Keane-Myers A, Maliszewski CR, Finkelman FD, Nickell SP: Recombinant IL-4 treatment augments resistance to *Borrelia burgdorferi* infections in both normal susceptible and antibody-deficient susceptible mice. J Immunol 1996, 156:2488-2494

5. Duray PH, Steere AC: Clinical pathologic correlations of Lyme disease by stage. Ann N Y Acad Sci 1988, 539:65-79

6. Lawrence T, Gilroy DW: Chronic inflammation: a failure of resolution? Int J Exp Pathol 2007, 88:85-94

7. Krishnaswamy G, Kelley J, Yerra L, Smith JK, Chi DS: Human endothelium as a source of multifunctional cytokines: molecular regulation and possible role in human disease. J Interferon Cytokine Res 1999, 19:91-104

8. Winsauer G, de Martin R: Resolution of inflammation: intracellular feedback loops in the endothelium. Thromb Haemost 2007, 97:364-369

9. Ryan GB, Majno G: Acute inflammation. A review. Am J Pathol 1977, 86:183-276

10. Sherwood ER, Toliver-Kinsky T: Mechanisms of the inflammatory response. Best Pract Res Clin Anaesthesiol 2004, 18:385-405

11. Henson PM: Dampening inflammation. Nat Immunol 2005, 6:1179-1181

12. Hanada T, Yoshimura A: Regulation of cytokine signaling and inflammation. Cytokine Growth Factor Rev 2002, 13:413-421

13. Cannon JG: Inflammatory Cytokines in Nonpathological States. News Physiol Sci 2000, 15:298-303

14. Dinarello CA: Biologic basis for interleukin-1 in disease. Blood 1996, 87:2095-2147

15. Dawson J, Rordorf-Adam C, Geiger T, Towbin H, Kunz S, Nguyen H, Zingel O, Chaplin D, Vosbeck K: Interleukin-1 (IL-1) production in a mouse tissue chamber model of inflammation. II. Identification of (tissue) macrophages as the IL-1 producing cells and the effect of anti-inflammatory drugs. Agents Actions 1993, 38:255-264

16. Marceau F, Grassi J, Frobert Y, Bergeron C, Poubelle PE: Effects of experimental conditions on the production of interleukin-1 alpha and -1 beta by human endothelial cells cultured in vitro. Int J Immunopharmacol 1992, 14:525-534

17. Geiger T, Towbin H, Cosenti-Vargas A, Zingel O, Arnold J, Rordorf C, Glatt M, Vosbeck K: Neutralization of interleukin-1 beta activity in vivo with a monoclonal antibody alleviates collagen-induced arthritis in DBA/1 mice and prevents the associated acute-phase response. Clin Exp Rheumatol 1993, 11:515-522

18. Pober JS: Effects of tumour necrosis factor and related cytokines on vascular endothelial cells. Ciba Found Symp 1987, 131:170-184

19. Ikuta S, Kirby JA, Shenton BK, Givan AL, Lennard TW: Human endothelial cells: effect of TNF-alpha on peripheral blood mononuclear cell adhesion. Immunology 1991, 73:71-76

20. Bellingan GJ, Caldwell H, Howie SE, Dransfield I, Haslett C: In vivo fate of the inflammatory macrophage during the resolution of inflammation: inflammatory macrophages do not die locally, but emigrate to the draining lymph nodes. J Immunol 1996, 157:2577-2585

21. Hughes J, Johnson RJ, Mooney A, Hugo C, Gordon K, Savill J: Neutrophil fate in experimental glomerular capillary injury in the rat. Emigration exceeds in situ clearance by apoptosis. Am J Pathol 1997, 150:223-234

22. Mitchell S, Thomas G, Harvey K, Cottell D, Reville K, Berlasconi G, Petasis NA, Erwig L, Rees AJ, Savill J, Brady HR, Godson C: Lipoxins, aspirin-triggered epi-lipoxins, lipoxin stable analogues, and the resolution of inflammation: stimulation of macrophage phagocytosis of apoptotic neutrophils in vivo. J Am Soc Nephrol 2002, 13:2497-2507

23. Heasman SJ, Giles KM, Ward C, Rossi AG, Haslett C, Dransfield I: Glucocorticoid-mediated regulation of granulocyte apoptosis and macrophage phagocytosis of apoptotic cells: implications for the resolution of inflammation. J Endocrinol 2003, 178:29-36

24. Huynh ML, Fadok VA, Henson PM: Phosphatidylserine-dependent ingestion of apoptotic cells promotes TGF-beta1 secretion and the resolution of inflammation. J Clin Invest 2002, 109:41-50

25. Serhan CN, Savill J: Resolution of inflammation: the beginning programs the end. Nat Immunol 2005, 6:1191-1197

26. Le Y, Zhou Y, Iribarren P, Wang J: Chemokines and chemokine receptors: their manifold roles in homeostasis and disease. Cell Mol Immunol 2004, 1:95-104

27. Homey B, Zlotnik A: Chemokines in allergy. Current Opinion in Immunology 1999, 11:626-634

28. Luster AD: Chemokines--chemotactic cytokines that mediate inflammation. N Engl J Med 1998, 338:436-445

29. Ehrt S, Schnappinger D, Bekiranov S, Drenkow J, Shi S, Gingeras TR, Gaasterland T, Schoolnik G, Nathan C: Reprogramming of the macrophage transcriptome in response to interferon-gamma and *Mycobacterium tuberculosis*: signaling roles of nitric oxide synthase-2 and phagocyte oxidase. J Exp Med 2001, 194:1123-1140

30. Moser B, Wolf M, Walz A, Loetscher P: Chemokines: multiple levels of leukocyte migration control. Trends Immunol 2004, 25:75-84

31. Furie MB, Randolph GJ: Chemokines and tissue injury. Am J Pathol 1995, 146:1287-1301

32. Bendall L: Chemokines and their receptors in disease. Histol Histopathol 2005, 20:907-926

33. Szekanecz Z, Vegvari A, Szabo Z, Koch AE: Chemokines and chemokine receptors in arthritis. Front Biosci (Schol Ed) 2010, 2:153-167

34. Koch AE: Chemokines and their receptors in rheumatoid arthritis: future targets? Arthritis Rheum 2005, 52:710-721

35. Qin S, Rottman JB, Myers P, Kassam N, Weinblatt M, Loetscher M, Koch AE, Moser B, Mackay CR: The chemokine receptors CXCR3 and CCR5 mark subsets of T cells associated with certain inflammatory reactions. J Clin Invest 1998, 101:746-754

36. Katschke KJ, Jr., Rottman JB, Ruth JH, Qin S, Wu L, LaRosa G, Ponath P, Park CC, Pope RM, Koch AE: Differential expression of chemokine receptors on peripheral blood, synovial fluid, and synovial tissue monocytes/macrophages in rheumatoid arthritis. Arthritis Rheum 2001, 44:1022-1032

37. Szekanecz Z, Szucs G, Szanto S, Koch AE: Chemokines in rheumatic diseases. Curr Drug Targets 2006, 7:91-102

38. Koch AE, Kunkel SL, Burrows JC, Evanoff HL, Haines GK, Pope RM, Strieter RM: Synovial tissue macrophage as a source of the chemotactic cytokine IL-8. J Immunol 1991, 147:2187-2195

39. Koch AE, Kunkel SL, Shah MR, Hosaka S, Halloran MM, Haines GK, Burdick MD, Pope RM, Strieter RM: Growth-related gene product alpha. A chemotactic cytokine for neutrophils in rheumatoid arthritis. J Immunol 1995, 155:3660-3666

40. Kadl A, Leitinger N: The role of endothelial cells in the resolution of acute inflammation. Antioxid Redox Signal 2005, 7:1744-1754

41. Becker BF, Heindl B, Kupatt C, Zahler S: Endothelial function and hemostasis. Z Kardiol 2000, 89:160-167

42. Michiels C: Endothelial cell functions. J Cell Physiol 2003, 196:430-443

43. Middleton J, Patterson AM, Gardner L, Schmutz C, Ashton BA: Leukocyte extravasation: chemokine transport and presentation by the endothelium. Blood 2002, 100:3853-3860

44. Ali S, Palmer AC, Fritchley SJ, Maley Y, Kirby JA: Multimerization of monocyte chemoattractant protein-1 is not required for glycosaminoglycan-dependent transendothelial chemotaxis. Biochem J 2001, 358:737-745

45. Muller WA: Leukocyte-endothelial-cell interactions in leukocyte transmigration and the inflammatory response. Trends Immunol 2003, 24:327-334

46. Langer HF, Chavakis T: Leukocyte-endothelial interactions in inflammation. J Cell Mol Med 2009, 13:1211-1220

47. Nourshargh S, Hordijk PL, Sixt M: Breaching multiple barriers: leukocyte motility through venular walls and the interstitium. Nat Rev Mol Cell Biol 2010, 11:366-378

48. Mayadas TN, Johnson RC, Rayburn H, Hynes RO, Wagner DD: Leukocyte rolling and extravasation are severely compromised in P selectin-deficient mice. Cell 1993, 74:541-554

49. Ley K: The role of selectins in inflammation and disease. Trends Mol Med 2003, 9:263-268

50. Patel KD, Cuvelier SL, Wiehler S: Selectins: critical mediators of leukocyte recruitment. Semin Immunol 2002, 14:73-81

51. Grailer JJ, Kodera M, Steeber DA: L-selectin: role in regulating homeostasis and cutaneous inflammation. J Dermatol Sci 2009, 56:141-147

52. Walcheck B, Moore KL, McEver RP, Kishimoto TK: Neutrophil-neutrophil interactions under hydrodynamic shear stress involve L-selectin and PSGL-1. A mechanism that amplifies initial leukocyte accumulation of P-selectin in vitro. J Clin Invest 1996, 98:1081-1087

53. Crockett-Torabi E, Sulenbarger B, Smith CW, Fantone JC: Activation of human neutrophils through L-selectin and Mac-1 molecules. J Immunol 1995, 154:2291-2302

54. Lorenzon P, Vecile E, Nardon E, Ferrero E, Harlan JM, Tedesco F, Dobrina A: Endothelial cell E- and P-selectin and vascular cell adhesion molecule-1 function as signaling receptors. J Cell Biol 1998, 142:1381-1391

55. Arfors KE, Lundberg C, Lindbom L, Lundberg K, Beatty PG, Harlan JM: A monoclonal antibody to the membrane glycoprotein complex CD18 inhibits polymorphonuclear leukocyte accumulation and plasma leakage in vivo. Blood 1987, 69:338-340

56. Cook-Mills JM, Deem TL: Active participation of endothelial cells in inflammation. J Leukoc Biol 2005, 77:487-495

57. Dustin ML, Rothlein R, Bhan AK, Dinarello CA, Springer TA: Induction by IL 1 and interferon-gamma: tissue distribution, biochemistry, and function of a natural adherence molecule (ICAM-1). J Immunol 1986, 137:245-254

58. Albelda SM, Smith CW, Ward PA: Adhesion molecules and inflammatory injury. FASEB J 1994, 8:504-512

59. Sano H, Nakagawa N, Chiba R, Kurasawa K, Saito Y, Iwamoto I: Cross-linking of intercellular adhesion molecule-1 induces interleukin-8 and RANTES production through the activation of MAP kinases in human vascular endothelial cells. Biochem Biophys Res Commun 1998, 250:694-698

60. Wang Q, Doerschuk CM: The p38 mitogen-activated protein kinase mediates cytoskeletal remodeling in pulmonary microvascular endothelial cells upon intracellular adhesion molecule-1 ligation. J Immunol 2001, 166:6877-6884

61. Ley K, Laudanna C, Cybulsky MI, Nourshargh S: Getting to the site of inflammation: the leukocyte adhesion cascade updated. Nat Rev Immunol 2007, 7:678-689

62. Mamdouh Z, Kreitzer GE, Muller WA: Leukocyte transmigration requires kinesin-mediated microtubule-dependent membrane trafficking from the lateral border recycling compartment. J Exp Med 2008, 205:951-966

63. Mamdouh Z, Chen X, Pierini LM, Maxfield FR, Muller WA: Targeted recycling of PECAM from endothelial surface-connected compartments during diapedesis. Nature 2003, 421:748-753

64. Lou O, Alcaide P, Luscinskas FW, Muller WA: CD99 is a key mediator of the transendothelial migration of neutrophils. J Immunol 2007, 178:1136-1143

65. Schenkel AR, Mamdouh Z, Chen X, Liebman RM, Muller WA: CD99 plays a major role in the migration of monocytes through endothelial junctions. Nat Immunol 2002, 3:143-150

66. Bixel G, Kloep S, Butz S, Petri B, Engelhardt B, Vestweber D: Mouse CD99 participates in T-cell recruitment into inflamed skin. Blood 2004, 104:3205-3213

67. Wegmann F, Petri B, Khandoga AG, Moser C, Khandoga A, Volkery S, Li H, Nasdala I, Brandau O, Fassler R, Butz S, Krombach F, Vestweber D: ESAM supports neutrophil extravasation, activation of Rho, and VEGF-induced vascular permeability. J Exp Med 2006, 203:1671-1677

68. Fabbri M, Smart C, Pardi R: T lymphocytes. Int J Biochem Cell Biol 2003, 35:1004-1008

69. von Andrian UH, Mackay CR: T-cell function and migration. Two sides of the same coin. N Engl J Med 2000, 343:1020-1034

70. Shortman K, Liu YJ: Mouse and human dendritic cell subtypes. Nat Rev Immunol 2002, 2:151-161

71. Santana MA, Rosenstein Y: What it takes to become an effector T cell: the process, the cells involved, and the mechanisms. J Cell Physiol 2003, 195:392-401

72. Murphy KM, Reiner SL: The lineage decisions of helper T cells. Nat Rev Immunol 2002, 2:933-944

73. Berry N, Ase K, Kikkawa U, Kishimoto A, Nishizuka Y: Human T cell activation by phorbol esters and diacylglycerol analogues. J Immunol 1989, 143:1407-1413

74. Summers C, Rankin SM, Condliffe AM, Singh N, Peters AM, Chilvers ER: Neutrophil kinetics in health and disease. Trends Immunol 2010, 31:318-324

75. Faurschou M, Borregaard N: Neutrophil granules and secretory vesicles in inflammation. Microbes Infect 2003, 5:1317-1327

76. Burdon PC, Martin C, Rankin SM: Migration across the sinusoidal endothelium regulates neutrophil mobilization in response to ELR + CXC chemokines. Br J Haematol 2008, 142:100-108

77. Robinson JM: Phagocytic leukocytes and reactive oxygen species. Histochem Cell Biol 2009, 131:465-469

78. Robinson JM: Reactive oxygen species in phagocytic leukocytes. Histochem Cell Biol 2008, 130:281-297

79. Muller I, Munder M, Kropf P, Hansch GM: Polymorphonuclear neutrophils and T lymphocytes: strange bedfellows or brothers in arms? Trends Immunol 2009, 30:522-530

80. Moretta A, Marcenaro E, Sivori S, Della CM, Vitale M, Moretta L: Early liaisons between cells of the innate immune system in inflamed peripheral tissues. Trends Immunol 2005, 26:668-675

81. Morris MA, Ley K: Trafficking of natural killer cells. Curr Mol Med 2004, 4:431-438

82. Timonen T: Natural killer cells: endothelial interactions, migration, and target cell recognition. J Leukoc Biol 1997, 62:693-701

83. Biron CA, Nguyen KB, Pien GC, Cousens LP, Salazar-Mather TP: Natural killer cells in antiviral defense: function and regulation by innate cytokines. Annu Rev Immunol 1999, 17:189-220

84. Biron CA, Brossay L: NK cells and NKT cells in innate defense against viral infections. Curr Opin Immunol 2001, 13:458-464

85. Wallin RP, Screpanti V, Michaelsson J, Grandien A, Ljunggren HG: Regulation of perforin-independent NK cell-mediated cytotoxicity. Eur J Immunol 2003, 33:2727-2735

86. Eischen CM, Schilling JD, Lynch DH, Krammer PH, Leibson PJ: Fc receptor-induced expression of Fas ligand on activated NK cells facilitates cell-mediated cytotoxicity and subsequent autocrine NK cell apoptosis. J Immunol 1996, 156:2693-2699

87. Auffray C, Sieweke MH, Geissmann F: Blood monocytes: development, heterogeneity, and relationship with dendritic cells. Annu Rev Immunol 2009, 27:669-692

88. Gordon S, Taylor PR: Monocyte and macrophage heterogeneity. Nat Rev Immunol 2005, 5:953-964

89. Leon B, Ardavin C: Monocyte-derived dendritic cells in innate and adaptive immunity. Immunol Cell Biol 2008, 86:320-324

90. Geissmann F, Jung S, Littman DR: Blood Monocytes Consist of Two Principal Subsets with Distinct Migratory Properties. Immunity 2003, 19:71-82

91. Serbina NV, Jia T, Hohl TM, Pamer EG: Monocyte-mediated defense against microbial pathogens. Annu Rev Immunol 2008, 26:421-452

92. Dominguez PM, Ardavin C: Differentiation and function of mouse monocyte-derived dendritic cells in steady state and inflammation. Immunol Rev 2010, 234:90-104

93. Belge KU, Dayyani F, Horelt A, Siedlar M, Frankenberger M, Frankenberger B, Espevik T, Ziegler-Heitbrock L: The proinflammatory CD14+CD16+DR++ monocytes are a major source of TNF. J Immunol 2002, 168:3536-3542

94. Mizuno K, Toma T, Tsukiji H, Okamoto H, Yamazaki H, Ohta K, Ohta K, Kasahara Y, Koizumi S, Yachie A: Selective expansion of CD16high. Clin Exp Immunol 2005, 142:461-470

95. Nahrendorf M, Swirski FK, Aikawa E, Stangenberg L, Wurdinger T, Figueiredo JL, Libby P, Weissleder R, Pittet MJ: The healing myocardium sequentially mobilizes two monocyte subsets with divergent and complementary functions. J Exp Med 2007, 204:3037-3047

96. Fairweather D, Cihakova D: Alternatively activated macrophages in infection and autoimmunity. J Autoimmun 2009, 33:222-230

97. Pestka S, Krause CD, Walter MR: Interferons, interferon-like cytokines, and their receptors. Immunol Rev 2004, 202:8-32

98. Schroder K, Hertzog PJ, Ravasi T, Hume DA: Interferon-gamma: an overview of signals, mechanisms and functions. J Leukoc Biol 2004, 75:163-189

99. Zhang SY, Boisson-Dupuis S, Chapgier A, Yang K, Bustamante J, Puel A, Picard C, Abel L, Jouanguy E, Casanova JL: Inborn errors of interferon (IFN)-mediated immunity in humans: insights into the respective roles of IFN-alpha/beta, IFN-gamma, and IFN-lambda in host defense. Immunol Rev 2008, 226:29-40

100. Celada A, Gray PW, Rinderknecht E, Schreiber RD: Evidence for a gamma-interferon receptor that regulates macrophage tumoricidal activity. J Exp Med 1984, 160:55-74

101. Boehm U, Klamp T, Groot M, Howard JC: Cellular responses to interferon-gamma. Annu Rev Immunol 1997, 15:749-795

102. Schroder K, Hertzog PJ, Ravasi T, Hume DA: Interferon-gamma: an overview of signals, mechanisms and functions. J Leukoc Biol 2004, 75:163-189

103. Schroecksnadel K, Frick B, Winkler C, Fuchs D: Crucial role of interferon-gamma and stimulated macrophages in cardiovascular disease. Curr Vasc Pharmacol 2006, 4:205-213

104. Singh SK, Girschick HJ: Molecular survival strategies of the Lyme disease spirochete *Borrelia burgdorferi*. Lancet Infect Dis 2004, 4:575-583

105. Rosa PA: Microbiology of Borrelia burgdorferi. Semin Neurol 1997, 17:5-10

106. Rosa PA, Tilly K, Stewart PE: The burgeoning molecular genetics of the Lyme disease spirochaete. Nat Rev Microbiol 2005, 3:129-143

107. Fraser CM, Casjens S, Huang WM, Sutton GG, Clayton R, Lathigra R, White O, Ketchum KA, Dodson R, Hickey EK, Gwinn M, Dougherty B, Tomb JF, Fleischmann RD, Richardson D, Peterson J, Kerlavage AR, Quackenbush J, Salzberg S, Hanson M, van VR, Palmer N, Adams MD, Gocayne J, Weidman J, Utterback T, Watthey L, McDonald L, Artiach P, Bowman C, Garland S, Fuji C, Cotton MD, Horst K, Roberts K, Hatch B, Smith HO, Venter JC: Genomic sequence of a Lyme disease spirochaete, Borrelia burgdorferi. Nature 1997, 390:580-586

108. Tokarz R, Anderton JM, Katona LI, Benach JL: Combined effects of blood and temperature shift on *Borrelia burgdorferi* gene expression as determined by whole genome DNA array. Infect Immun 2004, 72:5419-5432

109. Schwan TG, Piesman J, Golde WT, Dolan MC, Rosa PA: Induction of an outer surface protein on Borrelia burgdorferi during tick feeding. Proc Natl Acad Sci U S A 1995, 92:2909-2913

110. Alitalo A, Meri T, Ramo L, Jokiranta TS, Heikkila T, Seppala IJ, Oksi J, Viljanen M, Meri S: Complement evasion by *Borrelia burgdorferi*: serum-resistant strains promote C3b inactivation. Infect Immun 2001, 69:3685-3691

111. Kraiczy P, Skerka C, Brade V, Zipfel PF: Further characterization of complement regulator-acquiring surface proteins of *Borrelia burgdorferi*. Infect Immun 2001, 69:7800-7809

112. Kraiczy P, Skerka C, Kirschfink M, Zipfel PF, Brade V: Mechanism of complement resistance of pathogenic *Borrelia burgdorferi* isolates. Int Immunopharmacol 2001, 1:393-401

113. Hellwage J, Meri T, Heikkila T, Alitalo A, Panelius J, Lahdenne P, Seppala IJ, Meri S: The complement regulator factor H binds to the surface protein OspE of *Borrelia burgdorferi*. J Biol Chem 2001, 276:8427-8435

114. Bykowski T, Babb K, von Lackum K, Riley SP, Norris SJ, Stevenson B: Transcriptional regulation of the *Borrelia burgdorferi* antigenically variable VlsE surface protein. J Bacteriol 2006, 188:4879-4889

115. Zhang JR, Norris SJ: Genetic variation of the *Borrelia burgdorferi* gene vlsE involves cassette-specific, segmental gene conversion. Infect Immun 1998, 66:3698-3704

116. Liang FT, Brown EL, Wang T, Iozzo RV, Fikrig E: Protective niche for Borrelia burgdorferi to evade humoral immunity. Am J Pathol 2004, 165:977-985

117. Duray PH: The surgical pathology of human Lyme disease. An enlarging picture. Am J Surg Pathol 1987, 11 Suppl 1:47-60

118. Codolo G, Amedei A, Steere AC, Papinutto E, Cappon A, Polenghi A, Benagiano M, Paccani SR, Sambri V, Del PG, Baldari CT, Zanotti G, Montecucco C, D'Elios MM, de BM: Borrelia burgdorferi NapA-driven Th17 cell inflammation in lyme arthritis. Arthritis Rheum 2008, 58:3609-3617

119. Gross DM, Steere AC, Huber BT: T helper 1 response is dominant and localized to the synovial fluid in patients with Lyme arthritis. J Immunol 1998, 160:1022-1028

120. Shin JJ, Glickstein LJ, Steere AC: High levels of inflammatory chemokines and cytokines in joint fluid and synovial tissue throughout the course of antibiotic-refractory Lyme arthritis. Arthritis Rheum 2007, 56:1325-1335

121. Barthold SW, Persing DH, Armstrong AL, Peeples RA: Kinetics of *Borrelia burgdorferi* dissemination and evolution of disease after intradermal inoculation of mice. Am J Pathol 1991, 139:263-273

122. Ruderman EM, Kerr JS, Telford SR, III, Spielman A, Glimcher LH, Gravallese EM: Early murine Lyme carditis has a macrophage predominance and is independent of major histocompatibility complex class II-CD4+ T cell interactions. J Infect Dis 1995, 171:362-370

123. Barthold SW, Beck DS, Hansen GM, Terwilliger GA, Moody KD: Lyme borreliosis in selected strains and ages of laboratory mice. J Infect Dis 1990, 162:133-138

124. Barthold SW, de Souza MS, Janotka JL, Smith AL, Persing DH: Chronic Lyme borreliosis in the laboratory mouse. Am J Pathol 1993, 143:959-971

125. Brown CR, Blaho VA, Loiacono CM: Susceptibility to experimental Lyme arthritis correlates with KC and monocyte chemoattractant protein-1 production in joints and requires neutrophil recruitment via CXCR2. J Immunol 2003, 171:893-901

126. Steere AC, Batsford WP, Weinberg M, Alexander J, Berger HJ, Wolfson S, Malawista SE: Lyme carditis: cardiac abnormalities of Lyme disease. Ann Intern Med 1980, 93:8-16

127. Armstrong AL, Barthold SW, Persing DH, Beck DS: Carditis in Lyme disease susceptible and resistant strains of laboratory mice infected with *Borrelia burgdorferi*. Am J Trop Med Hyg 1992, 47:249-258

128. Montgomery RR, Booth CJ, Wang X, Blaho VA, Malawista SE, Brown CR: Recruitment of macrophages and polymorphonuclear leukocytes in Lyme carditis. Infect Immun 2007, 75:613-620

129. Kelleher DM, Telford SR, III, Criscione L, Lin SR, Spielman A, Gravallese EM: Cytokines in murine Lyme carditis: Th1 cytokine expression follows expression of proinflammatory cytokines in a susceptible mouse strain. J Infect Dis 1998, 177:242-246

130. Thaisetthawatkul P, Logigian EL: Peripheral nervous system manifestations of lyme borreliosis. J Clin Neuromuscul Dis 2002, 3:165-171

131. Ebnet K, Brown KD, Siebenlist UK, Simon MM, Shaw S: *Borrelia burgdorferi* activates nuclear factor-kappa B and is a potent inducer of chemokine and adhesion molecule gene expression in endothelial cells and fibroblasts. J Immunol 1997, 158:3285-3292

132. Sellati TJ, Burns MJ, Ficazzola MA, Furie MB: *Borrelia burgdorferi* upregulates expression of adhesion molecules on endothelial cells and promotes transendothelial migration of neutrophils in vitro. Infect Immun 1995, 63:4439-4447

133. Sellati TJ, Abrescia LD, Radolf JD, Furie MB: Outer surface lipoproteins of *Borrelia burgdorferi* activate vascular endothelium in vitro. Infect Immun 1996, 64:3180-3187

134. Burns MJ, Sellati TJ, Teng EI, Furie MB: Production of interleukin-8 (IL-8) by cultured endothelial cells in response to *Borrelia burgdorferi* occurs independently of secreted IL-1 and tumor necrosis factor alpha and is required for subsequent transendothelial migration of neutrophils. Infect Immun 1997, 65:1217-1222

135. Burns MJ, Furie MB: *Borrelia burgdorferi* and interleukin-1 promote the transendothelial migration of monocytes in vitro by different mechanisms. Infect Immun 1998, 66:4875-4883

136. Huang AJ, Furie MB, Nicholson SC, Fischbarg J, Liebovitch LS, Silverstein SC: Effects of human neutrophil chemotaxis across human endothelial cell monolayers on the permeability of these monolayers to ions and macromolecules. J Cell Physiol 1988, 135:355-366

137. Gergel EI, Furie MB: Activation of endothelium by *Borrelia burgdorferi* in vitro enhances transmigration of specific subsets of T lymphocytes. Infect Immun 2001, 69:2190-2197

138. Gergel EI, Furie MB: Populations of human T lymphocytes that traverse the vascular endothelium stimulated by *Borrelia burgdorferi* are enriched with cells that secrete gamma interferon. Infect Immun 2004, 72:1530-1536

139. Schrier D, Gilbertsen RB, Lesch M, Fantone J: The role of neutrophils in type II collagen-induced arthritis in rats. Am J Pathol 1984, 117:26-29

140. Santos LL, Morand EF, Hutchinson P, Boyce NW, Holdsworth SR: Anti-neutrophil monoclonal antibody therapy inhibits the development of adjuvant arthritis. Clin Exp Immunol 1997, 107:248-253

141. Lusitani D, Malawista SE, Montgomery RR: Borrelia burgdorferi are susceptible to killing by a variety of human polymorphonuclear leukocyte components. J Infect Dis 2002, 185:797-804

142. Ritzman AM, Hughes-Hanks JM, Blaho VA, Wax LE, Mitchell WJ, Brown CR: The chemokine receptor CXCR2 ligand KC (CXCL1) mediates neutrophil recruitment and is critical for development of experimental Lyme arthritis and carditis. Infect Immun 2010, 78:4593-4600

143. Xu Q, Seemanapalli SV, Reif KE, Brown CR, Liang FT: Increasing the recruitment of neutrophils to the site of infection dramatically attenuates Borrelia burgdorferi infectivity. J Immunol 2007, 178:5109-5115

144. Yssel H, Nakamoto T, Schneider P, Freitas V, Collins C, Webb D, Mensi N, Soderberg C, Peltz G: Analysis of T lymphocytes cloned from the synovial fluid and blood of a patient with Lyme arthritis. Int Immunol 1990, 2:1081-1089

145. Yssel H, Shanafelt MC, Soderberg C, Schneider PV, Anzola J, Peltz G: *Borrelia burgdorferi* activates a T helper type 1-like T cell subset in Lyme arthritis. J Exp Med 1991, 174:593-601

146. Yin Z, Braun J, Neure L, Wu P, Eggens U, Krause A, Kamradt T, Sieper J: T cell cytokine pattern in the joints of patients with Lyme arthritis and its regulation by cytokines and anticytokines. Arthritis Rheum 1997, 40:69-79

147. Salazar JC, Pope CD, Sellati TJ, Feder HM, Jr., Kiely TG, Dardick KR, Buckman RL, Moore MW, Caimano MJ, Pope JG, Krause PJ, Radolf JD: Coevolution of markers of innate and adaptive immunity in skin and peripheral blood of patients with erythema migrans. J Immunol 2003, 171:2660-2670

148. Wang X, Ma Y, Yoder A, Crandall H, Zachary JF, Fujinami RS, Weis JH, Weis JJ: T cell infiltration is associated with increased Lyme arthritis in TLR2-/- mice. FEMS Immunol Med Microbiol 2008, 52:124-133

149. Dong Z, Edelstein MD, Glickstein LJ: CD8+ T cells are activated during the early Th1 and Th2 immune responses in a murine Lyme disease model. Infect Immun 1997, 65:5334-5337

150. Matyniak JE, Reiner SL: T helper phenotype and genetic susceptibility in experimental Lyme disease. J Exp Med 1995, 181:1251-1254

151. Keane-Myers A, Nickell SP: T cell subset-dependent modulation of immunity to *Borrelia burgdorferi* in mice. J Immunol 1995, 154:1770-1776

152. Defosse DL, Johnson RC: In vitro and in vivo induction of tumor necrosis factor alpha by Borrelia burgdorferi. Infect Immun 1992, 60:1109-1113

153. Montgomery RR, Nathanson MH, Malawista SE: The fate of *Borrelia burgdorferi*, the agent for Lyme disease, in mouse macrophages. Destruction, survival, recovery. J Immunol 1993, 150:909-915

154. Salazar JC, Duhnam-Ems S, La VC, Cruz AR, Moore MW, Caimano MJ, Velez-Climent L, Shupe J, Krueger W, Radolf JD: Activation of human monocytes by live *Borrelia burgdorferi* generates TLR2-dependent and -independent responses which include induction of IFN-beta. PLoS Pathog 2009, 5:e1000444

155. Radolf JD, Arndt LL, Akins DR, Curetty LL, Levi ME, Shen Y, Davis LS, Norgard MV: Treponema pallidum and Borrelia burgdorferi lipoproteins and synthetic lipopeptides activate monocytes/macrophages. J Immunol 1995, 154:2866-2877

156. Ma Y, Weis JJ: *Borrelia burgdorferi* outer surface lipoproteins OspA and OspB possess B-cell mitogenic and cytokine-stimulatory properties. Infect Immun 1993, 61:3843-3853

157. Moore MW, Cruz AR, LaVake CJ, Marzo AL, Eggers CH, Salazar JC, Radolf JD: Phagocytosis of *Borrelia burgdorferi* and *Treponema pallidum* potentiates innate immune activation and induces gamma interferon production. Infect Immun 2007, 75:2046-2062

158. Dame TM, Orenzoff BL, Palmer LE, Furie MB: IFN-gamma alters the response of *Borrelia burgdorferi*-activated endothelium to favor chronic inflammation. J Immunol 2007, 178:1172-1179

159. Keane-Myers A, Nickell SP: Role of IL-4 and IFN-gamma in modulation of immunity to *Borrelia burgdorferi* in mice. J Immunol 1995, 155:2020-2028

160. Brown CR, Reiner SL: Experimental Lyme arthritis in the absence of interleukin-4 or gamma interferon. Infect Immun 1999, 67:3329-3333

161. Glickstein L, Edelstein M, Dong JZ: Gamma interferon is not required for arthritis resistance in the murine Lyme disease model. Infect Immun 2001, 69:3737-3743

162. Brown CR, Blaho VA, Fritsche KL, Loiacono CM: Stat1 deficiency exacerbates carditis but not arthritis during experimental Lyme borreliosis. J Interferon Cytokine Res 2006, 26:390-399

163. Satoskar AR, Elizondo J, Monteforte GM, Stamm LM, Bluethmann H, Katavolos P, Telford SR, III: Interleukin-4-deficient BALB/c mice develop an enhanced Th1-like response but control cardiac inflammation following *Borrelia burgdorferi* infection. FEMS Microbiol Lett 2000, 183:319-325

164. Olson CM, Jr., Bates TC, Izadi H, Radolf JD, Huber SA, Boyson JE, Anguita J: Local production of IFN-gamma by invariant NKT cells modulates acute lyme carditis. J Immunol 2009, 182:3728-3734

165. Furie MB, Cramer EB, Naprstek BL, Silverstein SC: Cultured endothelial cell monolayers that restrict the transendothelial passage of macromolecules and electrical current. J Cell Biol 1984, 98:1033-1041

166. Randolph GJ, Furie MB: A soluble gradient of endogenous monocyte chemoattractant protein-1 promotes the transendothelial migration of monocytes in vitro. J Immunol 1995, 155:3610-3618

167. Stanley ER, Heard PM: Factors regulating macrophage production and growth. Purification and some properties of the colony stimulating factor from medium conditioned by mouse L cells. J Biol Chem 1977, 252:4305-4312

168. Forestal CA, Gil H, Monfett M, Noah CE, Platz GJ, Thanassi DG, Benach JL, Furie MB: A conserved and immunodominant lipoprotein of Francisella tularensis is proinflammatory but not essential for virulence. Microb Pathog 2008, 44:512-523

169. Rival Y, Del Maschio A, Rabiet MJ, Dejana E, Duperray A: Inhibition of platelet endothelial cell adhesion molecule-1 synthesis and leukocyte transmigration in endothelial cells by the combined action of TNF-alpha and IFN-gamma. J Immunol 1996, 157:1233-1241

170. Muller WA, Weigl SA, Deng X, Phillips DM: PECAM-1 is required for transendothelial migration of leukocytes. J Exp Med 1993, 178:449-460

171. Dufour EM, Deroche A, Bae Y, Muller WA: CD99 is essential for leukocyte diapedesis *in vivo*. Cell Commun Adhes 2008,1-13

172. Steere AC, Coburn J, Glickstein L: The emergence of Lyme disease. J Clin Invest 2004, 113:1093-1101

173. Robertson MJ: Role of chemokines in the biology of natural killer cells. J Leukoc Biol 2002, 71:173-183

174. Dalbeth N, Gundle R, Davies RJ, Lee YC, McMichael AJ, Callan MF: CD56bright NK cells are enriched at inflammatory sites and can engage with monocytes in a reciprocal program of activation. J Immunol 2004, 173:6418-6426

175. Berman ME, Xie Y, Muller WA: Roles of platelet/endothelial cell adhesion molecule-1 (PECAM-1, CD31) in natural killer cell transendothelial migration and beta 2 integrin activation. J Immunol 1996, 156:1515-1524

176. Liston A, McColl S: Subversion of the chemokine world by microbial pathogens. Bioessays 2003, 25:478-488

177. Zhao Z, Chang H, Trevino RP, Whren K, Bhawan J, Klempner MS: Selective up-regulation of matrix metalloproteinase-9 expression in human erythema migrans skin lesions of acute lyme disease. J Infect Dis 2003, 188:1098-1104

178. Van den Steen PE, Opdenakker G, Wormald MR, Dwek RA, Rudd PM: Matrix remodelling enzymes, the protease cascade and glycosylation. Biochim Biophys Acta 2001, 1528:61-73

179. Meerschaert J, Furie MB: Monocytes use either CD11/CD18 or VLA-4 to migrate across human endothelium in vitro. J Immunol 1994, 152:1915-1926

180. Pinola M, Saksela E, Tiisala S, Renkonen R: Human NK cells expressing alpha 4 beta 1/beta 7 adhere to VCAM-1 without preactivation. Scand J Immunol 1994, 39:131-136

181. Woodfin A, Voisin MB, Imhof BA, Dejana E, Engelhardt B, Nourshargh S: Endothelial cell activation leads to neutrophil transmigration as supported by the sequential roles of ICAM-2, JAM-A, and PECAM-1. Blood 2009, 113:6246-6257

182. Romer LH, McLean NV, Yan HC, Daise M, Sun J, DeLisser HM: IFN-gamma and TNF-alpha induce redistribution of PECAM-1 (CD31) on human endothelial cells. J Immunol 1995, 154:6582-6592

183. Woodfin A, Voisin MB, Nourshargh S: PECAM-1: a multi-functional molecule in inflammation and vascular biology. Arterioscler Thromb Vasc Biol 2007, 27:2514-2523

184. Proost P, Verpoest S, Van de Borne K, Schutyser E, Struyf S, Put W, Ronsse I, Grillet B, Opdenakker G, Van DJ: Synergistic induction of CXCL9 and CXCL11 by Toll-like receptor ligands and interferon-gamma in fibroblasts correlates with elevated levels of CXCR3 ligands in septic arthritis synovial fluids. J Leukoc Biol 2004, 75:777-784

185. Proost P, Vynckier AK, Mahieu F, Put W, Grillet B, Struyf S, Wuyts A, Opdenakker G, Van DJ: Microbial Toll-like receptor ligands differentially regulate CXCL10/IP-10 expression in fibroblasts and mononuclear leukocytes in synergy with IFN-gamma and provide a mechanism for enhanced synovial chemokine levels in septic arthritis. Eur J Immunol 2003, 33:3146-3153

186. Loos T, Dekeyzer L, Struyf S, Schutyser E, Gijsbers K, Gouwy M, Fraeyman A, Put W, Ronsse I, Grillet B, Opdenakker G, Van DJ, Proost P: TLR ligands and cytokines induce CXCR3 ligands in endothelial cells: enhanced CXCL9 in autoimmune arthritis. Lab Invest 2006, 86:902-916

187. Miller JC, Ma Y, Bian J, Sheehan KC, Zachary JF, Weis JH, Schreiber RD, Weis JJ: A critical role for type I IFN in arthritis development following Borrelia burgdorferi infection of mice. J Immunol 2008, 181:8492-8503

188. Cruz AR, Moore MW, La Vake CJ, Eggers CH, Salazar JC, Radolf JD: Phagocytosis of Borrelia burgdorferi, the Lyme disease spirochete, potentiates innate immune activation and induces apoptosis in human monocytes. Infect Immun 2008, 76:56-70

189. Hayakawa Y, Huntington ND, Nutt SL, Smyth MJ: Functional subsets of mouse natural killer cells. Immunol Rev 2006, 214:47-55

190. Hirsch S, Gordon S: The use and limitation of monoclonal antibodies against mononuclear phagocytes. Immunobiology 1982, 161:298-307

191. Steere AC, Duray PH, Butcher EC: Spirochetal antigens and lymphoid cell surface markers in Lyme synovitis. Comparison with rheumatoid synovium and tonsillar lymphoid tissue. Arthritis Rheum 1988, 31:487-495

192. Miura M, El-Sawy T, Fairchild RL: Neutrophils mediate parenchymal tissue necrosis and accelerate the rejection of complete major histocompatibility complex-disparate cardiac allografts in the absence of interferon-gamma. Am J Pathol 2003, 162:509-519

193. Zehntner SP, Brickman C, Bourbonniere L, Remington L, Caruso M, Owens T: Neutrophils that infiltrate the central nervous system regulate T cell responses. J Immunol 2005, 174:5124-5131

194. Schenkel AR, Dufour EM, Chew TW, Sorg E, Muller WA: The murine CD99-related molecule CD99-like 2 (CD99L2) is an adhesion molecule involved in the inflammatory response. Cell Commun Adhes 2007, 14:227-237

195. Bixel MG, Petri B, Khandoga AG, Khandoga A, Wolburg-Buchholz K, Wolburg H, Marz S, Krombach F, Vestweber D: A CD99-related antigen on endothelial cells mediates neutrophil but not lymphocyte extravasation in vivo. Blood 2007, 109:5327-5336

196. Bixel MG, Li H, Petri B, Khandoga AG, Khandoga A, Zarbock A, Wolburg-Buchholz K, Wolburg H, Sorokin L, Zeuschner D, Maerz S, Butz S, Krombach F, Vestweber D: CD99 and CD99L2 act at the same site as, but independently of, PECAM-1 during leukocyte diapedesis. Blood 2010, 116:1172-1184

197. Ramesh G, Alvarez X, Borda JT, Aye PP, Lackner AA, Sestak K: Visualizing cytokine-secreting cells in situ in the rhesus macaque model of chronic gut inflammation. Clin Diagn Lab Immunol 2005, 12:192-197